

**Design and Development of an Automated Fiber Optic Gyroscope Coil Winding Machine**

by

**Stephen M. Lin**

**B.S. Mechanical Engineering (1995)**

**Massachusetts Institute Of Technology, Cambridge**

**Submitted to the Department of Mechanical Engineering  
in Partial Fulfillment of the Requirements for the Degree of  
Master of Science**

at the

**Massachusetts Institute of Technology**

**September 1997**

**© 1997 Massachusetts Institute of Technology  
All Rights Reserved**

Signature of Author .....

**Department of Mechanical Engineering  
August 20, 1997**

Certified by .....

**Dr. Andre Sharon  
Executive Officer of the Manufacturing Institute  
Thesis Supervisor**

Accepted by.....

**Ain A. Sonin  
Chairman, Department Committee on Graduate Students**

FEB 12 1998

ARCHIVE

# Design and Development of an Automated Fiber Optic Gyroscope Coil Winding Machine

by

Stephen M. Lin

Submitted to the Department of Mechanical Engineering  
on August 20, 1997 in Partial Fulfillment of the  
Requirements for the Degree of Master of Science

## Abstract

Fiber optic gyroscopes (FOGs) continue to represent an increasingly attractive solid-state alternative to the traditional spinning-mass gyroscopes which still dominate the gyroscope market. However, the benefits of FOGs do not come cheaply. At the heart of a FOG is a fiber optic sensing coil wound in one of several special patterns to improve gyroscopic performance. Winding a fiber optic sensing coil traditionally is performed on a semi-automated machine with the constant or frequent attention of an operator and is a long and involved process, thus driving up costs.

A DARPA funded project was created to cost reduce many components of manufacturing FOGs including the winding of fiber optic sensing coils. The MIT Manufacturing Institute (MIT/MI) was subcontracted through a corporate customer to develop an automated machine for the winding of fiber optic sensing coils. The MIT/MI designed, developed, and delivered a fully automated machine to the corporate customer capable of winding fiber optic sensing coils with significantly lower operator intervention, and at significantly faster speeds than previously available. This document will cover various aspects in the design and development of the automated winding machine. These topics include, but are not limited to, the development of an active tension control system capable of continuously varying the desired tension level on the fiber as it is being wound into a FOG coil. And, a method for automatically swapping the two supply spools used in winding a FOG that allows the machine to wind all patterns dictated by the project will be discussed.

Thesis Supervisor: Dr. Andre Sharon  
Title: Director of the MIT Manufacturing Institute

# Table of Contents

<b>1. Introduction .....</b>	<b>14</b>
1.1. What Is A Gyroscope .....	14
1.2. How A Fiber Optic Gyro Works.....	17
1.3. The Components Of A FOG .....	20
1.3.1. The Light Source .....	21
1.3.2. The Source Coupler .....	21
1.3.3. The Integrated Optics Chip (IOC).....	21
1.3.4. The Photodetector.....	22
1.3.5. The Coil .....	22
1.4. The Drive to Automation .....	30
<b>2. Overall System Design .....</b>	<b>33</b>
2.1. The Customer .....	33
2.2. The Design Process .....	34
2.3. Basic Requirements For Winder Topology .....	36
2.4. The Supply Unit Concept.....	41
2.5. Fiber guiding .....	42
2.5.1. Fiber Guiding Requirements.....	42
2.5.2. Lead and Lag Angles .....	43
2.5.3. Fiber Manipulators.....	45
2.5.4. The Guide Wheel .....	46
2.5.5. Concept Selection .....	48
2.6. Overall Design Validation.....	48
2.7. Process Experiments .....	49
<b>3. Machine Subsystems: Detailed Design and Validation .....</b>	<b>50</b>
3.1. Introduction .....	50
3.2. Supply Units.....	51

3.3. Flange Design.....	52
3.3.1. Introduction.....	52
3.3.2. Flange Designs .....	53
3.3.2.1. Routing The Fiber Out Early .....	53
3.3.2.2. Vertical Slots .....	54
3.3.2.3. Horizontal Layered Slots .....	56
3.3.3. Test Results .....	57
3.4. Payout Clamp - Coupling To The Supply Unit .....	58
3.4.1. Introduction.....	58
3.4.2. Functional Requirements.....	59
3.4.3. Concept Generation and selection .....	61
3.4.3.1. Simple Mechanical Stop.....	61
3.4.3.2. Kinematic Coupling .....	62
3.4.3.3. Quasi-Kinematic Coupling.....	64
3.4.3.4. Clamping Actuator Selection.....	66
3.4.4. Testing and Results.....	68
3.5. The Roller .....	70
3.5.1. Introduction.....	70
3.5.2. Development of the Roller Concept.....	71
3.5.3. Roller Design Details .....	73
3.5.3.1. Flat Surface Engagement .....	73
3.5.3.2. Fitted Roller Vs. Single Multi-Purpose Roller .....	75
3.5.4. Testing and Results.....	77
<b>4. Supply Units: Detailed Design, Control and Validation .....</b>	<b>80</b>
4.1. Introduction .....	80
4.2. Guide Wheel Runout .....	81
4.2.1. Introduction.....	81
4.2.2. Guide Wheel Development.....	83
4.2.2.1. Single-Piece Guide Wheel .....	83

4.2.2.2. Optimized Hub and Retainer Guide Wheels .....	85
4.2.3. Interpretation of Guide Wheel Runout Profile .....	87
4.2.3.1. Measurement Technique .....	87
4.2.4. Further Improving Runout.....	90
4.3. Guide Wheel Fine Alignment .....	91
4.3.1. Introduction.....	91
4.3.2. The Fine Alignment Mechanisms .....	92
4.3.3. Testing and Results.....	94
4.4. Guide Wheel Registration .....	95
4.4.1. Introduction.....	95
4.4.2. Registration Concept Selection .....	96
4.4.2.1. High Precision External Sensor .....	97
4.4.2.2. Electrical Contact of the Guide Wheel to the Flange .....	98
4.4.2.3. Physical Contact of the Guide Wheel to the Flange.....	98
4.4.3. Testing and Results.....	99
4.5. Inactive Fiber Immobilization .....	102
4.5.1. Introduction.....	102
4.5.2. Concept Generation and Selection.....	103
4.5.2.1. Applying Tension With A Motor Bias.....	103
4.5.2.2. Applying Tension Using a Spring .....	104
4.6. Active Tension Control.....	106
4.6.1. Introduction.....	106
4.6.2. Tension Control Methods .....	107
4.6.2.1. Constant Tension Control Methods.....	107
4.6.2.2. Inertia De-coupled Tension Control Using A Magnetic Brake	107
4.6.2.3. Dancerless Tension Control.....	109
4.6.2.4. Active Dancer Tension Control .....	110
4.6.3. Tension Control Models.....	112
4.6.3.1. Introduction .....	112
4.6.3.2. Dancerless Tension Control Model .....	112

4.6.3.3. Active Dancer Tension Control Model.....	115
4.6.3.4. Simulated Tension Control Results .....	118
4.6.4. Choosing A Tension Control Method: Experimental Results.....	124
4.6.4.1. Introduction .....	124
4.6.4.2. Load Cell Noise.....	124
4.6.4.3. Tension Control While Winding .....	126
4.6.4.4. Tension Profiling While Winding .....	128
4.6.4.5. Making The Choice .....	129
4.6.5. The Automated Coil Winder: Tension Control Experiments .....	130
4.6.5.1. Introduction .....	130
4.6.5.2. Load Cell Noise.....	131
4.6.5.3. Tension Control While Winding At Constant Speed.....	132
4.6.5.4. Tension Control While Winding With A Slow Down Zone ....	133
4.6.5.5. Tension Profiling While Winding With A Slow Down Zone ...	135
4.6.6. Auto Load Cell Calibration.....	137
<b>5. Automated Control of the Coil Winding Process .....</b>	<b>138</b>
5.1. Introduction .....	138
5.2. The Scripting Language.....	139
5.2.1. Basic Operation - Cmd File Execution.....	140
5.2.2. Basic Unit Of Instruction - The Cmd .....	140
5.2.3. Flow Control .....	141
5.2.4. Interactive Control And Cmd Development .....	142
5.3. Undo Support.....	142
5.4. Rapid Process Development .....	143
5.4.1. Development And Tweaking On The Fly .....	144
5.4.2. Automatic Process Steps History Generation .....	145
5.5. Error Handling And Recovery .....	146
5.6. Results And Conclusions .....	147

**6. Conclusions.....149**

**7. Bibliography .....151**

# Table of Figures

Figure 1.1: A representation of a FOG coil.....	17
Figure 1.2. Balls rolling relative to a plank.....	18
Figure 1.3: The Sagnac Interferometer .....	20
Figure 1.4. Diagram of Fiber Optic Gyroscope.....	20
Figure 1.5: Demonstration of symmetry concept.....	23
Figure 1.6: A fiber optic gyroscope coil. ....	24
Figure 1.7: Winding Sequence .....	26
Figure 1.8: Quadrupole Cross Section .....	27
Figure 1.9: Helical Winding Technique.....	28
Figure 1.10: Helical Wind Cross Section.....	29
Figure 1.11: Orthocyclic Winding .....	30
Figure 2.1: Test-Bed Winder .....	36
Figure 2.2: Basic layout for a machine design to wind a quadrupole coil.....	37
Figure 2.3: Four basic requirements for winding all the patterns desired by the Customer.....	39
Figure 2.4: Each supply unit must be able to occupy two ride positions and one payout position to satisfy the four basic requirements.....	40
Figure 2.5: Three basic fiber guiding situations.....	43
Figure 2.6: The use of lead and lag angles for guiding fiber onto the product spool.....	44
Figure 2.7: Fixed manipulator for constraining fiber placement. ....	45
Figure 2.8: Adjustable finger-like manipulator for fiber guiding. ....	46
Figure 2.9: The guide wheel.....	47
Figure 3.1: The automated fiber optic gyroscope coil winding machine. A) Supply units, B) Main positioning system, C) Main winding shaft, D) Payout clamps, E) Ride clamps, F) Product spool, G) Roller.....	51
Figure 3.2: Traditional flange. The inactive fiber routes around the flange outer diameter towards the supply spool in ride position.....	52



Figure 3.3: Ideally the inactive fiber makes a 90 degree turn as soon as the winding pattern dictates and phases through the flange wall. ....54

Figure 3.4: Vertical slots flange design. The inactive fiber is routed through one of two vertical slots in the flange.....55

Figure 3.5: Routing fiber into the vertical slot. The fiber must be routed over the top edge of the slot and down into it.....56

Figure 3.6: Horizontal layered slots flange design. The inactive fiber is routed through the nearest slot in the flange for the given layer in the coil that the wind has progressed to. ....57

Figure 3.7: Rotational and lateral misalignment of the supply unit on the payout clamp as seen from the front. ....60

Figure 3.8: Rotational misalignment of the supply unit on top of the payout clamp as seen from above. ....61

Figure 3.9: A simple mechanical stop for the payout clamp.....62

Figure 3.10: Payout clamp using a kinematic coupling approach. Three spherical locators on the supply unit base seat into three wedges on the payout clamp.....64

Figure 3.11: Payout clamp utilizing a quasi-kinematic approach. Two locating pin and wedge pairs and one spherical locator constrain the supply unit in the most important degrees of freedom.....65

Figure 3.12: Engaging the quasi-kinematic clamp. The locating pins contact the locating wedges in two places while the spherical locator engages the locating pad at a point. ....66

Figure 3.13: Available space for payout clamp actuator. ....68

Figure 3.14: The clamp motor engages the clamp wedge to lock the supply unit down to the payout clamp base.....68

Figure 3.15: Payout clamp positioning repeatability as measured by a dial indicator at the location of the guide wheel. Left: results for supply unit A. Right: results for supply unit B. Solid lines indicate test type 1 results. Dashed lines indicate test type 2 results. ....69

Figure 3.16: Jog zone cross-section. Each series of cross-sections for a “clean” and “unclean” jog zone depict the jog start, two mid-jog, and jog end diagrams.....72

Figure 3.17: Roller mis-alignment with coil surface can compromise the integrity of the underlying layers. ....74

Figure 3.18: Self-aligning roller properly engages the coil surface and enforces the jog zone.....75

Figure 3.19: Left: Roller fitted to the width of the product spool rollers entire coil at once. Right: Thin roller capable of rolling any size product spool rollers coil little by little.....76

Figure 3.20: Overhead photo was taken of one edge of the jog zone as indicated. ....78

Figure 3.21: Overhear view of fiber near one edge of the jog zone before rolling.....79

Figure 3.22: Overhead view of fiber near one edge of the jog zone after rolling.79

Figure 4.1: Supply unit. A) Guide wheel, B) Tension sensor, C) Guide wheel fine alignment system, D) Base plate, E) Dancer pulley, F) Passive tension spring, G) Supply spool, H) Ride arm, I) Brake .....81

Figure 4.2: Guide wheel dimensions. The thickness of the guide wheel and its depth of reach are dictated by the fiber diameter and the flange depth. ..82

Figure 4.3: Asymmetric guide wheel incorporates support structure into the guide wheel itself.....84

Figure 4.4: Optimized guide wheel assembly redesign. The redesign of the original guide wheel assembly minimized the overall size of the guide wheel in an attempt to achieve lower runout. ....86

Figure 4.5: Runout profile of original guide wheel assembly. The ‘potato chip’ profile is distinguished by its two peaks and two valleys. ....88

Figure 4.6: Runout profile of an actual redesigned guide wheel assembly. This profile reveals only one peak and valley.....89

Figure 4.7: Runout profile remounting repeatability test.....90

Figure 4.8: Guide wheel misalignment. Improper alignment of the guide wheel with respect to the flange interferes with its ability to wind against the flange.....	92
Figure 4.9: Fine alignment of the guide wheel about the Y axis. Opposing set screws adjust and lock down the angle of the guide wheel about the pivot.	93
Figure 4.10: Fine alignment of the guide wheel about the Z axis. Opposing set screws adjust and lock the angle of the guide wheel about the pivot.....	94
Figure 4.11: Guide wheel registration using a high precision external sensor. ....	97
Figure 4.12: Guide wheel registration repeatability test. ....	101
Figure 4.13: Flange registration location data over several layers of winding for supply units A and B.....	102
Figure 4.14: Inactive fiber immobilization using battery power to apply a bias current to the supply spool motor. ....	104
Figure 4.15: Inactive fiber immobilization using a tension spring to apply a tension to the fiber through a dancer arm and pulley. The brake pad engages the supply spool to prevent it from rotating and releasing tension from the line.....	105
Figure 4.16: Inertia de-coupled tension control method using a magnetic brake. Feedback loops are indicated by the dashed lines.....	108
Figure 4.17: Dancerless tension control system. The dashed line indicated a feedback loop from the load cell to the supply spool motor.....	110
Figure 4.18: Active dancer tension control method.....	111
Figure 4.19: Idealized mechanical system for the dancerless tension control method. ....	113
Figure 4.20: Bond graph representation of the dancerless tension control system.....	114
Figure 4.21: Idealized mechanical system for the active dancer tension control method. ....	116
Figure 4.22: Bond graph representation of the active dancer tension control system.....	118

Figure 4.23: Simulink™ block diagram model of the dancerless tension control system.....	119
Figure 4.24: Results from simulated winding tests on the dancerless tension control model. Top: Normal winding. Fiber accelerates to constant speed and then decelerates back to zero. Mid: Desired tension is stepped in the middle of winding. Bot: A low amplitude broad band noise signal is inserted in to the feedback line.....	120
Figure 4.25: Simulink™ block diagram model of the active dancer tension control system.....	122
Figure 4.26: Results from simulated winding tests on the active dancer tension control model. Top: Normal winding. Fiber accelerates to constant speed and then decelerates back to zero. Mid: Desired tension is stepped in the middle of winding. Bot: A low amplitude broad band noise signal is inserted in to the feedback line.....	123
Figure 4.27: Load cell noise. Fiber is routed from supply spool to the product spool, but tension control is not active, and no winding is taking place..	125
Figure 4.28: Dancerless tension control. Winding at approximately 0.5 rps while sampling tension at 500 Hz. Top: Raw tension data. Mid: tension averaged over 50 milliseconds. Bottom: Tension frequency spectrum.	126
Figure 4.29: Active dancer tension control. Winding at approximately 360 dps while sampling tension every 2 milliseconds. Top: Raw tension data. Mid: Tension averaged over 50 milliseconds. Bottom: Tension frequency spectrum.....	127
Figure 4.30: Tension profiling tests conducted by inducing a tension step while winding. Top: Results using dancerless tension control. Bottom: Results using active dancer tension control. ....	128
Figure 4.31: Tension noise levels on the automated coil winder. Top: Main shaft is turning, but no fiber connects the supply spool to the product spool. Bottom: same situation but the supply unit is jogged as if winding were occurring.....	132

Figure 4.32: Active dancer tension control while winding at a constant speed of 240 dps on the automated winder. Tension is being maintained at 9 grams. Top: Raw tension data. Bottom: Averaged tension data. ....133

Figure 4.33: Tension control while winding with a slow down zone. Full winding speed at 360 dps with a slow speed of 60 dps through the jog zone. Tension is being maintained at 6 grams.....135

Figure 4.34: Top: Average tension while winding with tension spiking inside the jog zone. Bottom: Average tension while winding with tension dithering inside the jog zone. ....136

Figure 5.1: Making multiple calls to a cmd file from another cmd file.....141

Figure 5.2: Cmd list for maneuvering the main positioning system to properly wind the second fiber turn of a layer where the first turn lies up against the flange.....144

Figure 6.1: First full length fiber optic gyroscope coil wound on the automated fiber optic gyroscope coil winding machine. ....149

# 1. Introduction

## 1.1. *What Is A Gyroscope*

A gyroscope is a sensor that is used to detect rotation. It finds use in a wide range of applications but is most frequently used in navigation. From submarines to single-engine planes to satellites, gyroscopes make it possible for vehicles to accurately and reliably chart out their courses, either automatically or with the aid of an operator. Gyroscopes perform operations as simple as telling a plane which way is up or as complex as telling a satellite in near-zero gravity if it has deviated a thousandth of a degree off course.

One of the most recent applications of navigation technology is Global Positioning System or GPS<sup>1</sup>. Cars and other vehicles can use GPS to find their position on the globe. With the aid of a computer, the locational information from GPS can be used to track a car's progress and help a driver chart a course. Communication with satellites is not without problems. It is expensive and doesn't work well when obscured by obstacles, such as mountains or tall buildings. By using a gyroscope and a simple computer instead of satellite communication for locational information, a vehicle can navigate in almost any set of conditions. The problem to date has been that gyroscopes have been too expensive to find use in consumer automobiles. New technology has made it possible to reduce cost of gyroscopes, enabling their use in GPS. A gyro senses any turns made by the vehicle and a computer keeps track of the distances and directions traveled. By comparing this information to known maps and knowing a reference starting position, the computer can locate the vehicle on a map contained in memory.

---

<sup>1</sup> Herdman, Craig T. "Fiber Optic Gyroscopes." Honeywell Technology Center.

Traditionally, gyroscopes have been mechanically based devices comprised of high precision parts that spin and then twist in response to rotations of the gyroscope<sup>2</sup>. Exactly how these parts turn inside the sensor is well defined by modern dynamic theory. Essentially all mechanical gyroscopes operate on the same basic principle: conservation of angular momentum of a spinning mass. For a discussion of the dynamic theory of a basic mechanical gyroscope, see Crandall<sup>3</sup>. By measuring the torques and forces generated as a gyroscope moves, the rotational motion of the gyroscope can be deduced. Different gyroscopes accomplish these measurements in different ways, depending on the application and accuracy grade of the sensor, but all give a measurement of the rotation of the sensor.

There are two significant disadvantages to using mechanical gyros. The first is that they are relatively expensive to produce, especially the highest accuracy varieties. The high precision components and accurately machined parts used inside these gyros are inherently expensive to produce<sup>4</sup>. Though great effort has been expended to cost-reduce these parts, the parts are still difficult to manufacture and remain an impediment to cost-reducing mechanical gyros. In addition, the electronics and sensors in the gyros add expense due to their high accuracy and low noise requirements.

Another drawback of mechanical gyros is that they contain moving parts which are subject to failure over time. For example, a bearing may wear out, or a part of the structure may fatigue and break. In these cases, the gyroscope would become useless and would have to be replaced. On vehicles such as satellites, this is not easy and could render the satellite useless. If moving parts could be eliminated altogether, these problems could be avoided.

---

<sup>2</sup> Nauck, LCDR M. H. "Fiber-Optic Gyroscopes. History, Theory, And Application To Naval Systems." Multi-Redcom Technical Training Session, 1997

<sup>3</sup> Crandall, Karnopp, Kurtz, Pridmore-Brown. Dynamics of Mechanical and Electromechanical Systems, Robert E. Krieger Publishing Company Inc., FL 1982.

<sup>4</sup> Nauck, LCDR M. H.

Optical solid state technology has been shown in the last few years to be a viable substitute to the traditional mechanical technology used in gyroscopes. These solid state gyros incorporate no moving parts, relying on light traveling through an optical pathway to detect rotation. There are several ways that the optical pathway can be created. Ring Laser Gyros (RLGs) and Fiber Optic Gyros (FOGs) use two of the possible methods. As suggested by its name, the RLG uses a set of accurate mirrors arranged in a ring around which the light can travel. The FOG uses optical fiber to define the light path. For reasons of greater possible accuracy and lower cost, the FOG seems to be the more promising alternative<sup>5</sup>.

FOGs can reach and exceed the precision of current mechanical gyros and can operate under equal, or even harsher environmental conditions. The drawback to date has been the expense of building these solid state gyros. Only recently has the state of technology begun to progress enough to bring the cost of manufacturing the gyros down to competitive levels. Optical fiber has become less expensive and methods of interfacing the fiber with other components in the gyro have become better defined. Likewise, the lasers, which act as the light source for the sensor, have recently become far more affordable.

The main factor currently driving the price of solid state gyroscopes is the manufacturing and assembly time<sup>6</sup>. It can take up to three weeks to produce a working three-axis gyroscope. If this time can be reduced, through automation and other techniques, the cost of a solid state gyro can be brought significantly below that of a mechanical one. Given that they have no moving parts and could be made inexpensively, the solid state gyroscope could prove to be a superior alternative to its mechanical cousin.

---

<sup>5</sup> Herdman, Craig T. "Fiber Optic Gyroscopes." Honeywell Technology Center.

<sup>6</sup> DeFazio, Thomas L. "Development Issues For Quadrupole-Pattern Optical-Fiber Coil-Winding Machinery For Interferometric Fiber-Optic Gyro Manufacture and Automation" Draper Laboratories, 1992



## 1.2. How A Fiber Optic Gyro Works

The basic theory behind the FOG is fairly simple. Consider a long strand of optical fiber that is wrapped into a coil (see figure 1.1). The fiber is wound from its midpoint outwards so that half the fiber is wound counterclockwise around the coil and the other clockwise. The two ends of the fiber will then be located on the outside of the coil as shown in the figure. Light that is in phase is passed through both ends of the fiber coil. If the coil remains stationary, light coming out of the two ends will be in phase. However, if the coil turns along its axis, as indicated in figure 1, light traveling through the coil in the direction of the rotation

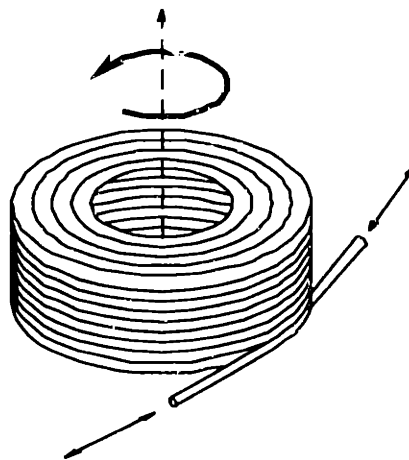


Figure 1.1: A representation of a FOG coil.

will take longer to travel the fiber length than the light traveling against the direction of rotation<sup>7</sup>.

A physical example may prove useful in understanding this concept. Consider two balls that are rolled along a plank of a given length from opposite ends, towards each other at equal speeds as shown in (see figure 1.2). The balls are rolled along the two edges of the plank so that they don't collide. If the plank is held stationary, the balls will take the same amount of time to reach the

---

<sup>7</sup> Lefevre, Herve C. "Fundamentals of the Interferometric Fiber-Optic Gyroscope." Photonetics.

ends of the plank. If, on the other hand, the plank is moved towards one of its ends while the balls are moving, the ball traveling in that direction will take longer to reach the end than the ball traveling in the opposing direction. The time difference between when the two balls reach the ends of the plank is related to the velocity of the plank.

This is a similar concept to that employed in the fiber optic gyroscope except that light takes the place of the balls and optical fiber takes the place of the plank. The primary conceptual difference is that the fiber is wound into a coil so that rotation rather than translation is measured. The light emerging from opposite ends of the coil can be recombined and measured for phase shift. If the coil has experienced rotation, the light traveling in opposite directions will take different times to traverse the length of the coil and will be shifted in phase when they emerge. This shift is directly related to the rotation rate of the coil.

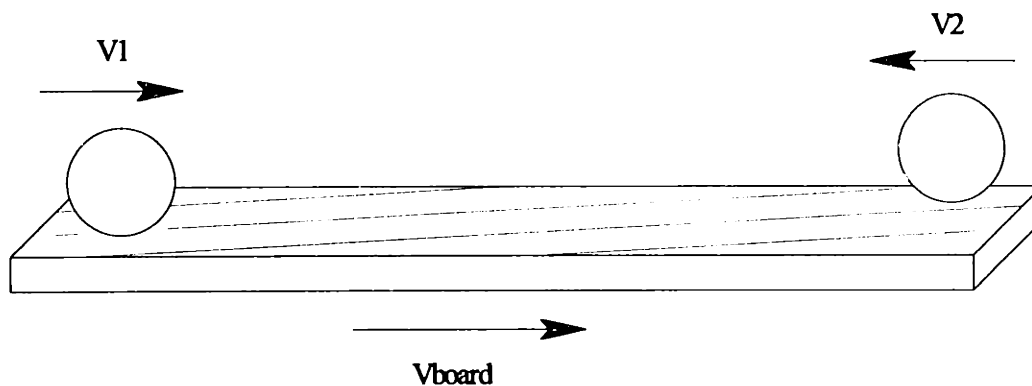


**Figure 1.2. Balls rolling relative to a plank**

In 1914, a French researcher by the name of Sagnac first proposed using this concept of phase shift for measurement<sup>8</sup>. He created a simple device consisting of bright light, a 45° beam splitter, and a ring of mirrors. With this device, he was able to successfully prove the above described concept, which is now commonly known as the Sagnac Effect. His device, called a Sagnac interferometer is shown in (see figure 1.3). The entire device was rotated at a

---

<sup>8</sup> Davis, James Lawrence. "Inertial Rotation Sensing Using a Fiber Sagnac Interferometer," Thesis (Ph.D.), MIT, Department of Electrical Engineering, 1981.

velocity  $\omega$  and the combined light was shown onto a screen. A fringe pattern was seen on the screen which corresponded directly to the rotation  $\omega$ . About sixty years later, in 1976, Vali and Shorthill proposed and implemented the first optical fiber gyroscope<sup>9</sup>. Since then, the technology has grown to the point where FOGs are as viable as their mechanical counterparts.

A few, simple mathematical relations are enough to entirely describe the Sagnac effect and relate the relative phase shift of the light to the rotation rate of the coil. When the light beams emerging from the coil are recombined, the beams will interfere, and there will be a power loss corresponding to the degree of phase shift between the beams. This relationship is described by the following equation:

$$P = \frac{1}{2}P_0(1 + \cos \Delta\phi)^{10} \quad (1)$$

where  $P$  is the detected output power,  $P_0$  is the power input to the coil, and  $\Delta\phi$  is the phase difference. By measuring the power output with a photodetector, and knowing the power input, the phase shift can be deduced. The rotation rate is related to the phase shift of the coil through the following relation:

$$\Omega = \frac{2\pi LD}{\lambda_0 c} \Delta\phi^{11} \quad (2)$$

where  $\lambda_0$  and  $c$  are the free-space wavelength and velocity of light, respectively,  $L$  is the length of fiber, and  $D$  is the diameter of the coil.  $\Delta\phi$  is the phase shift, as per equation 1, and  $\Omega$  is the rotation rate of the coil. Thus, from a measurement of the power output from the recombined beams that have passed through the sensing coil, a measure of the rate of rotation of the coil can be made. The majority of fiber optic gyroscopes use this basic concept in sensing rotation.

---

<sup>9</sup> V.Vali and R.W. Shorthill. "Fiber Ring Interferometer," Applied Optics, 1976. p. 15, 1099.

<sup>10</sup> Ibid

<sup>11</sup> Ibid

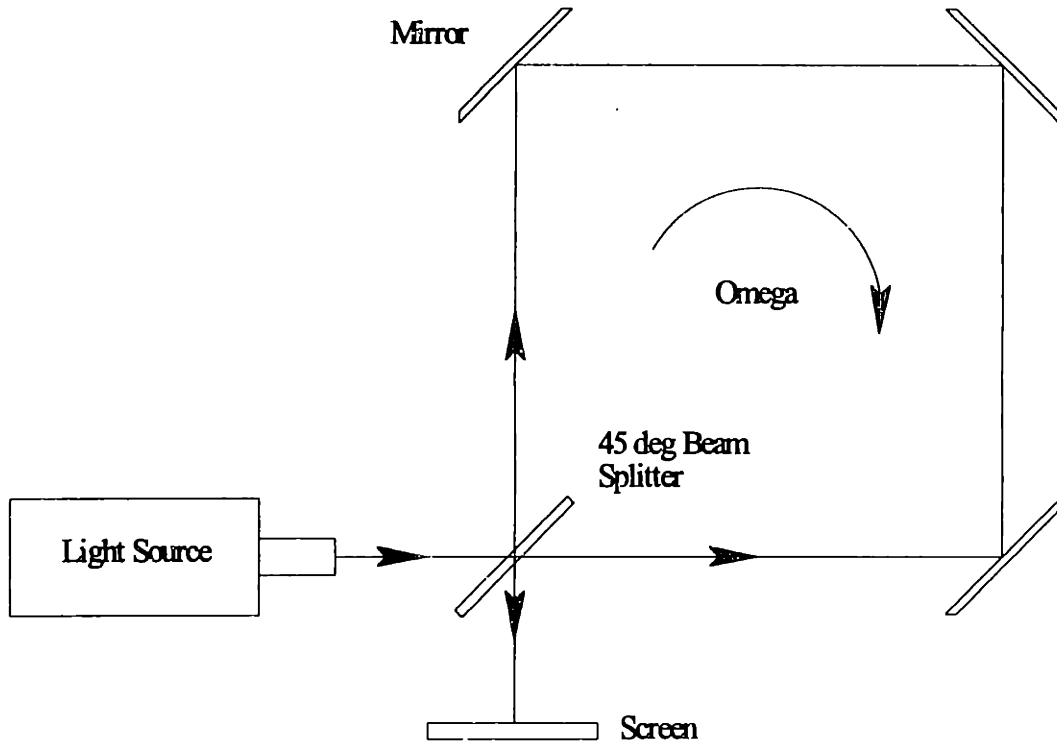


Figure 1.3: The Sagnac Interferometer

### 1.3. The Components Of A FOG

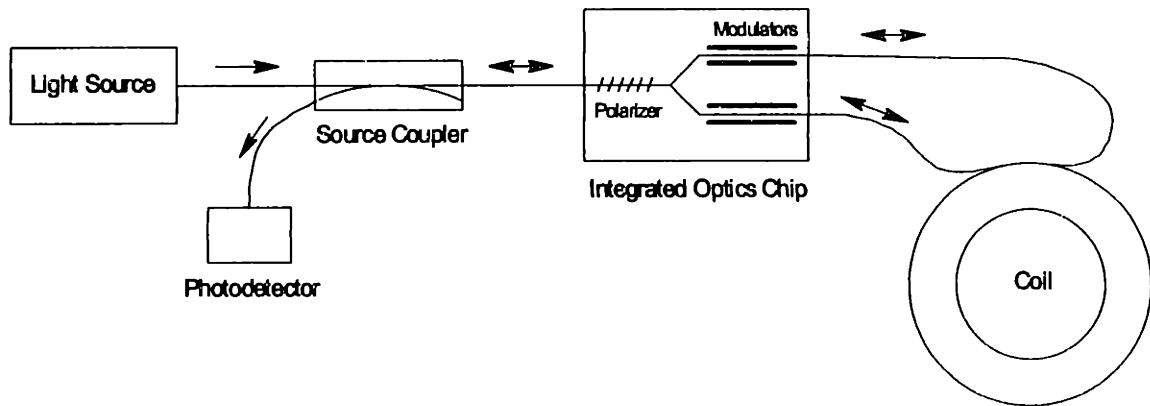


Figure 1.4. Diagram of Fiber Optic Gyroscope.

Each of the major components of the gyro can be seen in figure 1.4. These components are the light source, source coupler, integrated optics chip (IOC), coil, and photodetector. Each of these components will be discussed below.

### **1.3.1. The Light Source**

The laser is the light source for the gyro. It provides a constant, coherent beam of light that drives the Sagnac effect. Laser diodes are commonly used in FOGs as they are small and exhibit adequate performance. To meet power requirements, these diodes are coupled with a rare-earth doped fiber that acts to amplify the beam. Together, the diode and doped fiber generate the light beam for the gyro.

### **1.3.2. The Source Coupler**

The source coupler serves the basic function of routing the returning light beam from the coil to the photodetector. The coupler also allows for light to travel from the light source towards the coil. In order to accomplish this, two fibers are fused together along their sides and are reinforced for durability. A fiber lead coming from the laser attaches to the end of one of the fibers and the lead from the coil is attached to the other end of the same fiber. The photodetector lead is attached to the end of the other fiber in the coupler. Finally, the last coupler fiber end is left unattached.

### **1.3.3. The Integrated Optics Chip (IOC)**

In order to split the light beam as it enters the coil, a special beam splitter must be used. This splitter also serves the purpose of recombining the two light beams emerging from the coil. While there are various forms of splitters available, a special type called an Integrated Optics Chip (IOC) is commonly used in gyroscopes. Light pathways are formed within a specially designed chip

to efficiently guide the light between the single fiber and the two coil fiber ends. The IOC looks much like a rectangular piece of glass with the fibers attaching to the shorter ends of the rectangle. Where the IOC becomes unique from other beam splitters, is in the phase modulator contained within the IOC. The modulator acts to modulate the frequency of the light beam which aids in the operation of the gyro and significantly increases their accuracy. The IOC also acts to polarize the light beams which also increases operating efficiency.

#### **1.3.4. The Photodetector**

In order to detect the phase shift in the light emerging from the coil, a two different types of photodetectors are commonly used. Both the PIN and Avalanche photodiodes operate on the principle of photons of light creating free electrons upon contact with a specially designed surface. The surface is connected to an electrical circuit and the current is measured. By the nature of the interaction, current is proportional to light intensity; thus, providing a measure of the phase shift in the light beams.

#### **1.3.5. The Coil**

The fiber optic coil has the most bearing on this document of all the FOG components as the goal of the project was to develop a coil winding machine. Therefore, the many unique features of the coil will be covered in much more detail than the other components. Many of the references cited thoroughly discuss the other FOG components.

Among the many factors contributing to FOG performance, the quality of the sensing coil is one of the most important. The Sagnac effect relies on the fact that the shift in the phase of the light beams is due solely to the rotation of the coil. However, there are other factors that can create this shift. These factors act to change the local index of refraction of the optical fiber. Changes in the index of refraction will locally change the velocity of light in the fiber. And,

changes in the velocity of light could lead to an apparent shift in phase of the two propagating beams. Temperature variation and stress are the two most significant factors that can create these local changes in index of refraction. Coils are rigorously tested under thermal variations and severe vibration when determining the performance of the coils. A common measurement called drift, usually expressed in degrees per hour, corresponds to the rotation sensing error over time. The best coils have better than .0005 deg/hr of drift, termed strategic grade, the next best have .05 deg/hr, termed navigation grade, and the crudest coils have 1 deg/hr, termed tactical grade. With current technology, tactical grade coils are relatively easy to wind. Navigation grade coils are commonly produced but at high costs and at low production rates. Strategic grade coils can be wound but require a great deal of care and are highly labor intensive. To be used for navigation applications, the gyros must be of navigation grade or better to avoid excess error in the sensor readings.

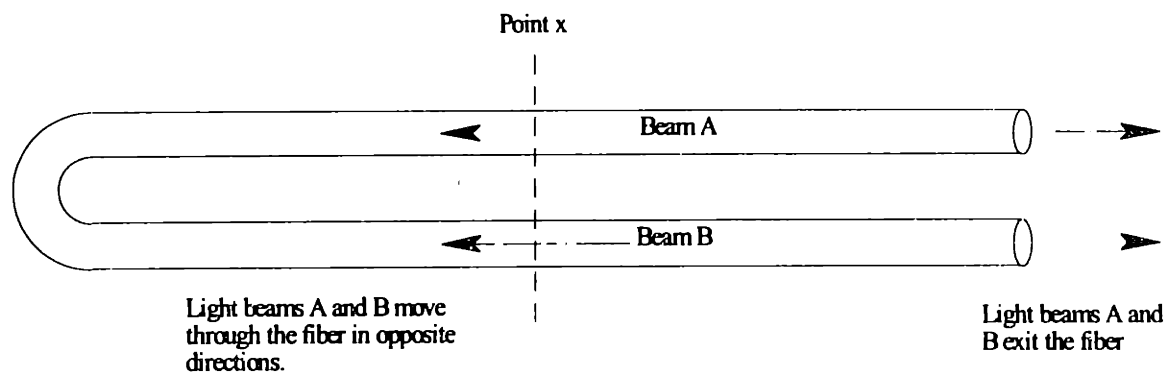


**Figure 1.5: Demonstration of symmetry concept.**

Different approaches can be taken to deal with these environmental variations. The coil could be carefully insulated and thus protected from thermal and vibration effects. This approach has been tested and works quite well. However, this type of insulation is bulky, and it is desirable to keep the gyroscope as small as possible in most applications. With this in mind, the problem can also be addressed by altering the winding of the coil. The approach has been to create patterns of winding that achieve maximum symmetry within

the coil. What is meant by symmetry in this case is that points in the fiber equidistant from its midpoint are located adjacent to each other within the coil. By doing this, the light traveling in opposite directions will see the same variations at the same time as it passes through the fiber. Hence, any change experienced by one of the beams should be virtually identical to that of the other, and when recombined, the two propagating light beams should only reflect phase shifts due to rotation.<sup>12</sup> Figure 1.5 provides a clarification of this concept. Consider that the fiber is only folded over once, as shown, rather than wound into a coil. If a temperature or vibration disturbance occurred at point x, light beams A and B traveling in both directions would experience this disturbance at the same time and at the same distance from each end of the fiber. Thus, the light beams emerging from the two ends of the fiber should exhibit the same phase shift caused by the disturbance. The two beams would therefore emerge in phase.

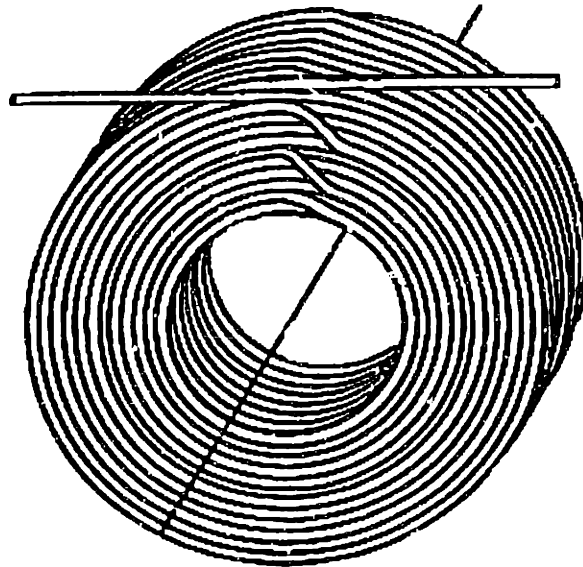


**Figure 1.6: A fiber optic gyroscope coil.<sup>13</sup>**

---

<sup>12</sup> Baron, Heidelberg et al. "RPM Measuring Device Utilizing An Optical Fiber Coil and Winding Method For Making The Coil" United States Patent, Patent No. 4,781,461

<sup>13</sup> Litton Systems Canada Ltd. "Fiber Optic Sensing Coil," United States Patent, Patent No. 4,793,708, Dec. 27, 1988.



To wind the fiber with such symmetry, the coil must actually be wound from the inside out. More specifically, winding must start with the midpoint of the fiber and proceed outwards towards the fiber ends. Half the fiber will be wound clockwise around the coil and the other half counterclockwise. This will lead to a coil that has the fiber ends exiting the coil on the outside diameter and in opposite directions, as shown in figure 1.6. To actually wind a coil this way, a length of fiber must first be wound half onto one supply spool and half on another, with the midpoint of the fiber between the supply spools.<sup>14</sup> During winding, the supply spools will pay out fiber onto the product spool, which holds the coil. At any one time during a wind, one supply spool will be actively paying out fiber while the other is locked in place, rotating as the product spool rotates. An example sequence of winding is shown in figure 1.7. Note the two supply spools containing half the fiber and the inactive and active positions for each spool.

---

<sup>14</sup> Litton Systems Canada Ltd. "Fiber Optic Sensing Coil," United States Patent, Patent No. 4,793,708, Dec. 27, 1988.

Keeping in mind that coils are wound in this inside-out manner, there are various patterns of fiber placement that can result in coil symmetry, some exhibiting better results than others. The most basic of these patterns is termed the “quadrupole.” Figure 1.8 depicts a cross-section of a coil wound with this

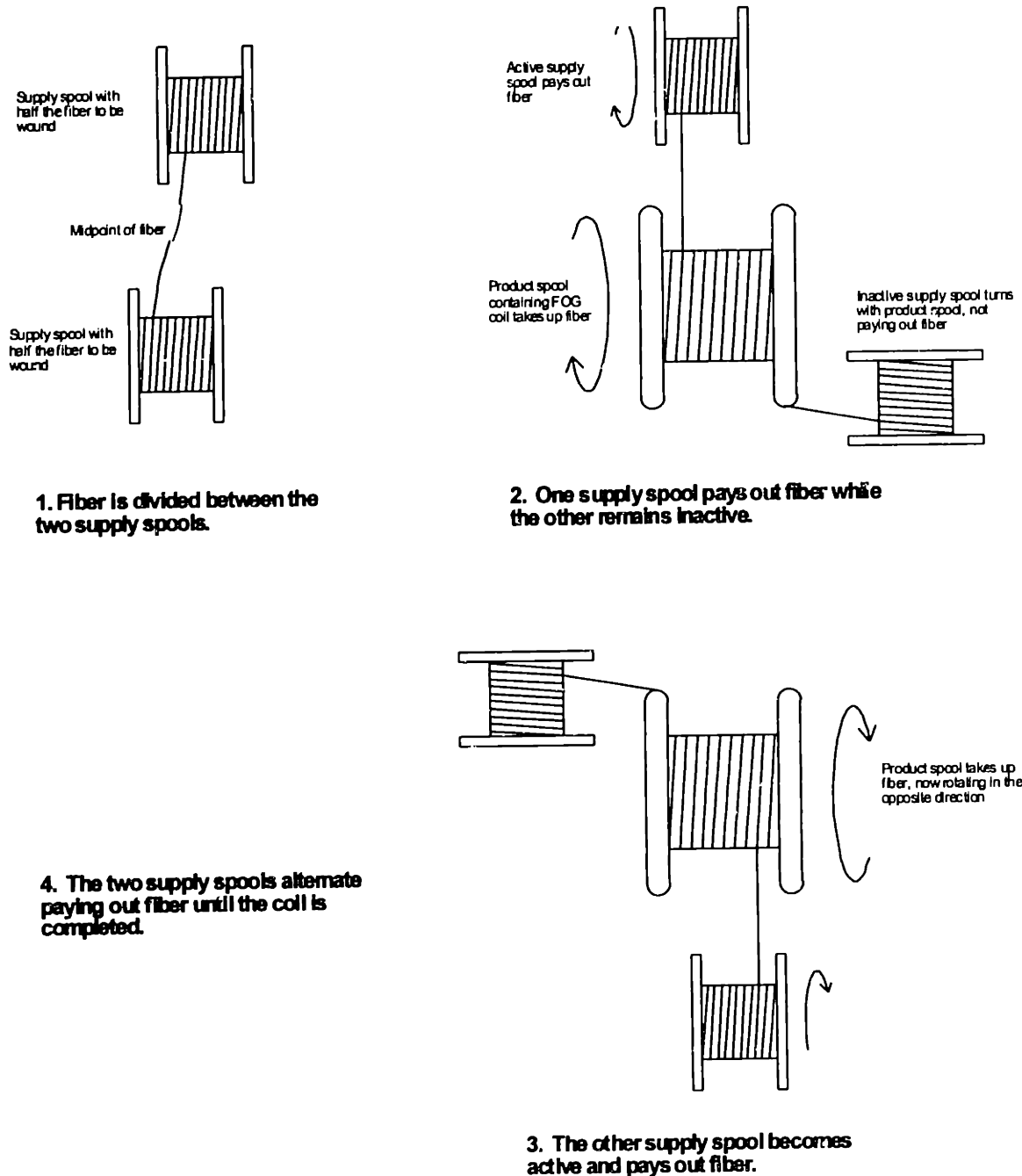
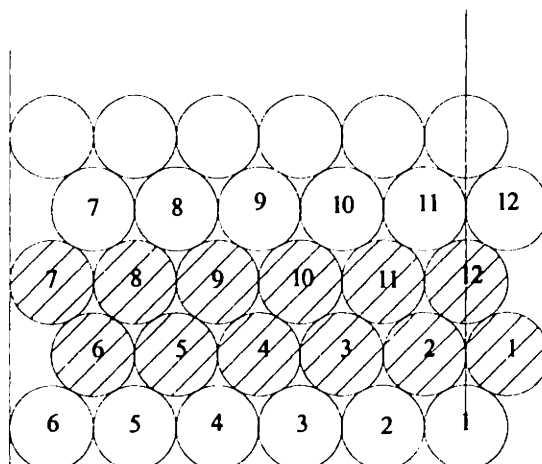


Figure 1.7: Winding Sequence



**Figure 1.8: Quadrupole Cross Section**

pattern. The white circles indicate fibers wound in one direction and the black indicate those fibers wound in the other. By examination, it can be seen that corresponding turns of the black and white fiber are in very close proximity within the fiber pack. Also note that fibers are placed into the grooves formed by the underlying layer of fiber. This helps in guiding the fiber and achieving a tighter pack. Variations on this basic pattern yield better symmetry which have been shown to improve coil performance. Coils that are wound without attention to this symmetry exhibit far inferior performance.

Regardless of what pattern is used in a coil, local areas of stress within the pack caused by poor winding can be quite detrimental to coil performance. Examples of poor winding would be lumps and voids within the fiber pack and severe variations in tension. Essentially any characteristic of the coil wind that can cause varying pressures on the fibers can lead to variations in index of refraction. What this means is, to obtain optimum performance, the coil must be wound as evenly as possible with minimal variations in tension. Not only must the tension be consistent, it must be low enough not to cause undue stress in the glass of the fiber. It has been shown that coils wound with low tensions yield

superior performance<sup>15</sup>. These facts lay out the most basic of restraints for any coil winding machine. The machine must be able to accurately place fibers during a wind and it must be able to accurately control tension.

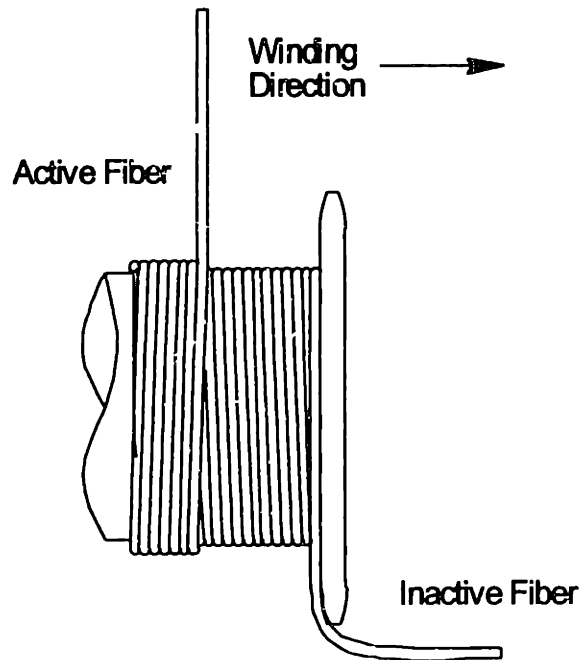


**Figure 1.9: Helical Winding Technique**

To aid in achieving a consistent wind throughout the coil, a specific winding technique is commonly employed. The simplest way to wind is to place the fiber in a spiral, or helix, allowing it to traverse across the fiber pack naturally as it is wound onto the coil. Fiber follows the groove formed by the previous layer when traversing in the direction of the helix and crosses those grooves when traversing against the helix as shown in figure 1.9. The problem is that the fiber can jump to the next groove at any location around the circumference of the coil. The circumferential location of the fiber can differ from turn to turn. It is easy to see that this phenomenon can cause inconsistency on the current layer, which can only get worse on progressing layers. An example of a cross-section

---

<sup>15</sup> Belsley, Kendall and Smith, Ron. "Exploratory Studies Of Optical Fiber Gyro Coil Winding Automation." Optelecom, Inc.

of a coil wound in this way is shown in figure 1.10. Dark circles correspond to fibers wound in the clockwise direction and light circles correspond to fibers wound counter clockwise. Note the uneven placement of the fibers which can lead to localized stresses. And, these stresses can severely differ from fiber to fiber. Needless to say, coils wound in this way have poor performance.

One alternative is to wind coils in an orthocyclic manner. This winding method was first developed by Phillips Industries in 1962 and is in common use today.<sup>16</sup> With this method, rather than winding in a helix, fibers are wound in

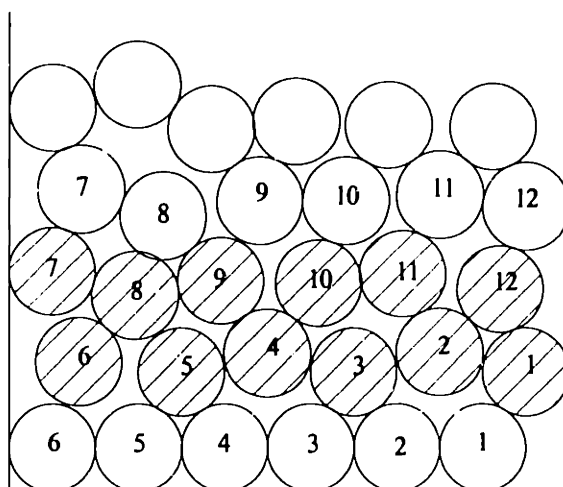


**Figure 1.10: Helical Wind Cross Section**

concentric hoops and cross over to adjacent grooves formed by the under-lying layer in well-defined zones. See figure 1.11 for an illustration of this type of wind. The zone where the fibers cross grooves is commonly termed the "jog zone" and is the only location in the coil where fibers deviate from a straight orientation. Many advantages are gleaned from orthocyclic winding. Local stresses due to crossing over are limited to one small area of the coil. Furthermore, adjacent

---

<sup>16</sup> Lenders, W. L. L. "The Orthocyclic Method of Coil Winding," Phillips Technical Review, Volume 23, October, 1962, No. 12. p. 365-404.

fibers in this zone will experience similar stresses at the same locations, and because of the symmetry of the coil, this should not effect the relative phase of the light emerging from the coil. Another benefit is that the majority of the circumference of the coil is wound with an even, closely packed profile much like that shown in figure 1.8. Any inconsistencies should then occur in the tight jog zone. Also, the close pack inherent to the orthocyclic wind has been shown to improve the thermal variation and vibration resistance of the coil.

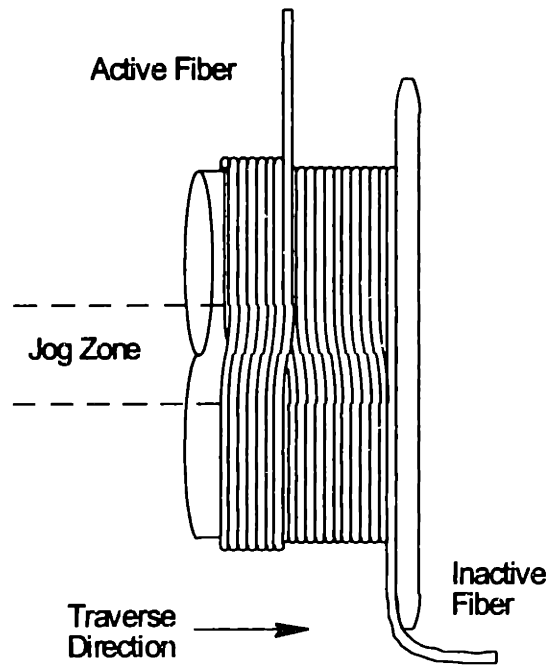


Figure 1.11: Orthocyclic Winding

### 1.4. The Drive to Automation

In review, for optimum performance, coils are wound in specific patterns in an orthocyclic manner, starting from the center of a length of fiber and winding outwards to the ends. Fiber placement and tension control are known to be important factors in winding a high performance coil. Any machine that is created to wind coils must be able to deal with many variables. It must accommodate the different patterns and allow for orthocyclic winding. It must be

able to very accurately guide fiber and maintain a constant, low tension. One of the greatest challenges is to be able to wind an entire coil with few or no errors. An error is considered any place in the coil where there is a deviation from the pattern, such as a gap. These errors can degrade the performance of the coil produced.

The current state of production is generally semi-automatic, requiring the presence of an operator. The operator monitors the winding of a coil at all times and interferes when an error occurs. Generally, the operator would use a small tool to manipulate the fiber into the correct place. With the current machines and control, these errors happen quite often and greatly extend the winding process. In addition, with most machines the operator must switch the two supply spools manually between their active and inactive positions (see figure 1.7), which takes time and adds a risk factor. Any time the operator must interact with the fiber, there is the possibility of damaging, or even breaking, the fiber. Winding in this manner has resulted in relatively long winding times, up to a week in many cases, and also yields a significant rejection rate.

There is a definite opportunity in the industry for improvement of the coil winding process. If FOGs are to become competitive, the cost of coils must be reduced without sacrificing quality. To accomplish this goal, winding times must be decreased and rejection rates lowered. This implies that operator intervention must be removed from the process, or at least minimized. In the past, that wasn't a feasible possibility as the process of coil winding was poorly understood and it was difficult, if not impossible, to design a machine that could account for all the variables. Through experiments that have been completed in recent years, the process of coil winding has become somewhat better characterized and it has become easier to predict the behavior of the fiber during a wind. These experiments have also made it possible to place more accurate specifications on parameters that were previously loosely defined. Along with this improvement in process understanding, the state of technology has greatly improved, facilitating the development of machine automation.

Given that the process and technology are in place, and the opportunity is present, there is a definite drive to automation. It is now possible to design and build a machine that can automatically wind coils and, in the end, reduce the cost per coil. This document describes the design and development of such a machine. The additional refinement of the process necessary to make the automation possible will also be presented. In chapter 2, an overview of the design process will be given, and some aspects of the top level design will also be discussed. Chapter 3 will discuss in detail the design and development of some of the subsystems of the machine. Chapter 4 will discuss in detail the design and development of the supply unit sub-system (see chapter 2) which played a disproportionately large role in the coil winding machine. Chapter 5 contains a discussion of the software automation scheme developed to control the machine. Finally, a discussion of the success of the machine and future recommendations will be presented in chapter 6.



## **2. Overall System Design**

This chapter will first cover the customer driven goals of the automated coil winding project. The design process followed in the development of the winder is then detailed. And, finally, a few key overall design choices are detailed and explained.

### **2.1. *The Customer***

Development of the automated coil winding machine was funded by an American company with aid from the federal government, to be referred to together hereafter as the Customer. In early 1995, the Customer approached the Manufacturing Institute at MIT (MIT/MI) with the automated coil winding project. The primary goal of the project was to cost reduce the winding of the fiber optic sensing coil used in FOGs. The current cost of FOGs derives heavily from the manual labor involved. Thus, the MIT/MI's main role in the project was to develop an automated coil winding machine. Two graduate students, Brian Sonnichsen and Stephen Lin, were placed onto the project and given responsibility over the design of the winding machine under the supervision of Dr. Andre Sharon, Director of the MIT/MI.

Specifications for the machine were drawn up early in the project. The precise details of these specifications cannot be revealed for reasons of confidentiality. The Customer desired a certain manufacturing throughput several times higher than conventional manual winding techniques. To achieve high quality coils winding errors were to be minimized and the tension on the fiber during winding was to be under tight control. The machine also had to meet various levels of flexibility. These included flexibility in the size and length of fiber it could wind, in the nominal winding tension, in the size of mandrel wound onto, and in the particular pattern to be wound. This flexibility would allow the

Customer to wind a variety of coils covering the range of performance grades to suit different applications.

## ***2.2. The Design Process***

To accomplish this task, MIT/MI followed a well defined design process. The process began with a review of existing technologies to learn the current state of the art in fiber optic coil winding. This review included reading through many articles over the last decade on coil winding to learn from the successes and failures of past experiences. The review also included site trips to three existing fiber optic winding centers across the United States to see actual production and experimental winding machines in action and to talk with the engineers and technicians involved first hand. In a meeting with the Customer immediately following these reviews it was determined that the state of the art in coil winding was not a sufficient foundation to begin design of an automated winding machine. The MIT/MI proposed, and the Customer agreed, that a test-bed winding machine should be built on which to conduct winding experiments. The goal of the test bed would be to provide a flexible vehicle for conducting winding process experiments and proving out designs for the final automated winder. It was believed that this test-bed would be essential for the success of the project.

The design of the test-bed itself began with brainstorming sessions both individually and as a group with periodic reviews with the Customer to insure the design was headed in an approved direction. Design constraints on the machine were taken from the specifications laid out by the customer as well as from information learned during the review of existing technologies. Design concepts were evaluated against the design constraints and each other and eliminated accordingly. Foam models followed detailed sketches of the more promising concepts. Detailed design of the test-bed winder began following a final design review with the Customer. A picture of the test-bed winder can be seen in figure 2.1.

Once the test-bed was built various experiments were run. The experiments served to prove out both hardware issues and process issues. For example, these experiments included determining the best mandrel and flange configurations for the product spool on which to wind the coil, how to wind fiber up against the flanges, how best to achieve tight tension control on the fiber while winding, how best to monitor the winding to detect errors, etc... Coils of three different pattern types were wound on the test-bed to prove out the overall concept for the final machine.

Design on the final machine began immediately after finishing experiments on the test-bed. Since the test-bed was very successful in its task, many of the issues in designing the final machine were related to automating those parts of the test-bed which were performed manually, and improving on the problem areas of the test-bed which were unable to be corrected at the time. For example, linear slides and swivels had to be replaced by motorized linear stages and rotary tables, and the mounting of the product spool had to be redesigned to eliminate runout while winding. The design process used during this period followed the same structure as when designing the test-bed machine. In some cases, working prototypes of competing ideas were constructed for evaluation.

The actual design of the test-bed won't be covered in this thesis. However, much of the design of the test-bed was used as a starting point for the design of the automated machine. Most of the process experiments discussed were performed on the prototype. This thesis will instead cover the design and development of the final automated winding machine. Many of the subsystem designs and various process development issues will be covered in another document by Brian Sonnichsen entitled "The Design Of An Automated Fiber Optic Coil Winder."

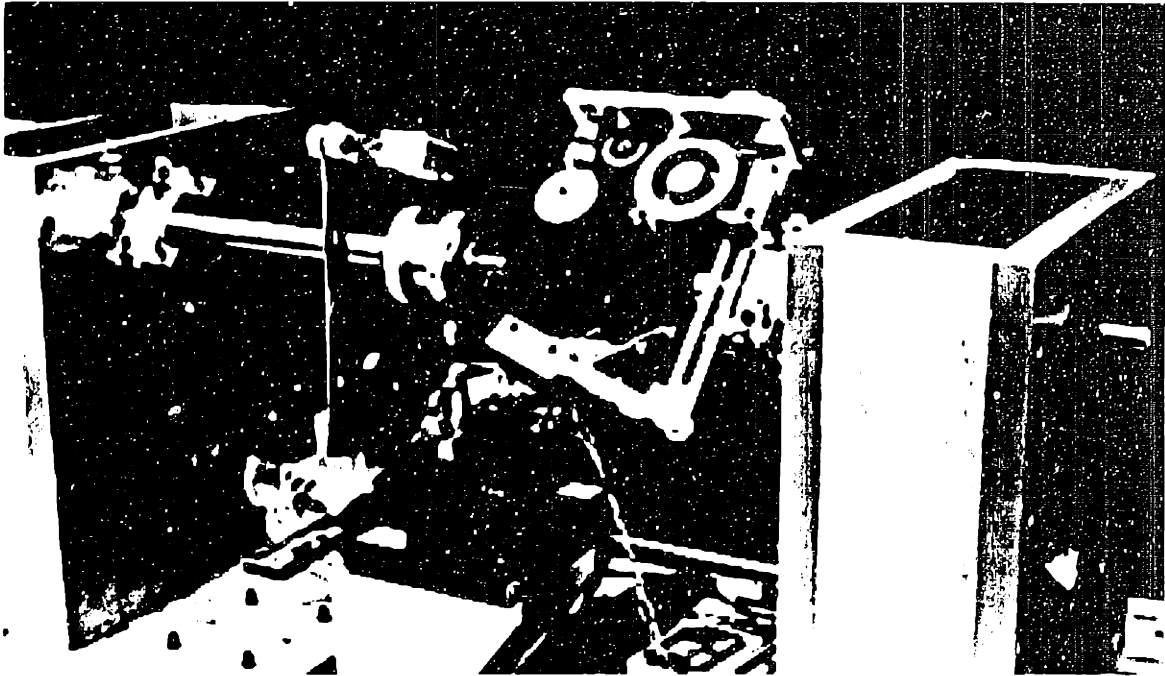
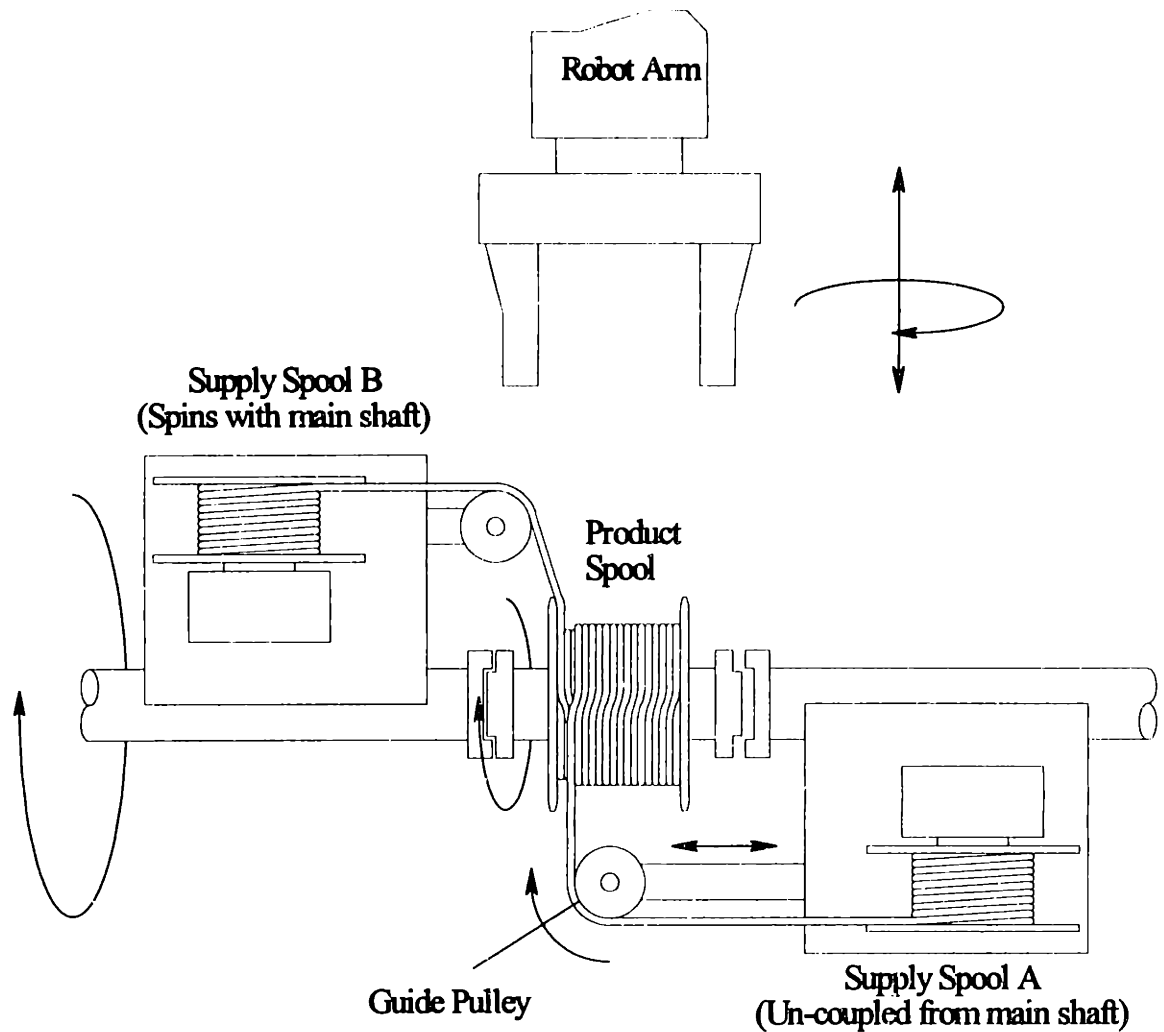


Figure 2.1: Test-Bed Winder

### ***2.3. Basic Requirements For Winder Topology***

In Chapter 1 the characteristics of a coil including one example pattern (i.e., the quadrupole) were detailed. In order to determine what shape an automated coil winding machine must take, the process steps in winding a full coil must be carefully considered for each pattern to be wound. The choice of patterns to be wound greatly influences the topology of the machine. Many of the existing machines surveyed during the design process were constructed with the quadrupole pattern in mind. Figure 2.2 shows a basic machine layout for winding a quadrupole coil. In this configuration both supply spools lie along the main shaft either rotating with it or remaining stationary depending on the state of two mechanical clutches. One supply spool remains clutched to the main shaft while the other pays out fiber onto the product spool as the product spool rotates. A guide pulley able to move laterally along the length of the product spool aims the fiber towards the proper location on the coil.



**Figure 2.2: Basic layout for a machine design to wind a quadrupole coil**

The quadrupole is considered one of the easier patterns to wind. One reason is that at all times during the wind each supply unit remains on its respective side of the product spool. Figure 2.2 shows supply spool A as it nears the end of a layer winding from right to left. The following layer would also be wound from supply spool A as it traverses back to its side of the product spool. Subsequently, supply spool B would be used to wind two layers first from left to

right and then right to left. This alteration continues until the coil is finished. Thus, the fiber from the two spools never have to cross each other.

Now, imagine that at the point in winding shown in figure 2.2 that the next layer was to be wound using supply spool B. This would, in fact, be impossible as the fiber would not be able to wind directly onto the product spool without first colliding with the fiber from supply spool A. This crossing of fibers on the same layer is a feature of a second winding pattern and also certain variations of a third pattern both of which will not be named or described in detail for reasons of proprietary nature.

After taking into consideration all the winding patterns desired by the Customer the basic requirements that the winder topology had to satisfy were determined. Each supply spool must be able to be placed on either side of the product spool and rotate with it while the other supply spool pays out fiber. Figure 2.3 illustrates these four basic requirements. Figure 2.3a shows supply A paying out fiber while supply B rides along on the left side of the product spool. Figure 2.3b shows the same only with supply B riding on the right side of the product spool. And, Figures 2.3c and 2.3d show supply B paying out fiber while supply A rides on either side of the product spool.

Looking again at the quadrupole winder in figure 2.2 it can be seen that the machine by itself can only satisfy two of the four basic requirements because it locks each supply spool to a particular side of the product spool. However, there is a way around this limitation. It is possible to equivalently move each supply spool to the other side of the product spool by keeping the supply spools stationary and instead flipping over the product spool itself. This technique has been proven to work manually by a subcontractor to the Customer. Figure 2.2 shows a proposed robotic arm which could perform the task of flipping over the product spool. The difficulties of this method in achieving the two remaining requirements include the design of such a mechanism to grasp the product spool, de-couple it from the main shaft, flip it over, reattach it to the main shaft,

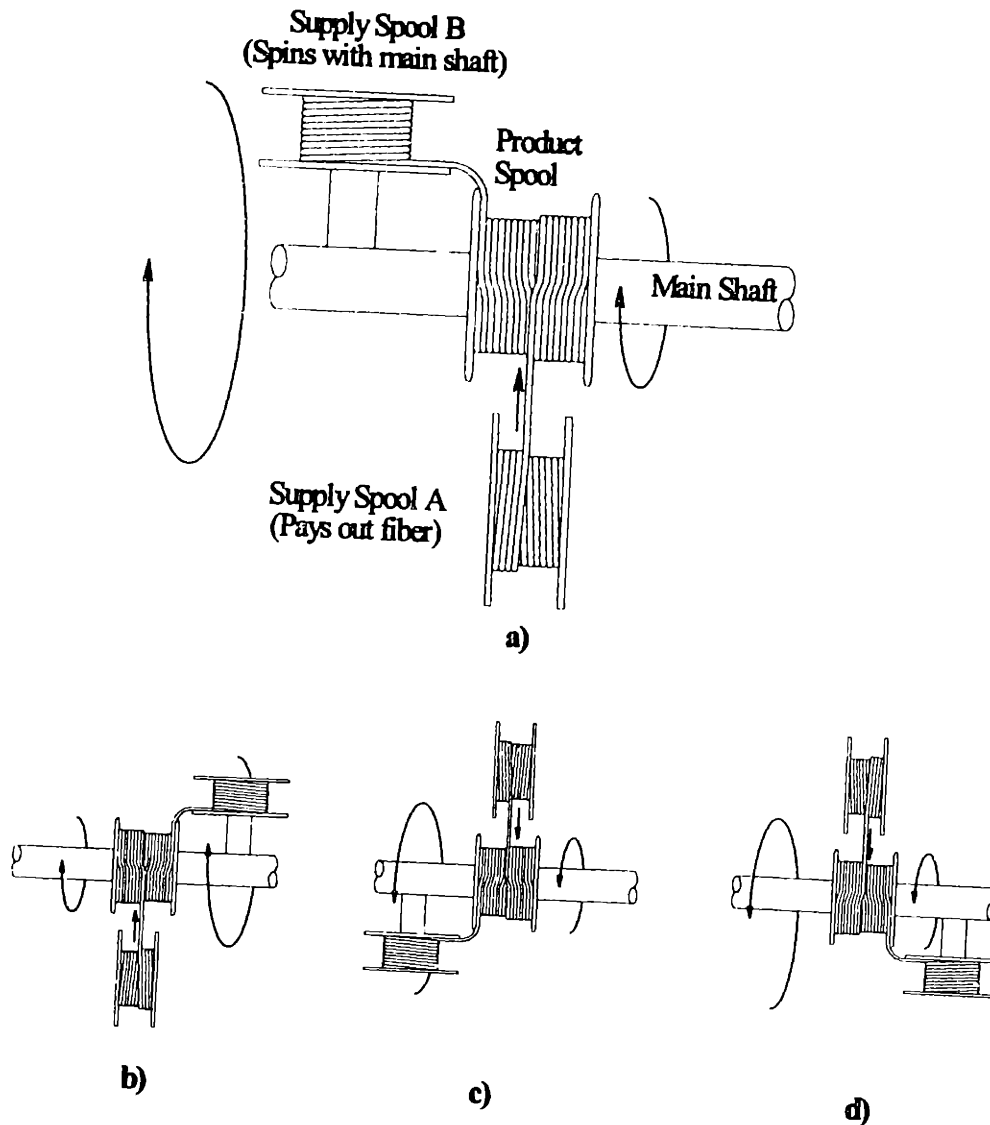


**Figure 2.3: Four basic requirements for winding all the patterns desired by the Customer.**

and then retract so as not to interfere with the winding. In addition, the act of performing this flip induces a half-twist into the fibers coming from both supply spools. Such twists can potentially affect the performance of the gyroscope the coil is placed into. Thus, this basic topology where both supply spools are tied to a particular side of the product spool was discarded as a possible basis for the automated winding machine.

The only remaining topology determined to satisfy all the basic requirements keeps the product spool fixed and instead moves the supply spools

as shown in figure 2.4. The difficulty here lies of course in actually moving the supply spools into these various locations without losing control of the fiber. The next sub-section describes in more detail the design choices considered and ultimately the design chosen.

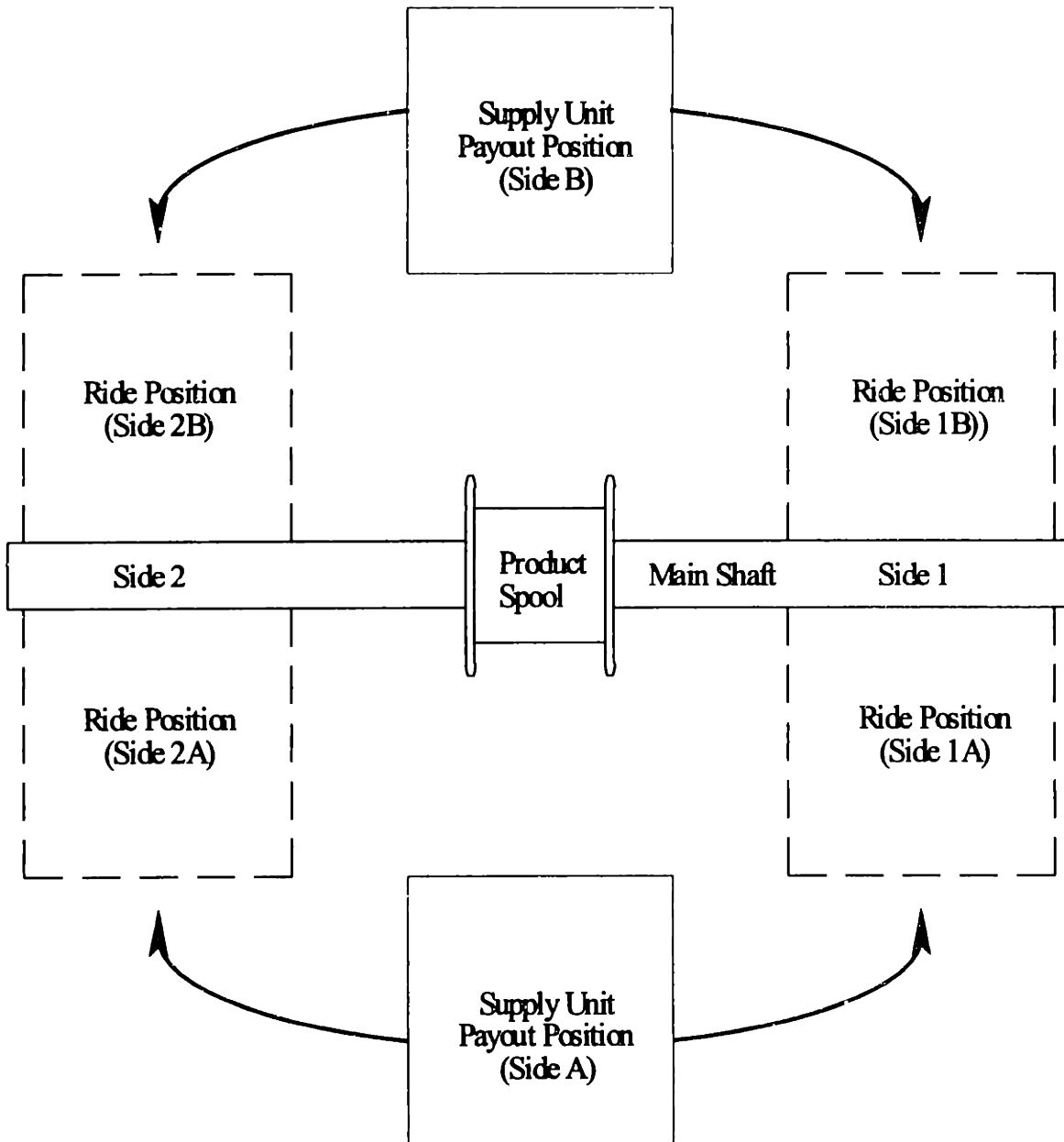


**Figure 2.4: Each supply unit must be able to occupy two ride positions and one payout position to satisfy the four basic requirements.**



## **2.4. The Supply Unit Concept**

Once it was decided that the product spool would remain fixed while the supply spools moved, a method for achieving this had to be chosen. There are two basic approaches to this task. The first approach seeks to minimize what is moved around by only moving the supply spool itself. In the second approach everything necessary for paying out fiber from a supply spool and maintaining tension on it is moved from side to side.

During the survey of existing machines an experimental winder was seen on site at a subcontractor to the Customer's facilities which satisfied the four basic requirements discussed and utilized the first approach described. However, this experimental apparatus was manually intensive. The operator was required to first secure the fiber to the product spool so that it would not unravel. Then, he would detach the supply spool from the motor driving it and unthread the fiber from the various pulleys it was routed around. As he performed this, the extra fiber would be wound back onto the supply spool and finally secured to the spool before attaching it along the main shaft.

The main difficulty of this approach is apparent. Not only must some method be found to attach/detach the supply spool to and from its drive system and the main shaft, but another method must also be found to thread and unthread the fiber through its various pulleys. In addition, the fiber must be prevented from simply hanging free without control lest it unwind from the product spool and also become impossible to rethread. Although, this approach seemed reasonable from the point of view of an operator it was clear that automating it would prove very difficult.

There is no reasonable compromise between the two approaches, so the second approach which was to become known as the Supply Unit approach was chosen. The advantages of this approach are many. With all the mechanisms

needed to payout fiber, guide it onto the product spool, and maintain tension on the fiber location on one modular unit suddenly there is only one task at hand. That task is to mechanically and electrically couple and de-couple the entire unit from either side of the main shaft and from its payout position. Figure 2.4 illustrates the three locations *each* supply unit must assume to satisfy the four basic requirements. Chapter 4 will cover the supply unit in more detail.

## **2.5. Fiber guiding**

Another issue affecting several areas of the machine design is the issue of fiber guiding. Fiber guiding is considered fundamental to winding a fiber optic coil as without a good method of guiding the fiber into the proper place on the coil winding errors are likely to occur. Any time a fiber is not placed where it is meant to be according to the pattern, a winding error is said to have occurred. Winding errors are known to degrade the ultimate performance of a fiber optic gyroscope.

Several methods were surveyed or designed for guiding the fiber onto the product spool, each with its own strengths and weaknesses and consequences for the rest of the machine (the supply units in particular). The most rudimentary approach involves simply using a lead or lag angle and the previously wound turn to guide the fiber. Another approach uses a very thin guide wheel to place the fiber onto the coil. And a third approach involves the use of a fiber manipulator. This section investigates the choice of the guide wheel as the final choice for the automated winding machine.

### **2.5.1. Fiber Guiding Requirements**

There are several situations that are encountered during the winding of any given pattern which require a slightly different form of fiber guiding. To be successful the automated winding machine must provide the ability to guide the

fiber satisfactorily in all situations. Figure 2.5 shows the three basic winding situations encountered during a wind. In 2.5a the next fiber turn is being placed adjacent to the previous fiber turn. In figure 2.5b the next fiber turn is spaced out by one fiber from the previous turn. And in figure 2.5c the next fiber turn lies against the flange of the product spool. In this case, the fiber is forced one layer up, but in a similar slightly different situation the fiber can remain on the same layer.

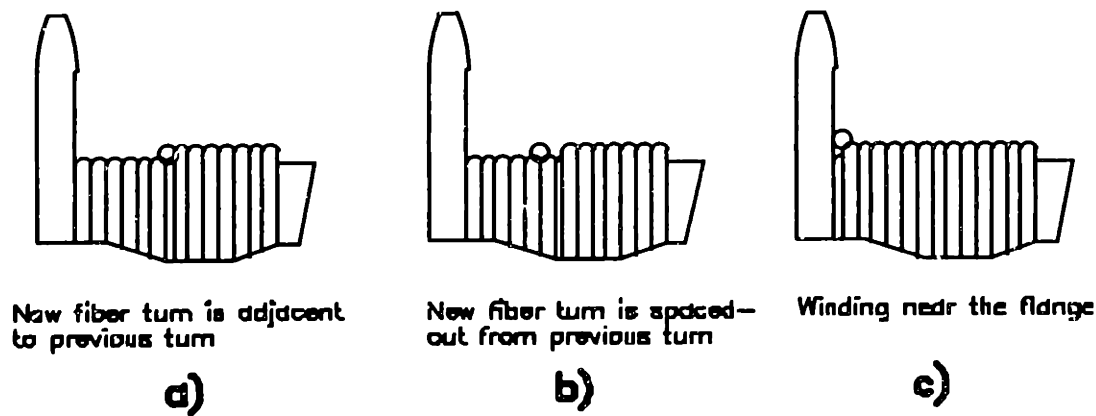
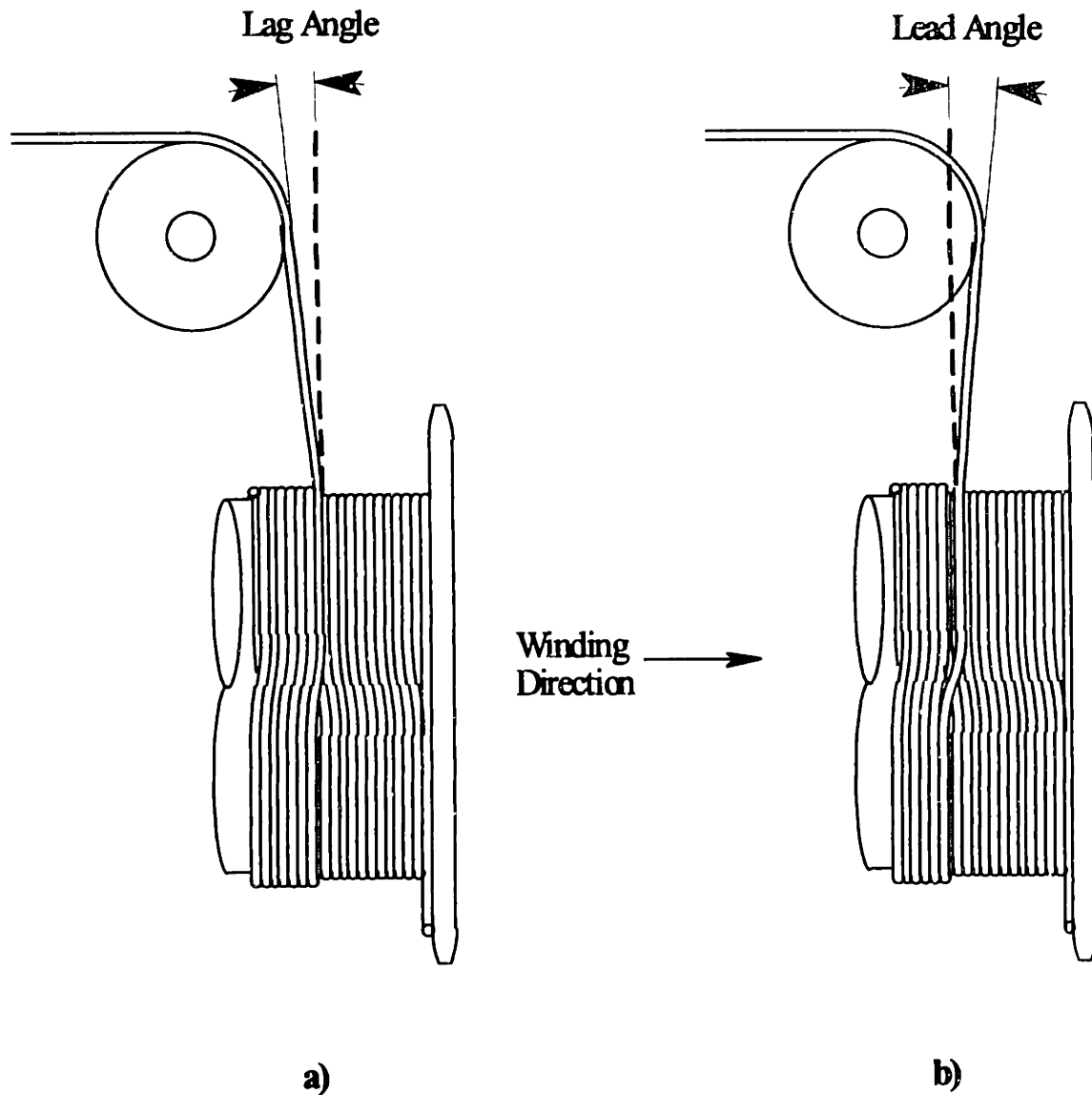


Figure 2.5: Three basic fiber guiding situations.

### 2.5.2. Lead and Lag Angles

Lead and lag angles offer the simplest method for fiber guiding. Figure 26 illustrates the use of both lead and lag angles. In this method the last pulley routing the fiber from the supply spool onto the product spool is used to align the fiber. If the placement of the pulley is located behind the current turn, as shown in figure 2.6a, then a lag angle is being used. Using a lag angle causes the fiber to push lightly against the previous turn, thus using it as a guide for the next turn. If, on the other hand, the placement of the pulley is located ahead of the current turn then a lead angle is being used. This would be useful in trying to achieve a spaced out fiber such as the one shown in figure 2.6b if required by the winding pattern.



**Figure 2.6: The use of lead and lag angles for guiding fiber onto the product spool**

The basic advantage of the purely lead/lag guiding scheme lies in its simplicity. By guiding the fiber from a distance there is no problem of interference of a guiding device with the flanges of the product spool. However, the simplicity of this method also limits its effectiveness. With such little control exercised over the fiber the use of lag angles can sometimes give rise to errors known as “climb” errors. This type of error occurs when a fiber lays down on top of the previous fiber turn rather than by its side. If no lead or lag angle is used the

nature of the orthocyclic wind will tend to cause another type of error known as a “gap” error where the fiber lays down with some space between it and the previous fiber turn, rather than right next to it. A lead angle can be used to purposely induce such a spaced out fiber. However, the control over the placement over the fiber in a typical lead/lag guiding scheme is very limited and historically winding-error prone.

### 2.5.3. Fiber Manipulators

Guiding the fiber from outside the flanges of the product spool is pretty much limited to the lead/lag scheme described previously. The next step in guiding is to attempt to place a fiber manipulator in-between the flanges to constrain the way the fiber lays down onto the coil.

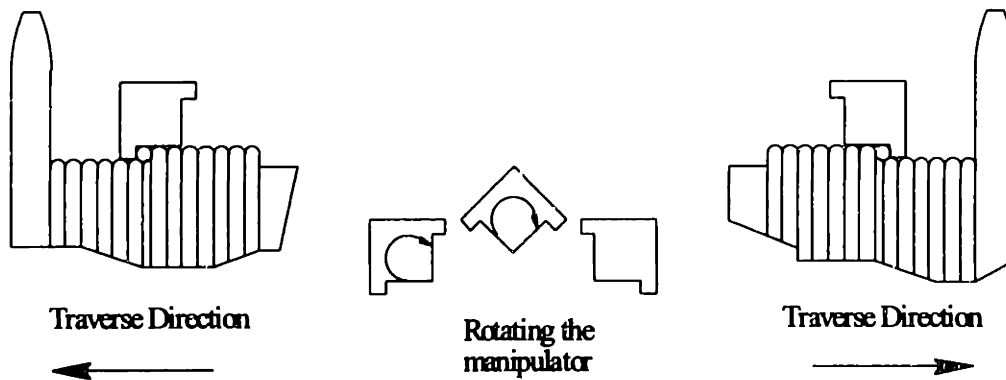
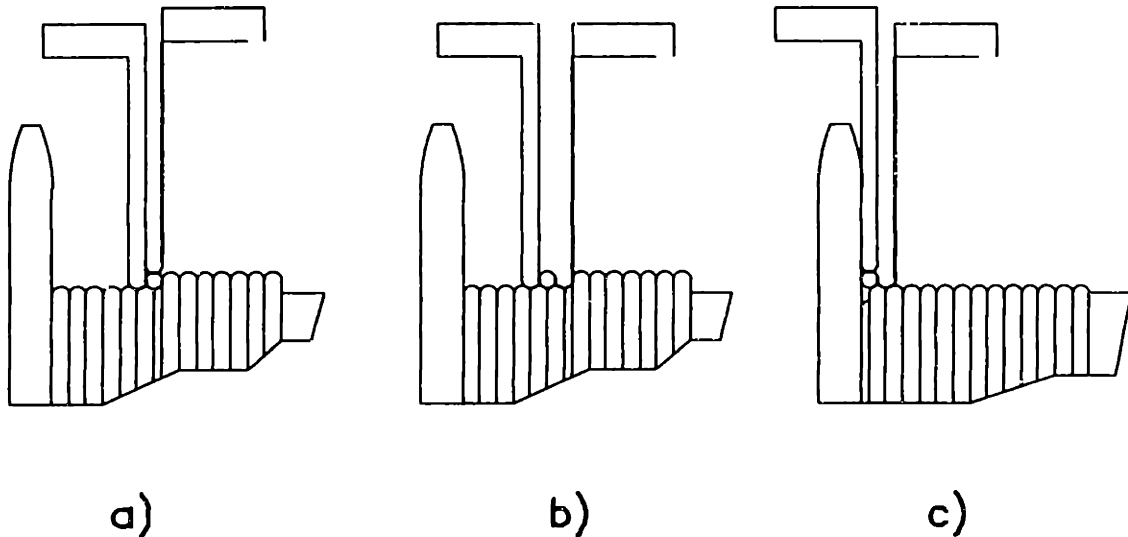


Figure 2.7: Fixed manipulator for constraining fiber placement.

Figure 2.7 shows one such concept taken from a subcontractor of the Customer where a tiny block utilizing a special shape is used to constrain fiber placement to only one possible place. This particular manipulator is capable of constraining the fiber while winding in either direction, although, the manipulator must be rotated to achieve this. The limitations on this form of manipulator is its inability to constrain winding right next to the flange and its inability to create spaced out fibers in a controlled fashion.



**Figure 2.8: Adjustable finger-like manipulator for fiber guiding.**

The concept for the manipulator shown in figure 2.8 was designed by the MIT/MI to address the limitations of the fixed block manipulator. As shown, by adjusting the relative positions of the two finger-like mechanisms this manipulator can be used to constrain the fiber in all three of the basic winding situations depicted in figure 2.8. However, the idea of this manipulator is not without its difficulties. Apparent in the adjustable finger-like manipulator, any such device would have to be very thin to accommodate winding against either flange. Though they appear to constrain the fiber completely, it is unclear that such control would be maintained when switching from one winding situation to another, and it is equally unclear how control could be regained automatically should the fiber get free of the manipulator. The Customer also voiced concerns that the use of tools in continual sliding contact with the fiber might cause micro-cracks in the fiber and thus degrade the final coil's ultimate performance.

#### **2.5.4. The Guide Wheel**

Another form of fiber guiding was borrowed from another subcontractor for the Customer. This method involves the use of a guide wheel such as the one shown in figure 2.9. The mechanism consists of the guide wheel itself which is a

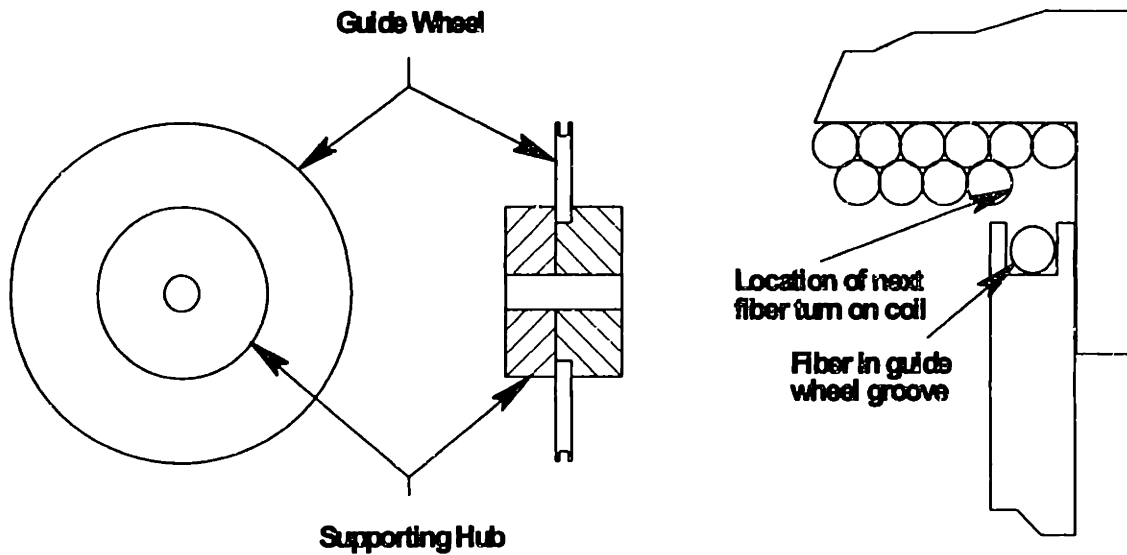


**Figure 2.9: The guide wheel.**

thin disc measuring no more than two fibers wide with a fine groove in its circumference in which the fiber can be placed, and external hubs to support the guide wheel.

The guide wheel's groove constrains the placement of the fiber onto the coil to only one possible place assuming the gap between the guide wheel and the coil is kept small enough. The ultra-thin profile of the guide wheel allows it to accurately place fibers onto the coil across the entire coil except for fibers which lie directly against the flange. The contact between the fiber and the guide wheel exhibit not sliding contact as does the manipulators previously mentioned.

The difficulties associated with the guide wheel result from its manufacture. To insure proper placement of the fiber the guide wheel must exhibit very low axial runout. For instance, a guide wheel having about .002" of axial runout would represent a runout of over 30% of a fiber diameter for the smaller fibers. Placement inaccuracies of this level would lead to many potential winding errors. Achieving low runout guide wheels was found by the mentioned subcontractor to the Customer to require a long and costly machining process.

### **2.5.5. Concept Selection**

Ultimately the guide wheel was chosen as the method for fiber guiding on the automated winding machine. It was clear that a method so simple as the use of pure lead/lag angles to guide the fiber from a distance from the actual coil would not be enough. Although, the manipulator covers more potential winding situations with its ability to adjust its shape to conform to the needs of the situation the issue of sliding contact with the fiber prevented the idea from getting beyond the drawing board. The guide wheel was a proven technology with only one real limitation, it's inability to wind a fiber right up against the flange. However, tests were performed on the test-bed winding machine to confirm the effectiveness of the guide wheel for positioning accuracy. These tests revealed that if the neighboring fiber turns are placed correctly, that the last turn on a layer up against the flange will be self-guided. With these results from the test-bed winder the guide wheel concept was again selected for use on the final machine.

## **2.6. Overall Design Validation**

As mentioned before, a test-bed winder was built prior to the final automated winding machine. The test-bed winder was built not only to perform experiments with the winding process itself but to validate the overall winder design concepts described earlier in this chapter. The test-bed was designed and built employing the supply unit concept allowing the supply units to swap to either side of the product spool. Both supply units used the guide wheel concept to place fiber onto the coil. The test-bed winder was successfully used in several winding experiments to wind test coils anywhere from a few layers of fiber to the tens of layers of fiber which would be required for an actual gyroscope sensing coil. The tests covered all three patterns mentioned and thus validated that the over all system design was flexible enough to meet the Customer requirements for pattern types to be wound. While noting some problems with runout of the guide wheels and of the product spool on the main shaft, the guide wheels were



validated as an effective means for accurately placing fiber onto the coil. Where guiding with the guide wheel was not possible, next to the flanges, it was discovered that a properly wound coil up to that point would provide a pathway for the next fiber turn against the shaft which would be naturally followed by the fiber.

## ***2.7. Process Experiments***

The other main purpose of the test-bed winder was to perform winding experiments to help characterize and define the winding process which was found to be lacking at the beginning of the project. When winding experts had previously been questioned about various issues in winding a FOG coil few answers were received. The process was not well understood. The MIT/MI sought to learn as many of these answers as possible for itself. Many of the questions were answered with experiments on the test-bed winder, and remaining questions were completed with test winds on the final automated coil winding machine whose greater precision and controls allowed for more accurate and conclusive tests. The experiments performed included the following objectives: characterization of winding on the base layer, characterization of winding in the jog zone, characterization of winding the transition turns, and determining the effect of various tension levels on the quality of the wind. These topics are addressed in detail later in this document and also in a document by Brian Sonnichsen entitled "The Design of an Automated Fiber Optic Coil Winder.

## **3. Machine Subsystems: Detailed Design and Validation**

### **3.1. Introduction**

The machine developed is broken down into subsystems each performing tasks necessary to winding a fiber optic coil. This chapter will cover the detailed design and validation of certain machine subsystems and subsystem features. The following generally describes the format for this chapter. Each subsystem's purpose will first be explained as well any problems it was designed to deal with. Design concept generation and selection will then be covered. And, finally any validation testing results will be presented and discussed.

Figure 3.1 shows the overall winding machine with its subsystems labeled. The supply units [A], as described in Chapter 2, contain the mechanisms for guiding the fiber, paying out fiber onto the product spool, and controlling tension on the fiber while it is actively paying out fiber and while the supply unit is rotating with the product spool. The main positioning system [B] contains several axes which enable the accurate positioning of either supply unit around the product spool in three dimensions. In addition, there are two rotational axes which facilitate the exchange of the supply units from their payout and ride positions. The payout position is defined as the position from which the supply unit can payout fiber onto the product spool. The ride position is defined as the situation where the supply unit is locked down to the main shaft [C] and thus rotates with it. The main shaft is split in two and coupled together by an unseen belting system. The payout clamp [D] is the subsystem which couples the supply units mechanically and electrically to the main positioning system. The ride clamp [E] is the subsystem which couples the supply units mechanically to the main shaft so that they may rotate with it. The product spool [F] is the fixture onto which the gyroscopic sensing coil is wound. It is connected to the

main shaft and rotates with it. The product spool is divided into the mandrel on top of which fiber is directly laid, and the flanges which are the side walls of the product spool which prevent the coil of fiber from falling apart at the sides as the layers of the coil build up. The roller [G] subsystem hangs from a support beam so that it is positioned near the product spool and is a device for improving the quality of the wind.

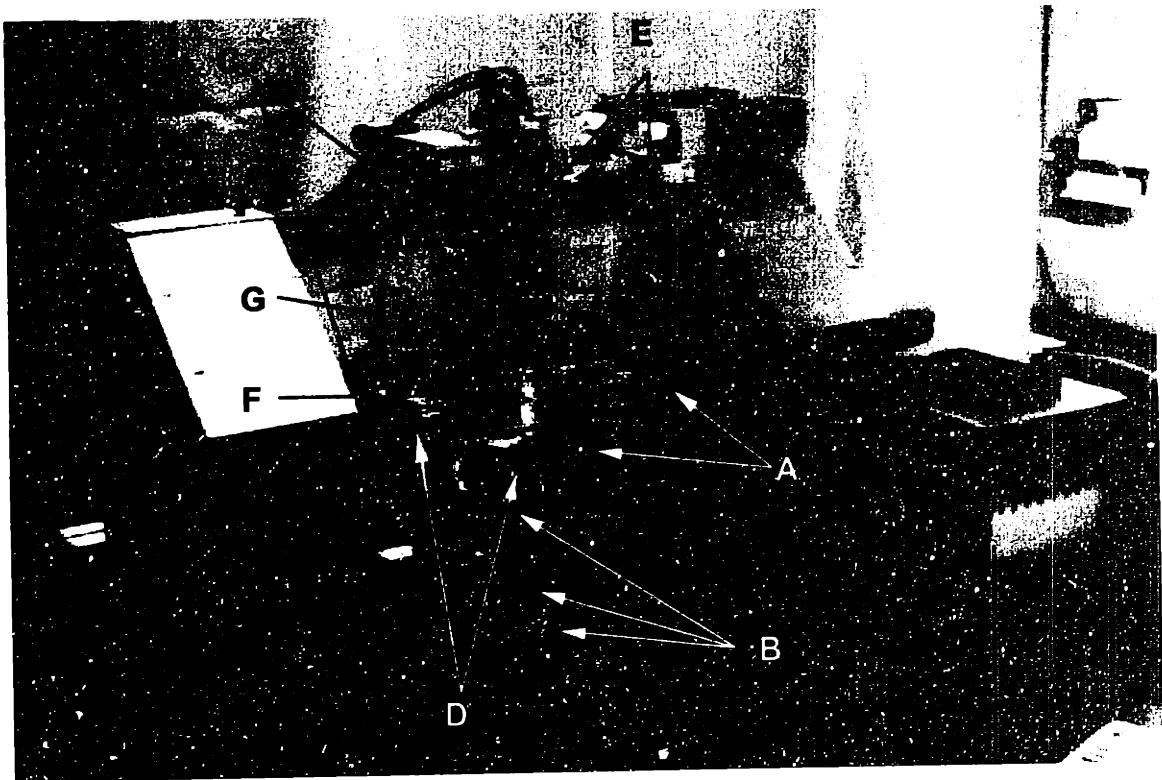


Figure 3.1: The automated fiber optic gyroscope coil winding machine. A) Supply units, B) Main positioning system, C) Main winding shaft, D) Payout clamps, E) Ride clamps, F) Product spool, G) Roller.

### **3.2. Supply Units**

The development of the supply unit was crucial to the success of the automated coil winding machine. Because of the disproportional importance of the supply unit subsystem to the coil winder it will be covered in its own chapter entitled "Supply Unit: Design, Control, and Validation."

### 3.3. Flange Design

#### 3.3.1. Introduction

The main purpose of the flanges of a product spool is to support the sides of a coil. This would seem a pretty simple task requiring only a flat surface for support, and in fact that is the sort of flange which has been used in traditional coil winding machines. However, such flanges themselves are the source of winding difficulties. When a winding pattern dictates that fiber should be wound from the other supply spool, the current supply spool must be routed out of the way. With a traditional flange this means that the fiber will hug the surface of the flange until it can be routed around the outer diameter of the flange as is the case in figure 3.2. Note that the term "inactive" fiber is used to indicate fiber which goes to the supply spool which is in its ride position. "Active" fiber would indicate fiber that is currently being paid out onto the product spool.

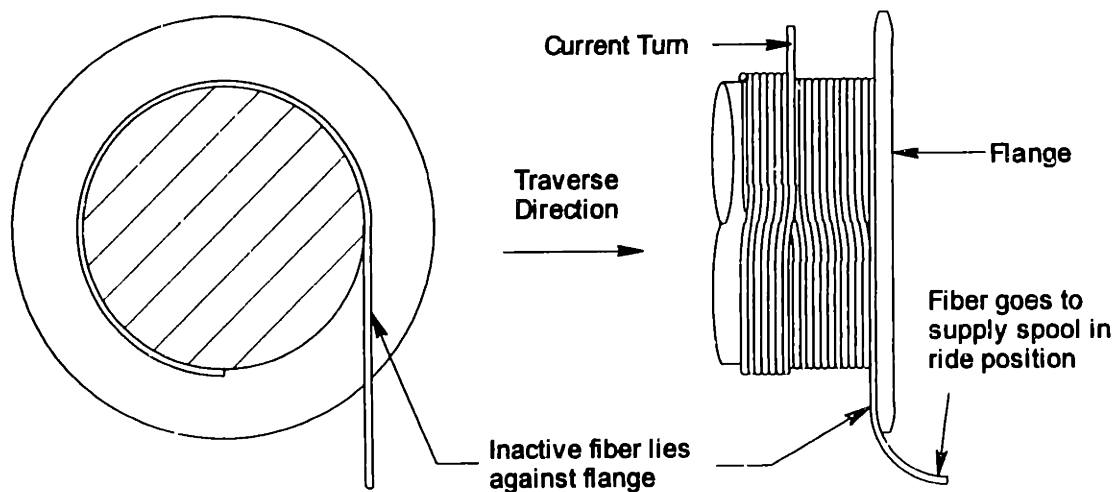


**Figure 3.2: Traditional flange. The inactive fiber routes around the flange outer diameter towards the supply spool in ride position.**

In the figure 3.2, winding has already begun using the fiber from the other supply spool. The current turn using this fiber is indicated as well as the traverse direction across the coil. Eventually, this fiber will wind all the way to the flange.

In this case this active fiber will collide with the inactive fiber which is occupying space right next to the flange. This means that the guide wheel will not be able to guide fiber near this space without potentially damaging the inactive fiber. This problem is resolved in traditional manual winding machines by the machine operator who would use a tool to guide the active fiber in behind and around the inactive fiber. This sort of maneuver requires a fair amount of dexterity and visual feedback as well as some trial and error on the operator's part, and is in no way a desirable maneuver to automate. The only other alternative to such a maneuver is to design a flange which allows the inactive fiber to be routed more immediately out of the way of the active fiber.

### **3.3.2. Flange Designs**

#### *3.3.2.1. Routing The Fiber Out Early*

The main purpose of designing a flange which is not flat is to be able to route the fiber outside of what is termed the "main winding area" as early as possible when it is no longer required by the winding pattern. Ideally, at the end of the last turn on a layer when a supply spool being swapped out to ride position the fiber would make a 90 degree angle and somehow phase through the flange itself. Figure 3.3 illustrates this situation. Of course, this situation is completely impossible. The fiber could not possibly make a right angle as shown because it would break, and the fiber also cannot phase through the flange. The Customer dictated a 0.5" minimum bend radius to prevent damage to the fiber. Consequently, clever flange geometries had to be design to allow the fiber to exit the main winding area without losing too much side support for the main fiber pack.

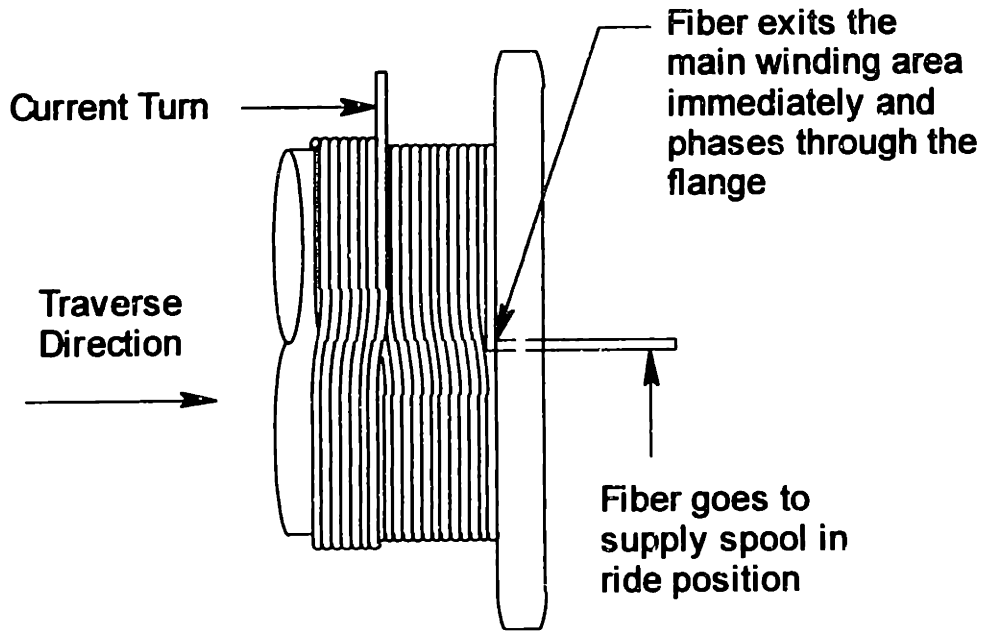


**Figure 3.3: Ideally the inactive fiber makes a 90 degree turn as soon as the winding pattern dictates and phases through the flange wall.**

### **3.3.2.2. Vertical Slots**

Figure 3.4 shows a flange design which allows the inactive fiber to be routed out as soon as possible given the 0.5" minimum bend radius constraint. The design incorporates two symmetric vertical slots. The slot used is determined by the winding direction of the fiber at the time it is routed out of the main winding area. Support for the fiber inside the main winding area is lost briefly where the slot begins in the flange wall, is picked up again in a line support where the bend radius is tangent to the plane of the inside-flange surface, and is lost briefly again when crossing the second slot. The loss of support is minimized by making the slot only as wide as necessary to route the fiber through it.

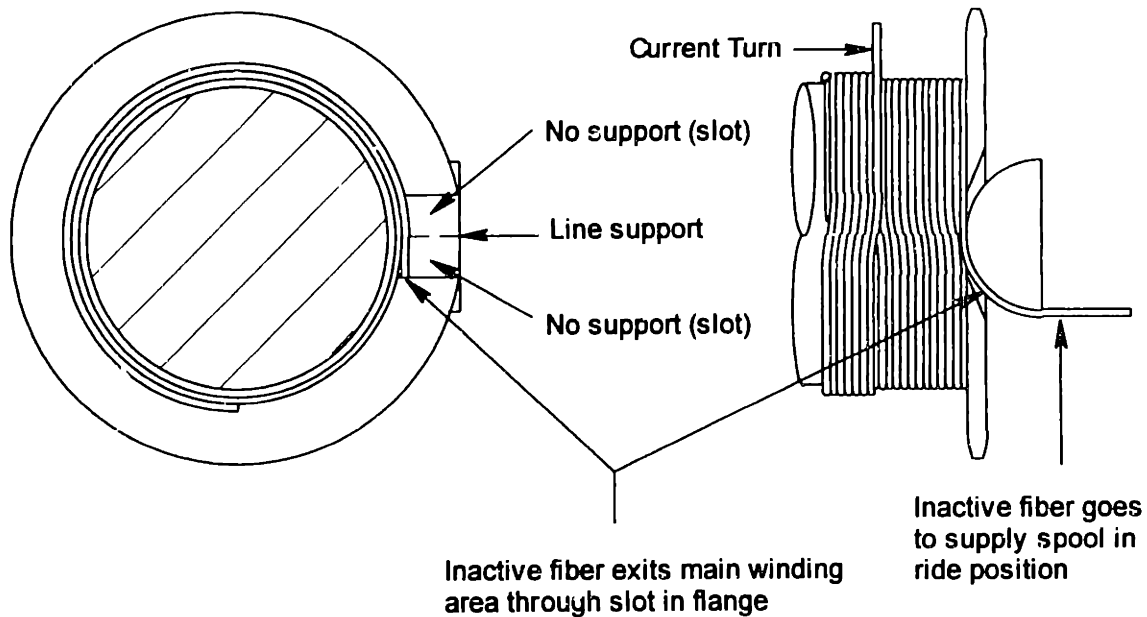


**Figure 3.4: Vertical slots flange design. The inactive fiber is routed through one of two vertical slots in the flange.**

The major disadvantage of using this flange design is the maneuvering that must be done to route the fiber into and out of the slot. Figure 3.5 shows how this would be accomplished. First the coil must be rotated such that the fiber is past the edge of the slot. The fiber can then be moved out of the main winding area and into the slot as the coil is rotated back to its original position.

The problem with this sort of maneuver is not in the mechanics of the maneuver which certainly can be automated. Rather, the problem results from when the fiber must be routed back into the main winding area. A similar maneuver must be performed. Only, this time, there would be another layer of fiber on top of the inactive fiber. Thus, rotating the coil to angle the inactive fiber back out of the slot and into the main winding area would threaten to pull the fiber out from under the layer which is covering it sooner than is dictated by the winding pattern.

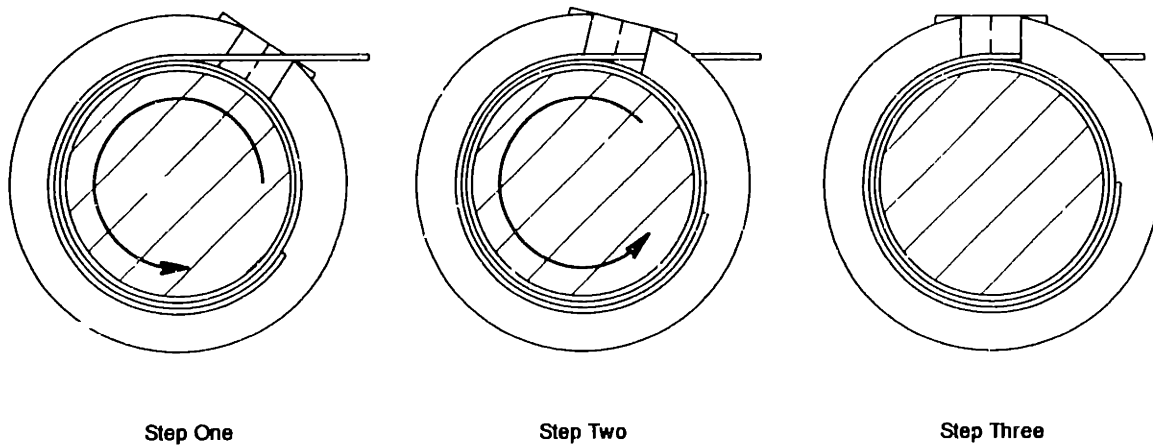


**Figure 3.5: Routing fiber into the vertical slot. The fiber must be routed over the top edge of the slot and down into it.**

### 3.3.2.3. Horizontal Layered Slots

Figure 3.6 shows another flange design which allows the fiber to be routed out of the main winding area immediately.<sup>17</sup> This method uses a series of horizontal layered slots. This flange design allows the fiber a way out of the main winding area while still providing adequate support on the sides to maintain the fiber pack's integrity. Support for the coil is lost when the fiber crosses over the first slot. Support is briefly picked up again as the fiber reaches the first fin (assuming there are enough layers for this to happen). This sporadic support continues until the tangent point of the bend radius is reached where, again, a line contact of support is provided. And, the sporadic support continues on the other side of this line.

The main advantage of this method over the vertical slots method is the ease with which the fiber can be routed into and out of the slot. The slots are lined up with the fiber just as a layer is finished and is ready to be swapped out with a single swinging motion.

---

<sup>17</sup> The horizontal layered slots flange concept was invented by Dr. Andre Sharon, Brian Sonnichsen, and Stephen Lin.



There are two disadvantages to this flange design. The first is that although when the fiber is lined up with a slot it is very easy to get the fiber out of the main winding area, it is not completely clear what happens when the fiber is lined up with one of the fins produced by the slots. The fiber must be routed to either the slot above or below the fin. Consequently, is it desirable to make the fins as thin as possible so that this situation where the fiber lines up directly with a fin occurs for a minimum number of layers for a given coil. The second disadvantage relates to the safety of the coil. The edges of the fins, after having been chamfered, still represent a danger to the fiber if it is pressed up against an edge with sufficient pressure.

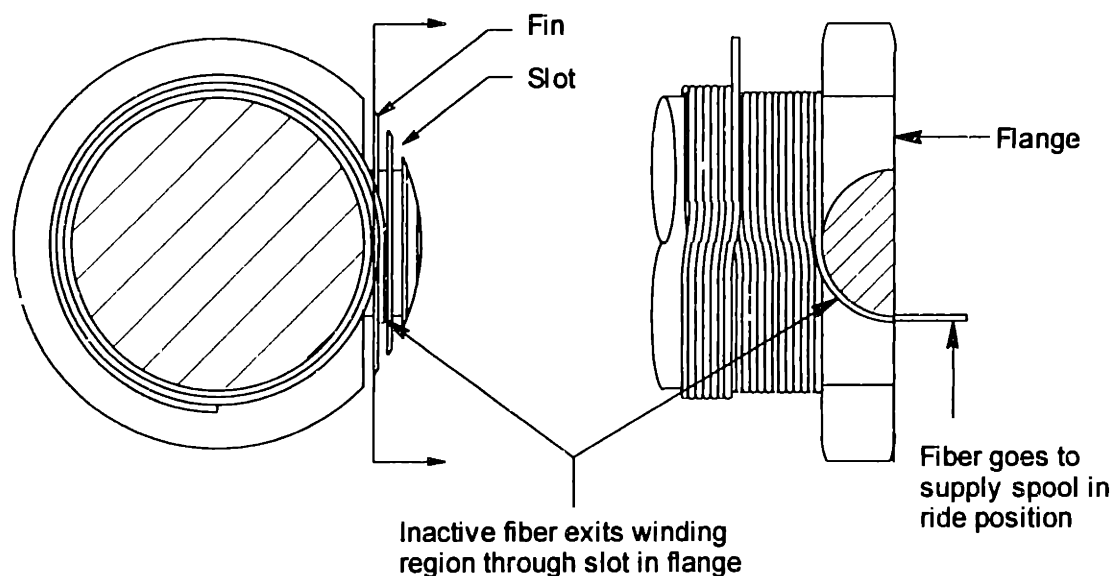


**Figure 3.6: Horizontal layered slots flange design. The inactive fiber is routed through the nearest slot in the flange for the given layer in the coil that the wind has progressed to.**

### 3.3.3. Test Results

Several small test coils were successfully wound onto mandrels with flanges incorporating the vertical slots concept. These test coils contained only about a dozen layers of relatively large diameter fiber. The flange depth of these coils were sized for the number of layers. The relatively shallow flange walls allowed

the fiber to be maneuvered into the slots without much of the rotation shown in figure 3.6. No significant loss of support at the slots was noticed in these coils.

Several test coils were also wound onto mandrels with flanges incorporating the layered horizontal slots concept. These flanges evolved through several iterations. The early iterations revealed the need to minimize the size of the slots, that is, the distance between adjacent fins. Coils wound with large slots relative to the size of the fiber, slots so large as to require about ten layers of fiber before reaching the second slot, showed problems with loss of support for the fiber. Fiber could be seen threatening to fall into the slots which in turn had an adverse effect when fiber on the overlying layer was attempted to be wound. The lack of support allowed gaps to form near the flange in the area of the slots. This lack of support problem was corrected by reducing the ratio of slot size to fiber diameter. Effectively, the size of the slots were reduced to just within manufacturing limits. Experiments performed on the redesigned flange showed no significant fiber support problems for tens of layers.

### ***3.4. Payout Clamp - Coupling To The Supply Unit***

#### **3.4.1. Introduction**

The payout clamp is the subsystem which holds a supply unit while it is paying out fiber to the product spool, as opposed to while it is rotating with the main coil in its ride position. The winding machine has two payout clamps, one for each of the supply units. The payout clamp couples the supply unit to the main positioning system both mechanically and electrically. The guide wheel on a supply unit is the device which guides the fiber onto the product spool (see Chapter 2). It is extremely important for the guide wheel to be in the proper position to effectively guide fiber onto the proper position of the coil. During the production of a coil a supply unit is frequently coupled and de-coupled to and from its payout clamp according to the demands of the pattern being wound. If a

supply unit is not clamped back into the same spot every time then the position of the guide wheel with respect to the product spool will not be known accurately, and consequently, winding an accurate coil will become impossible. Thus, the design of the payout clamp was important to the success of the automated winding machine.

### **3.4.2. Functional Requirements**

The functional requirements of the payout clamp involve the repeatable repositioning of a supply unit (as measured at the location of the guide wheel) in several dimensions. The critical dimensions were determined from experiments on the test-bed winding machine which showed that small errors in certain dimensions had little or no effect on the winding quality, while small errors in other dimensions produced drastically different winding results. Figure 3.7 depicts the supply unit above the payout clamp base as seen from its front. Rotational misalignment about the Y axis and lateral misalignment along the X axis both serve to place the guide wheel in a different position along the X axis than the previous clamping attempt indicated by the centerline. Figure 3.8 depicts the supply unit as seen from above. Rotational misalignment about the Z axis can cause lateral misalignment of the guide wheel along the X axis. In addition, such rotational misalignment can also impair the guide wheel's ability to guide fiber next to a flange (see section Guide Wheel: Fine Alignment in the chapter 4).

To complicate matters in the design of the payout clamp there was limited space available to house the subsystem. The space restrictions were imposed by the fact that at any given time, depending on the pattern being wound, there could be a supply unit in its ride position rotating on either side of the product spool. The payout clamp had to be designed to avoid being hit by this supply unit.

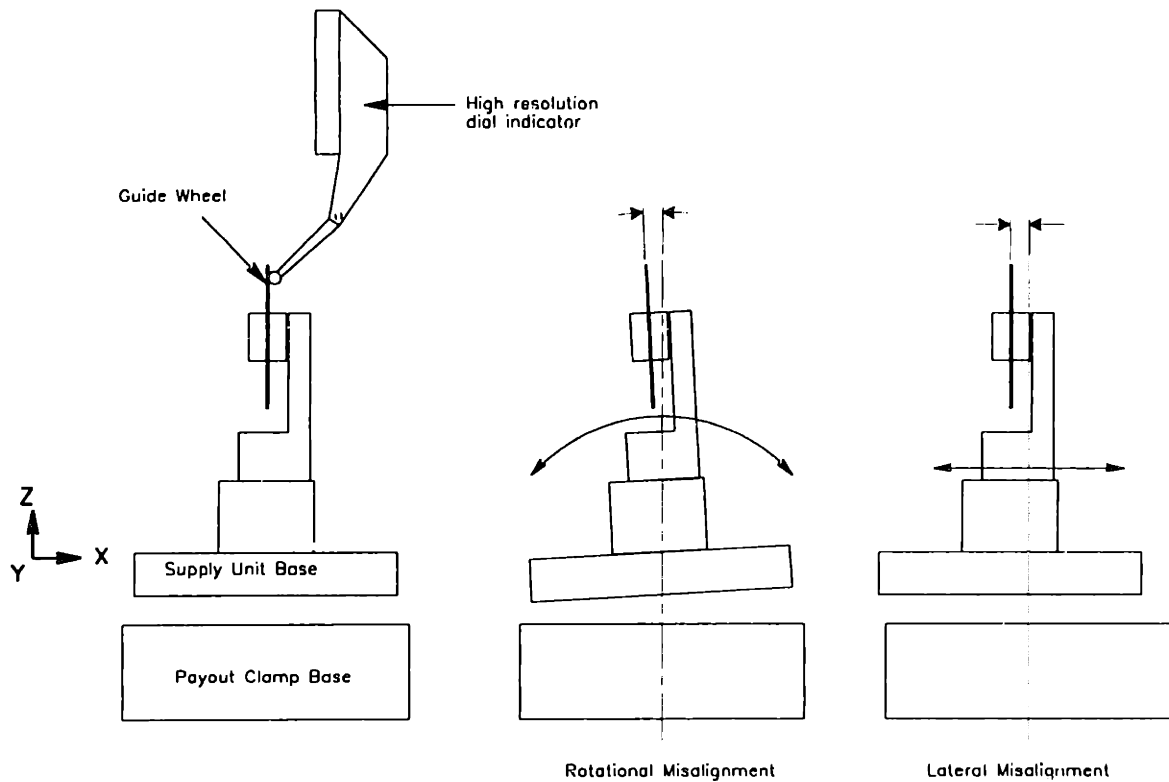


**Figure 3.7: Rotational and lateral misalignment of the supply unit on the payout clamp as seen from the front.**

A final functional requirement of the payout clamp was that the clamping force of the payout clamp be sufficient to survive the winding environment. This requirement stems from a few situations. To create the orthocyclic wind (described in chapter 1) the guide wheel (and thus the entire supply unit) must be jogged one or more fiber diameters during a portion of the rotation, i.e. inside the jog zone, for every rotation of the product spool. This jogging motion, when winding at high speeds, consists of a high acceleration and deceleration which would threaten to shake the supply unit out of its payout clamp. In addition, the machine operator must work with the machine itself during the setup and after the completion of a wind, and potentially in the middle of a wind if there are any problems. The clamping force of the supply unit had to be able to withstand potential bumping by the machine operator.

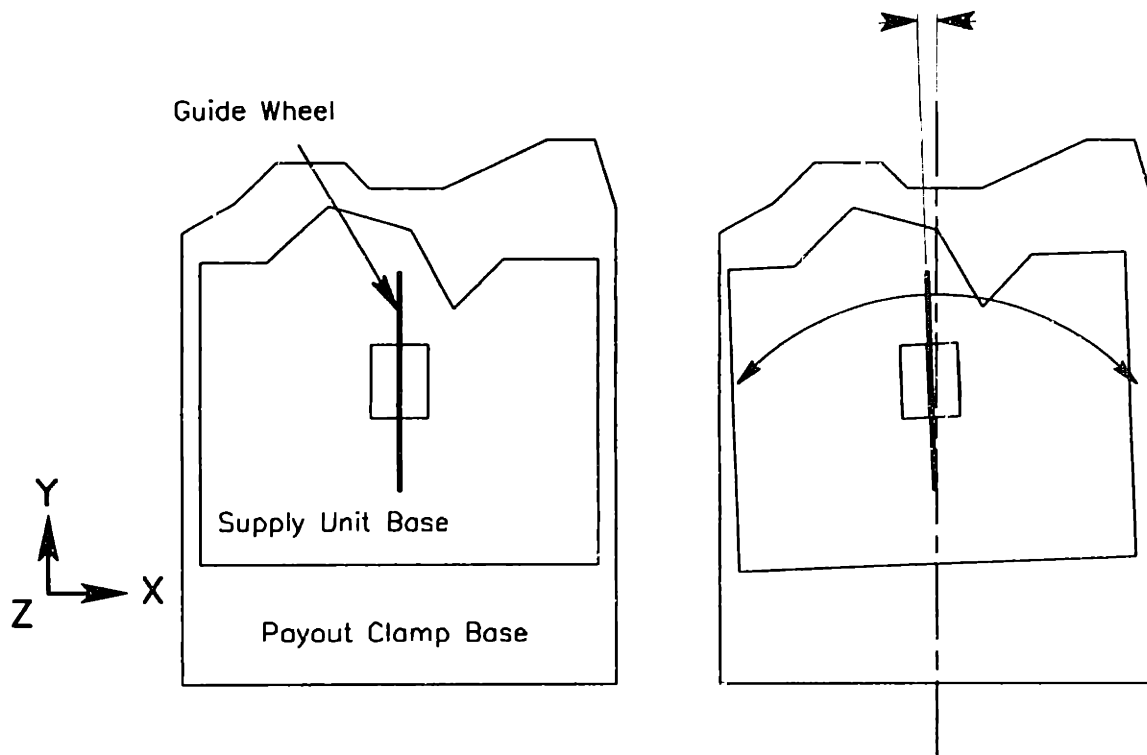


**Figure 3.8: Rotational misalignment of the supply unit on top of the payout clamp as seen from above.**

### **3.4.3. Concept Generation and selection**

#### **3.4.3.1. Simple Mechanical Stop**

The test-bed winder's payout clamp was design as a simple mechanical stop. Force was applied using thumb screws which pushed against the supply base pushing it into a mechanical stop build into the payout clamp. While sufficient for the purposes of the test-bed winding machine, working with this form of clamp highlighted its limitations for the final winder. Figure 3.9 illustrates this technique and its problems. The lip that was the mechanical stop was short to reduce the distance of vertical travel necessary to engage the supply unit base to the payout clamp base. However, without a large surface area to clamp against the supply unit could and would clamp against the mechanical stop at small angles (as shown in figure 3.9) which were not repeatable. This problem was complicated by the fact that small particles which occasionally found their way onto the payout clamp surfaces would also prevent the supply unit from seating flatly.

These problems were overcome by manually cleaning the payout clamp and manually ensuring a flat engagement. However, it could be seen that such a method would not be acceptable for the final automated winding machine.

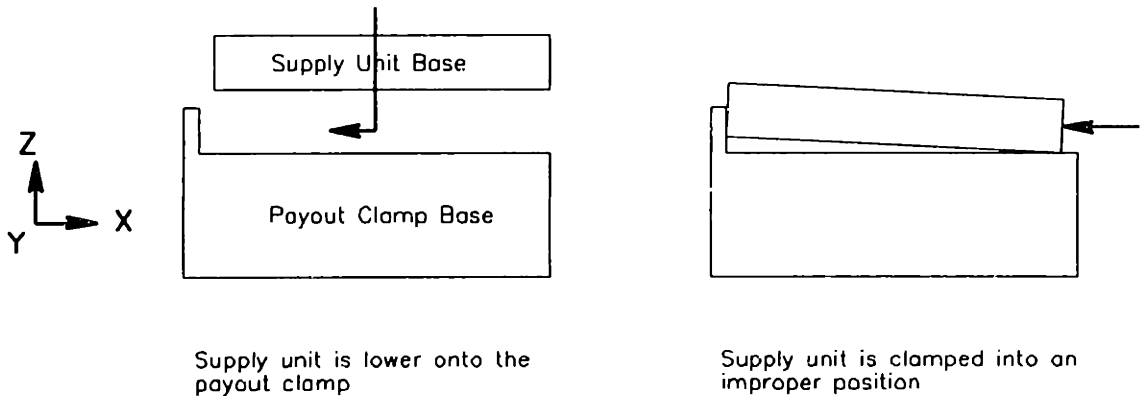


**Figure 3.9: A simple mechanical stop for the payout clamp.**

**3.4.3.2. Kinematic Coupling**

Kinematic couplings are designed in such a way as to deterministically constrain a mechanical interface without over constraint. This is accomplished by making contact at a number of points which is equal to the number of degrees of freedom that are to be restrained<sup>18</sup>. The concept of a kinematic coupling was applied to the interface between the base of the supply unit and the payout clamp. Figure 3.10 illustrates this concept. The supply unit is shown having three spherical locators attached to its underside. These three spherical locators are meant to seat into the three wedges located in the payout clamp base. Each of the spherical locator/wedge pairs provides two point contacts for a total of six point contacts which constrain the three translational and three rotational degrees of freedom.

A mock-up of this idea was made to test the concept. The nature of the kinematic coupling requires that the clamping force be applied in as pure a

---

<sup>18</sup> Slocum, Alexander H. Precision Machine Design. Prentice Hall, New Jersey, 1992. p. 401-404

vertical (Z axis in figure 3.10) direction as possible. The only convenient way of applying this force was to utilize magnets. Because the kinematic coupling was to do all the constraining on the supply unit the magnets were only to apply force to a base plate (simulating the supply unit base) through a very thin air gap. The results of experimenting with the mockup confirmed that the kinematic coupling would result in very repeatable clamping. Electromagnets were first utilized which advertised a strength of tens of pounds each. However, electromagnets function best when in actual contact with the object they are trying to attract, and their pulling strength is dramatically reduced as the distance from the object increases. An air gap of only 0.010" was enough to render the clamping force low enough that relatively small forces (such as an operator bumping into a supply unit) could threaten to cause the base plate to break free of the clamp. Larger electromagnets were not possible because of the space restrictions imposed on the payout clamp by the rest of the machine.

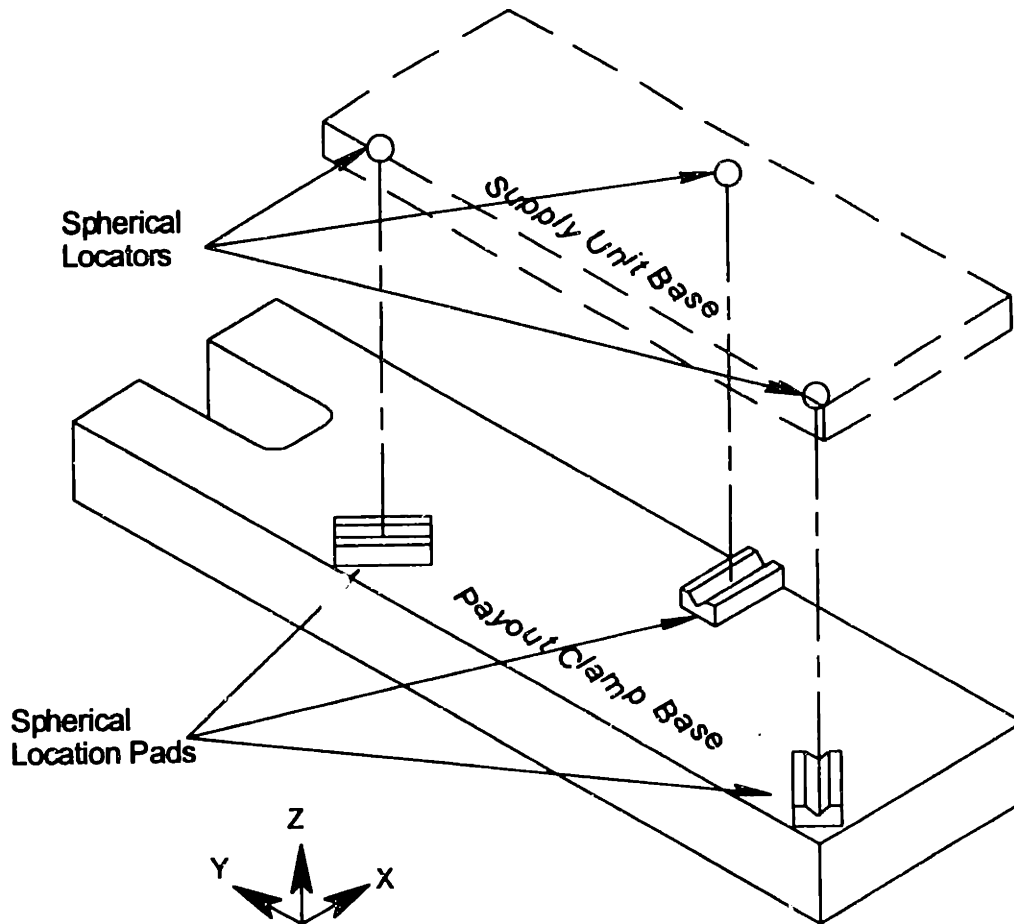


**Figure 3.10: Payout clamp using a kinematic coupling approach. Three spherical locators on the supply unit base seat into three wedges on the payout clamp.**

Natural ceramic magnets were tried afterwards because of their greater ability to attract objects at a distance. This resulted in better performance and certainly moving to rare earth magnets would have resulted in even better clamping ability. However, the dilemma with using natural magnets lies in the inability to turn their clamping force on and off as desired.

#### ***3.4.3.3. Quasi-Kinematic Coupling***

Although, the mockup of the kinematic coupling revealed the complications resulting from the need to apply a directly downward clamping force, the general idea of such a coupling was not abandoned. As noted in the functional



requirements for the payout clamp it is more important to achieve repeatability of positioning in only certain dimensions. The kinematic coupling of figure 3.10 succeeds in completely constraining the supply unit. A new quasi-kinematic coupling design to focus on the important degrees of freedom was devised.

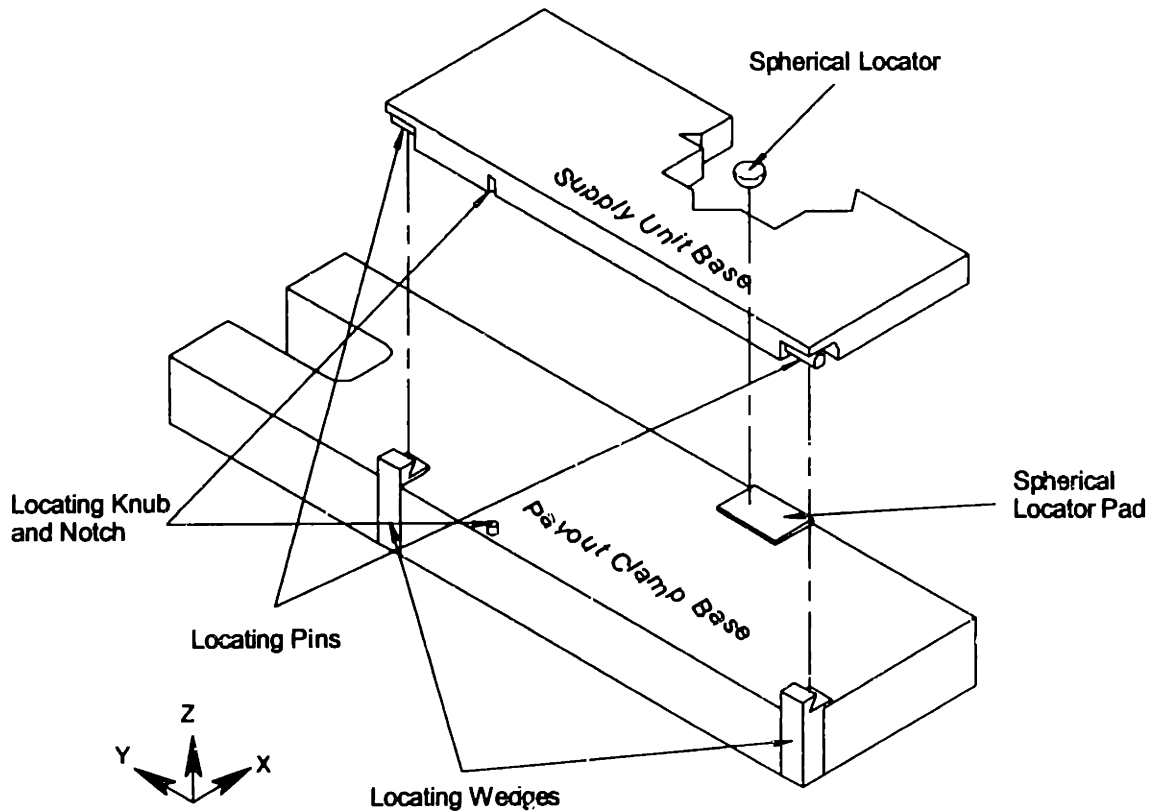


**Figure 3.11: Payout clamp utilizing a quasi-kinematic approach. Two locating pin and wedge pairs and one spherical locator constrain the supply unit in the most important degrees of freedom.**

Figure 3.11 illustrates this quasi-kinematic design. The design utilizes two locating pin and wedge pairs and one spherical locator. The two locating pins seat inside the locating wedges as shown in figure 3.12. Although, there is technically not a point contact between the pins and wedges, because of the distance that separates the two locating pins the contact with the wedges can be considered point contacts. The two pins together form a line about which the supply unit can rotate. The spherical locator is used to eliminate this rotation by providing a point contact against the spherical locating pad. The clamping force is applied at an angle pushing the supply unit up against the wedges as well

down against the pad. The locating pins and spherical locator together constrain the supply unit from translating along the X and Z axis as well as from rotating about the X, Y and Z axes. The remaining translational degree of freedom along the Y axis is loosely constrained by the locating nub and notch pair. The nub fits into the notch with several thousandths of an inch clearance allowing just a small amount of movement along the Y axis.

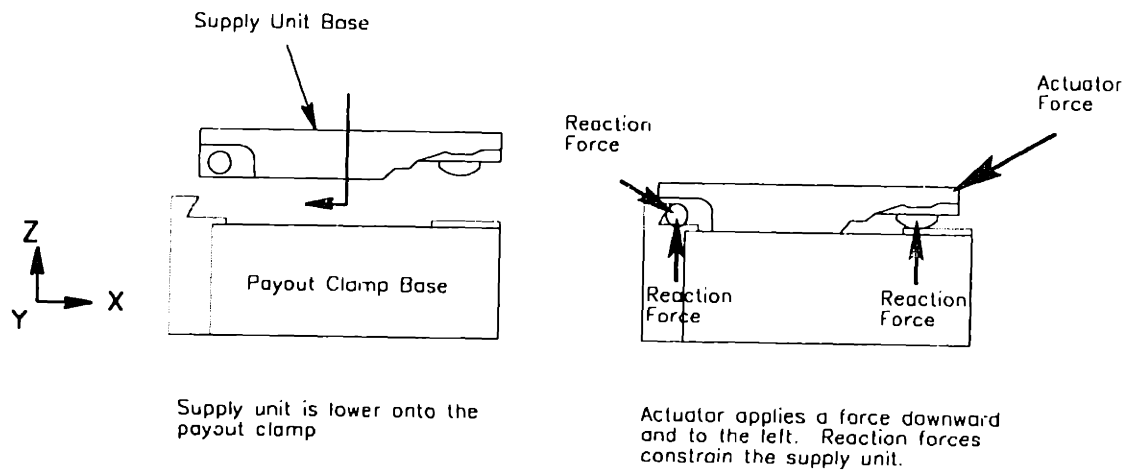


**Figure 3.12: Engaging the quasi-kinematic clamp. The locating pins contact the locating wedges in two places while the spherical locator engages the locating pad at a point.**

The change in design from the kinematic to the quasi-kinematic coupling design only sacrificed constraint in one degree of freedom which was previously determined not to be critical to the winding process. The design allowed for more options for the choice of clamping actuator.

#### 3.4.3.4. Clamping Actuator Selection

Recall that the main positioning system, on which the payout clamps ride, had to be able to pick up and drop off the supply units to and from each of their ride positions. This in addition to the need to avoid the path of supply units rotating with the main shaft dictated that the actuator, whatever it was, had to lie below the level of the supply unit base and could not stick out off to the sides of the payout clamp.

There were also additional limitations to the free space available to place an actuator. A small amount of space inside the payout clamp base had already been allocated for a small actuator for the supply unit brake (see Chapter 4). As mentioned before, the payout clamp served not only to mechanically couple the supply unit to the main positioning system, but also electrically. A bay of spring loaded contacts provided the electrical connection. In order that the spring force from this bay of contacts not bias the way in which the clamp closed it was allocated space between the two locating wedges. Figure 3.13 illustrates the amount of free space available for placement of the clamp actuator. The force was required to be applied along the X axis towards the locating wedges.

Two actuators were under consideration for the payout clamp. They were a piston and a geared DC motor. The piston offered a large amount of clamping force in a very small package with a quick actuation. The gear DC motor offered a comparable amount of clamping force in a slightly larger package, but with a slower actuation. The decision between the two forms of actuation was made on a geometric configuration basis. The use of a piston naturally suggests applying the force inline with the body of the piston itself. In order to obtain a force along the X axis as required the body of the piston would have to lie inline with the X axis. However, as can be seen in figure 3.13 placing such a piston in the middle of the payout clamp base would result in a geometric interference with the electrical contact bay. Instead a pair of pistons on either side of the contact bay could be used, or a mechanism to transform the pistons motion into a motion perpendicular to the stroke would have to be design and implemented. Therefore, a geared DC motor was utilized instead with a clamping arm rotating up against the supply unit base, the direction of motion being perpendicular to the body of the motor. This clamping action is shown in figure 3.14. The clamp arm contacts a clamp wedge attached to the base of the supply unit causing the force transmitted to be at an angle as desired.

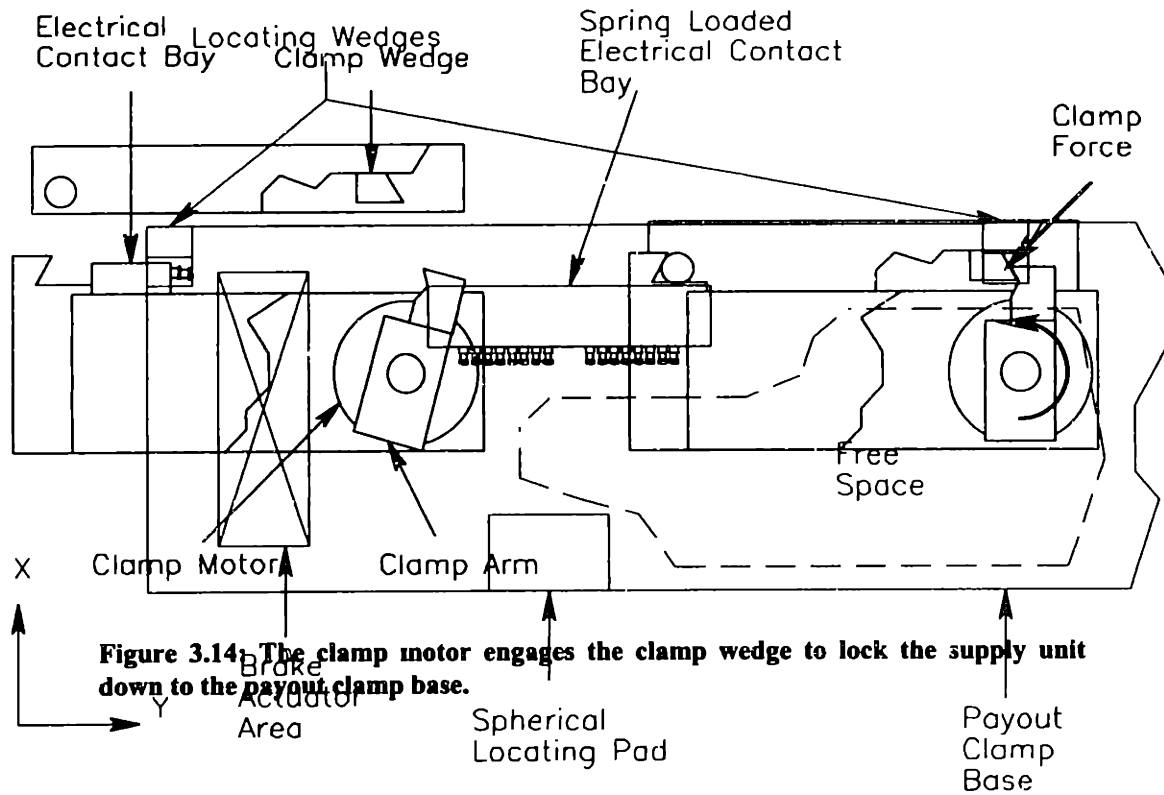


Figure 3.13: Available space for payout clamp actuator.

### 3.4.4. Testing and Results

Tests were run on the actual payout clamps which were manufactured and implemented on the final coil winding machine. The first test (type 1) simply involved toggling the clamp on and off allowing the spring loaded electrical contacts to push the supply unit out of the payout clamp locating wedges. A dial indicator was placed against the guide wheel to measure its lateral position along the X axis as shown in figure 3.7. The second test (type 2) also involved toggling the payout clamp on and off, only this time the supply unit was physically shifted into a slightly rotated position prior to clamping. The rotated angle was changed from trial to trial. Figure 3.15 shows the results of these tests for both supply unit A and supply unit B on the machine.

The results for test type 1 indicate excellent repeatability for both of the payout clamps being better than  $\pm 0.0001$ ". The resolution of the dial indicator

used to measure the position of the guide wheel was .0001". There was quite a

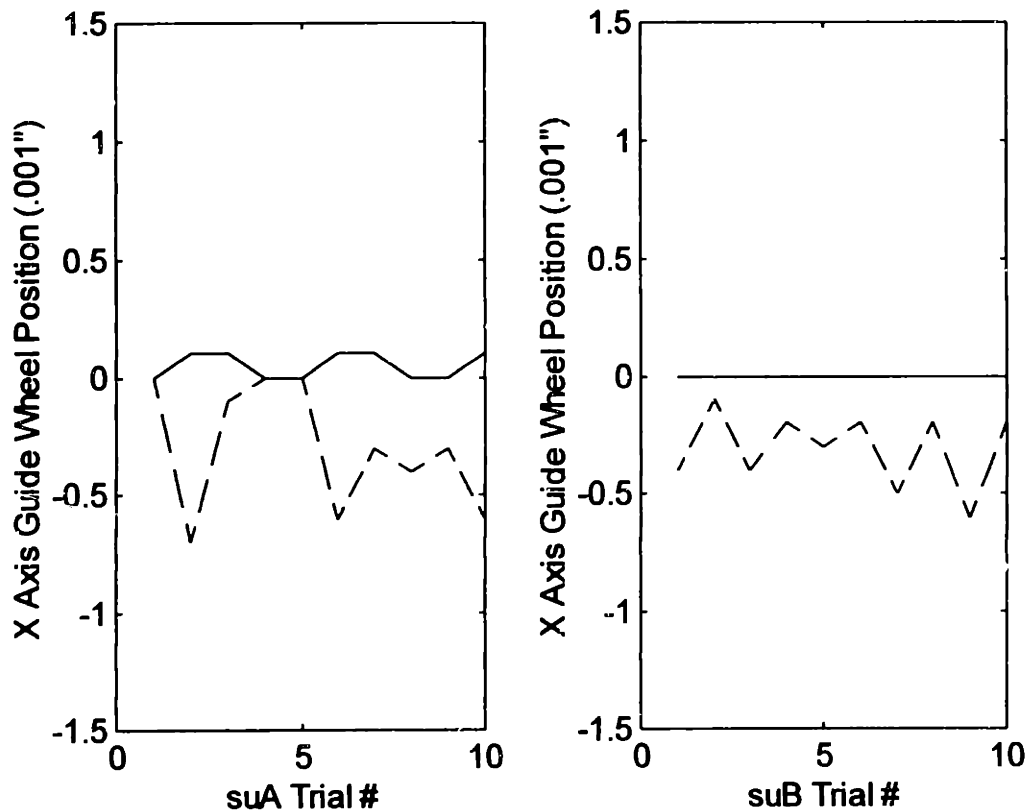


**Figure 3.15: Payout clamp positioning repeatability as measured by a dial indicator at the location of the guide wheel. Left: results for supply unit A. Right: results for supply unit B. Solid lines indicate test type 1 results. Dashed lines indicate test type 2 results.**

bit more spread in positioning repeatability for test type 2 for both the payout clamps. However, even for this test the spread was not more than  $\pm 0.0005$ ". It is curious to note that the discrepancy with the baseline trial for both payout clamps were always to one side of the baseline trial. This behavior is most likely the result of the baseline trial being far to one side of the trial spread. The results of the tests shown validate that the design of the payout clamp was successful in achieving a highly repeatable clamp in terms of the relative position of the guide wheel along the X axis from trial to trial.

The other functionality requirement that the payout clamp retain a firm enough hold on the supply unit to survive the winding environment was also

satisfied by the use of a dc geared motor. At no time did the clamp lose its clamping ability during any of the test winds performed, nor was the clamp susceptible to forced bumping of an operator's hands into a supply unit.

### **3.5. The Roller**

#### **3.5.1. Introduction**

Chapter 2 covered the selection of the guide wheel as the method of choice for guiding fiber onto the product spool. The ability of the guide wheel to accurately place fiber onto the product spool was confirmed through numerous winding experiments. However, placement accuracy is not 100% for several reasons. Outside of the jog zone, placement of the fiber is generally dictated by the grooves formed by the fibers from the underlying layer. This is not true in the jog zone where fibers cross over the fibers in the underlying layer. The relative runout of the guide wheel and the product spool grooves (see section "Guide Wheel Runout" in Chapter 4) places an absolute maximum possible accuracy on the placement of the fiber. The small amount of spacing between the guide wheel's groove and the fiber which passes through it allows the fiber to shift from side to side affecting its location on the product spool. Small dust particles which lie on the surface of the product spool can also affect the ultimate placement of fiber. And, small inaccuracies in the timing of the jogging axis which jogs the fiber from its current groove to the adjacent groove can affect the placement of the fiber. The culmination of all these possible variations is a coil, at the completion of the current layer, which does not have a well enforced jog zone. Figure 3.16 depicts a series of cross-sections taken at the jog zone start, two jog zone mid sections, and the jog zone end. The left series depicts what an ideal jog zone (termed "clean") looks like, while the right series depicts what a poorly enforced jog zone (termed "unclean") looks like.

Although, it is theoretically known that the size of the jog zone (measured angularly in degrees) should grow as more layers are wound onto the coil several experiments have shown that without some form of post-layer jog zone cleanup the jog zone will grow much faster. In addition, the "unclean" nature of a poorly enforced jog zone has been known to induce winding errors if variations in jog locations become so gross that overlying fibers are able to fall into gaps created by these variations.

### **3.5.2. Development of the Roller Concept**

Jog zone enforcement can easily be accomplished by pushing the exposed fibers on the current layer down into the grooves formed by the fibers in the underlying layers. Although, the exposed fibers cross over the fibers in the underlying layer in the jog zone, and thus cannot be pushed down into grooves in the jog zone, the act of making sure that the fibers just outside of the jog start and jog end are in their proper positions is also enough to move the fiber inside the zone to its proper position.

In traditional manual winding machines the operator is responsible for enforcing the jog zone. This is done generally at the completion of every layer. The operator, using the reflection of light on the fibers, can determine when all the turns on the layer begin and end their jogs at the same time. A tool of some sort, generally made of a soft material such as teflon to reduce the risk of damaging the fiber, is used to perform the jog zone enforcement. The tool is slid across the surface of the coil wherever the operator believes jog zone cleanup is needed.

This method of jog zone enforcement could be automated by placing the tool in the grip of a mechanism which applies the tool to the coil when and where necessary. However, as noted before the Customer expressed some concern about possible sliding contact against the fiber. Although, the use of teflon for

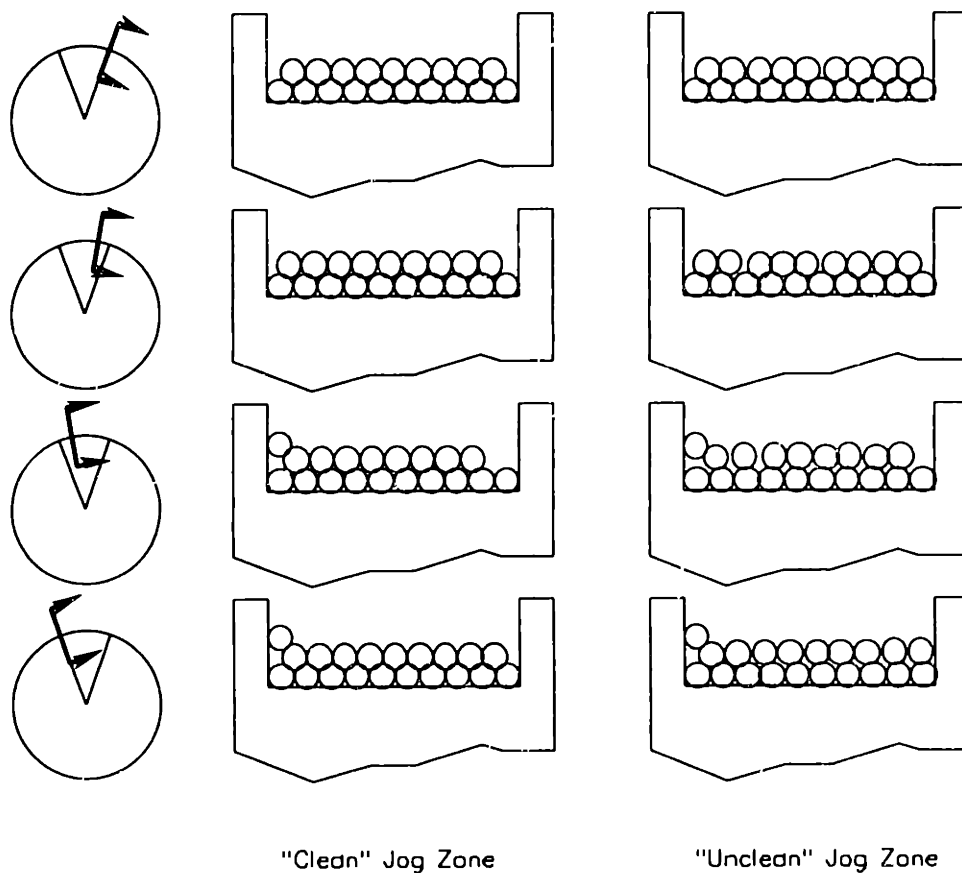


**Figure 3.16: Jog zone cross-section. Each series of cross-sections for a "clean" and "unclean" jog zone depict the jog start, two mid-jog, and jog end diagrams.**



the tool material was used partly to address this concern, the operators the MIT/MI talked to who utilized this method noted that their teflon tools would wear gradually. A tool which wears significantly poses not only a maintenance issue, but also possibly affects the tool's ability to perform its job properly and consistently over time. For these reasons an alternative was sought and found in the concept of a roller.

The roller is nothing more than a cylinder which rolls along the surface of the coil being wound applying pressure to the fiber pack, thus locally pushing the exposed fibers down into their natural positions. The rolling contact nature of the roller satisfied the Customer's concern about sliding contact against the coil.

### **3.5.3. Roller Design Details**

#### ***3.5.3.1. Flat Surface Engagement***

Experiments on the test-bed winding machine revealed that it is not enough for the roller to engage the coil but that the roller must engage the surface of the coil flatly. Any small misalignment between the surface of the roller with the surface of the coil will not only fail to enforce the jog zone in the desired manner, but will also risk compromising the integrity of the coil. Figure figure 3.17 illustrates this situation. The location where one side of the roller contacts the coil is under a lot of pressure because it is not distributed across the entire surface area of the roller.

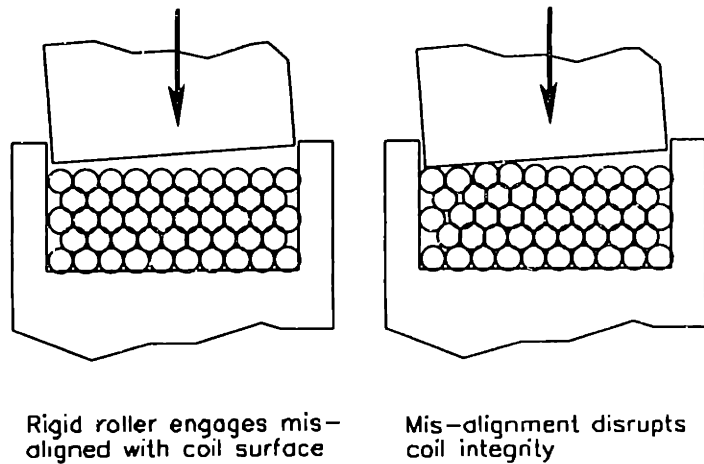


**Figure 3.17: Roller mis-alignment with coil surface can compromise the integrity of the underlying layers.**

It is possible to remedy the problem of mis-alignment by allowing for a fine-adjust of the roller angle so that it can be tweaked until the two surfaces are exactly parallel. The problem with this solution is that the two surfaces must be exactly matched; a difference of only a couple of thousandths of an inch could have a serious impact. In addition, a fixed roller does not account for the runout of the mandrel surface which influences the surface of any given layer. The product spool and it's mounting to the main shaft was design in such a way as to minimize such runout, but it can never be completely eliminated. Thus, even if the roller is tweaked to match the surface of the mandrel at one angular location of the main shaft, this will not necessarily remain true for an entire rotation of the main shaft.

Thus, the roller was designed to allow for self-alignment. Figure 3.18 shows the ideal situation where the roller approaches the coil with a small mis-alignment. As it contacts the coil surface it rotates and aligns itself with the surface, and finally applies an even pressure across its entire surface.

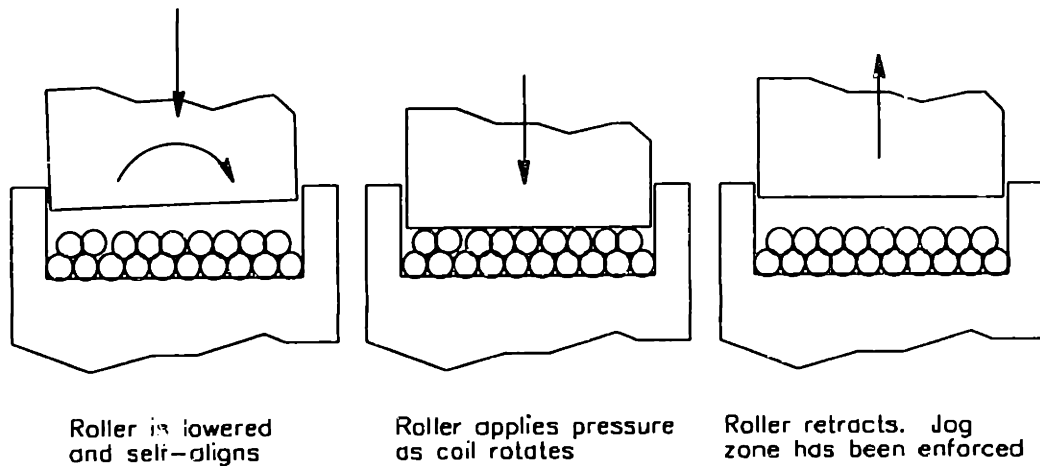


**Figure 3.18: Self-aligning roller properly engages the coil surface and enforces the jog zone**

### 3.5.3.2. Fitted Roller Vs. Single Multi-Purpose Roller

The roller had to be able to be used to roller many different sizes of coils from the very thin to the very wide, and those with small outer diameters to those with large outer diameters. There are two approaches to rolling given this constraint. Produce a new roller to match the width of each product spool, or use a roller which is thin enough to fit between the flanges of the thinnest product spool and reapply it several times over the width of the coil. Figure 3.19 shows these two approaches.

The disadvantage of fitting the roller to the product spool of course lies in the need to manufacture a new roller for every type of product spool. The advantage of this method, however, is that the coil need only be rolled once per layer. The opposite is true for the modular roller which need only be manufactured once for all product spools, but must roller the coil multiple times during a given layer.

The act of rolling just once can take between ten and twenty seconds. For a coil with dozens of layers, this can translate into several minutes worth of added process time to the production of the coil. If this task were the to be multiplied by as many times as necessary for a modular roller to roller and entire

layer, than the added process time could indeed be significant. Thus, the only way a modular roller would make sense would be if the roller could be applied continuously while the coil was being wound and moved laterally as necessary. However, experiments with continuous rolling showed that this technique actually worsened the placement of fiber in the jog zone (see next sub-section on rolling technique). Moreover, even if continuous rolling were possible, the roller would not be able to be moved laterally without pausing the winding since it would be in direct contact with the fiber. The roller would have to be

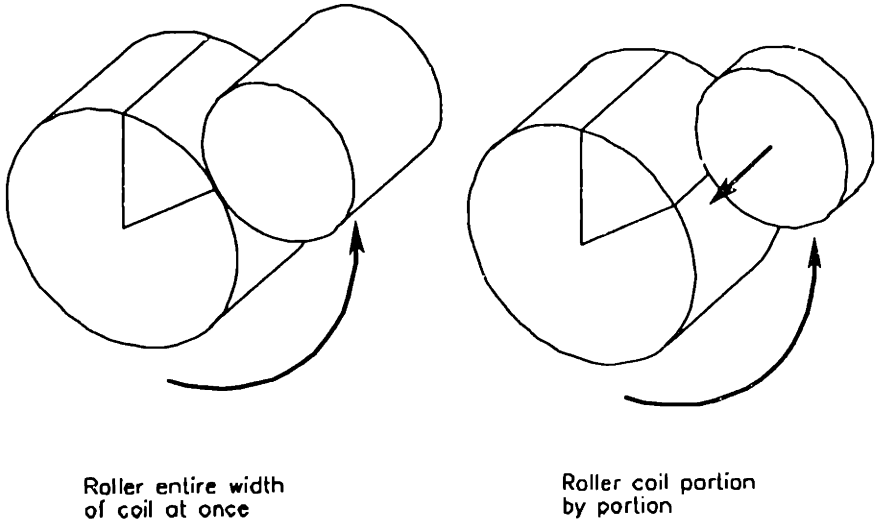


**Figure 3.19: Left: Roller fitted to the width of the product spool rollers entire coil at once. Right: Thin roller capable of rolling any size product spool rollers coil little by little.**

disengaged, moved laterally, and then re-engaged multiple times over the course of a given layer. And finally, since the roller mechanism hangs from overhead to engage the product spool, controlled lateral movement would require another linear positioning axis adding additional complexity to the machine. For these reasons, the fitted roller was chosen over the modular roller.

### **3.5.4. Testing and Results**

Performing a good rollering operation is not simply accomplished by just engaging the roller to the coil surface, applying pressure, and turning the coil until the whole circumference has been completed. As mentioned, the purpose of the roller is to enforce the jog zone of the coil. Various process techniques were tried to determine how best to roller a coil to achieve the best jog zone enforcement.

One of the early tests was to try continuous rollering of the coil while it was being wound. This actually proved to worsen the jog zone. The jog zone would look very nice on the side on which the roller approached the jog zone, but would then look poor on the other side where the roller receded from the jog zone causing it to spread out.

Further experimentation with various rollering techniques revealed the best way to apply the mechanism. The roller should be used only rolling towards the direction of the jog zone without rolling through it. The motion starts on the opposite side of the coil from the jog zone and moves towards it, and is performed alternatingly on both sides of the jog zone a few times.

The rollering aligns fibers that were mis-aligned with the grooves formed by the underlying layer. Of course, the act of doing this creates a local area of slack in the fiber which then gets pushed into the jog zone itself. This is a desirable result, as the slack can best be accommodated by the jog zone. That is, mis-alignments of fiber are more tolerated in the jog zone where fibers generally crossover the grooves formed by the underlying layer as opposed to seating inside those grooves.

Rollering must be performed on every layer and only when the layer is complete. Rollering a layer before layer completion runs the risk that the fiber adjacent to available space in the current layer, which exists because the layer is not complete, will get pushed into that space by the roller. This is not possible when the layer is complete.

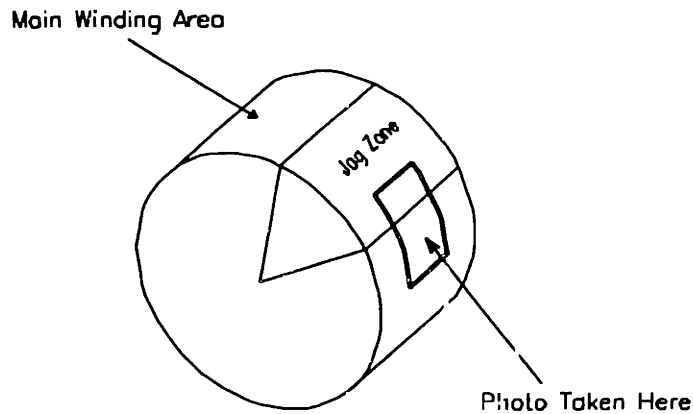


**Figure 3.20: Overhead photo was taken of one edge of the jog zone as indicated.**

Figures 3.21 and 3.22 show an overhead view of a layer before and after it has been rolled, respectively. The location of these photographs are indicated in figure 3.20. The left darker half, of the images shows fiber just outside the desired jog zone, and the right lighter half of the images shows fiber just inside the jog zone. The transition from light to dark is one edge of the jog zone. Notice how in the pre-rolled image the fiber just outside the zone forms a sort of tail. This tail is indicative of fibers starting their crossover at different angular positions. Thus, this is an “unclean” jog zone. Now, look how the post-rolled image does not exhibit this jog zone tail. All the fibers have been aligned to the underlying grooves right up to the edge of the jog zone so that they begin their crossovers at the same time. Winding experiments have shown that this enforcement of the jog zone helps to keep the jog zone size from growing dramatically as the number of layers in the coil increases, and in general to keep the coil geometry well-defined.

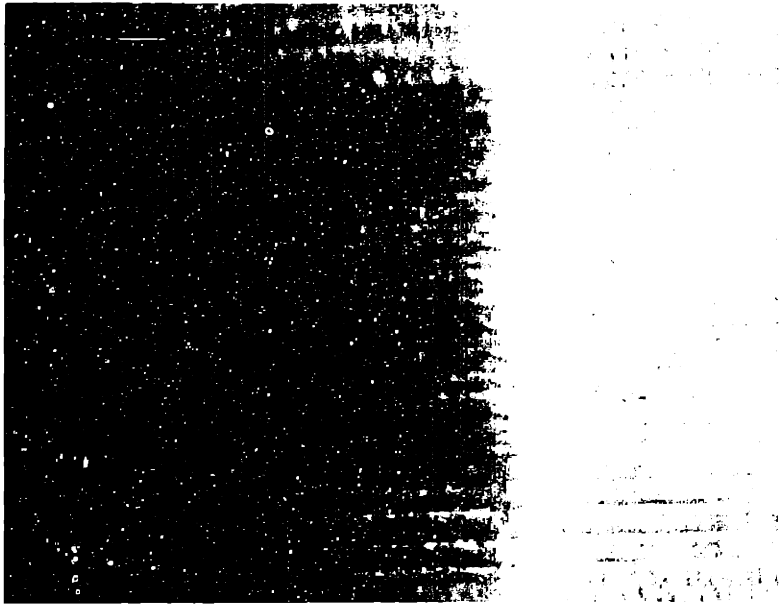


**Figure 3.21: Overhear view of fiber near one edge of the jog zone before rolling.**

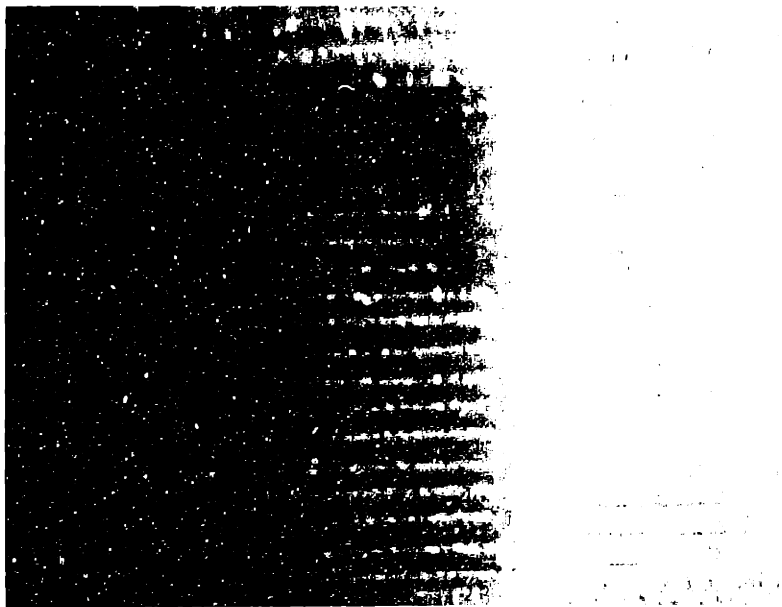


**Figure 3.22: Overhead view of fiber near one edge of the jog zone after rolling.**

## **4. Supply Units: Detailed Design, Control and Validation**

### **4.1. Introduction**

The supply unit concept, as explained in chapter 2, is key to the success of the automated coil winding machine. Figure 4.1 depicts a supply unit with each of its major components labeled. The guide wheel [A] is used to guide the fiber onto the product spool. The tension sensor [B] measures the tension on the fiber while the machine is winding and is used for tension control. The guide wheel fine alignment system [C] allows for the fine positioning of the guide wheel with respect to the product spool. The base plate [D] integrates all the components of the supply unit together and is the structure to which the payout clamp (see chapter 2) attaches. The dancer pulley [E] is used in the active tension control scheme. The tension spring [F] is used in the passive tension control scheme. The supply spool [G] contains the fiber which is being wound onto the product spool. The ride arm [H] is the structure through which the supply unit is attached to the main shaft of the machine. And, the brake [I] can be used to prevent motion of the supply spool.

The automated coil winder possesses two supply units each of which is responsible for supplying one half of the total fiber for a full coil. This chapter will cover in detail the various aspects of the supply unit's design and development. This includes fiber guiding and tension control. Tests results performed on the actual supply units developed will be presented.



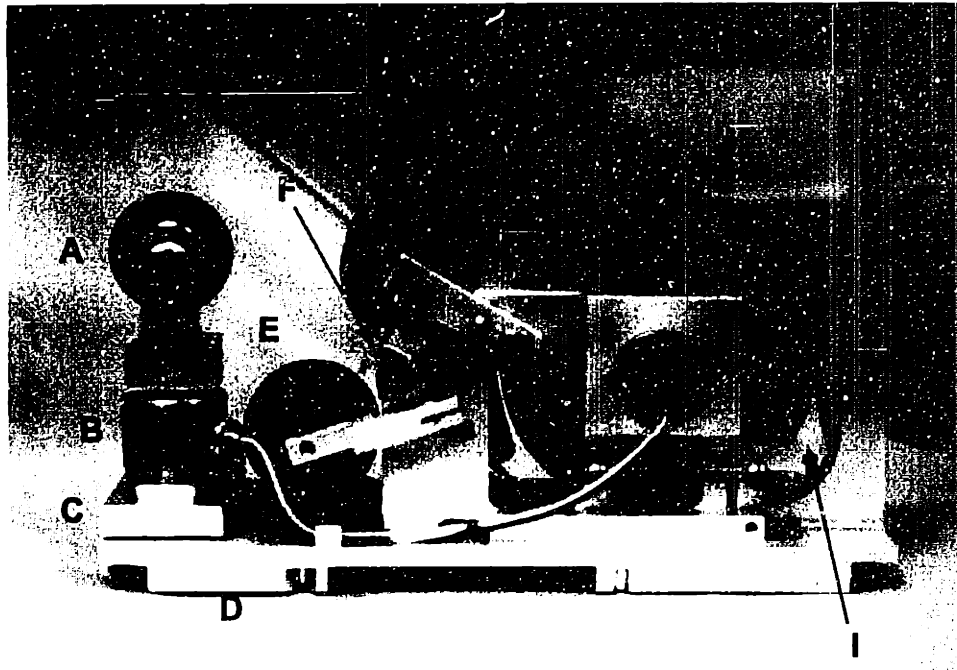


Figure 4.1: Supply unit. A) Guide wheel, B) Tension sensor, C) Guide wheel fine alignment system, D) Base plate, E) Dancer pulley, F) Passive tension spring, G) Supply spool, H) Ride arm, I) Brake

## 4.2. Guide Wheel Runout

### 4.2.1. Introduction

As mentioned in chapter 2 the guide wheel concept (see figure 2.9) was chosen as the method for guiding the placement of fiber onto the coil as it is being wound. However, the guide wheel concept is not without its difficulties. The guide wheel is expected to be able to guide fiber directly onto the coil at close range throughout the entire wind except for fibers which are suppose to lie directly against a flange of the product spool. The phrase 'at close range' indicates that the guide wheel is in fact positioned in between the two flanges of the product spool just below the surface of the coil at any given layer. In the worse case scenario the guide wheel is expected to guide a fiber which is only half a fiber away from the flange. Because the guide wheel must do this on next to either of the flanges this limits the overall thickness that the guide wheel can

be. For example, if the fiber to be wound is 250 microns in diameter, then the groove in the guide wheel must be slightly larger to accommodate the fiber and the walls on each side can be no larger than one half the fiber diameter, or 125 microns wide. Thus, the total width of this guide wheel is just greater than 500 microns, or about .020". That figure is for 250 micron fiber which is considered to be quite large for fiber optic gyroscopes.

To complicate matters, because the guide wheel is expected to be able to guide the fiber directly onto the product spool starting with the base layer, it must be able to reach all the way from outside the flange outer diameter to the product spool's core. Figure 4.2 illustrates how the fiber diameter and the flange depth dictate certain dimensions of the guide wheel.

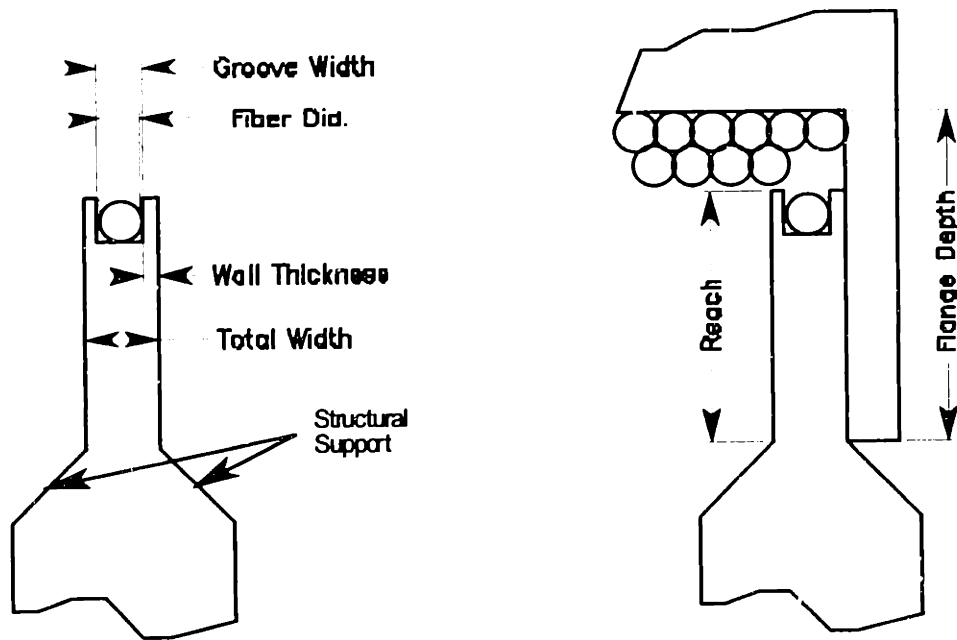


Figure 4.2: Guide wheel dimensions. The thickness of the guide wheel and its depth of reach are dictated by the fiber diameter and the flange depth.

Fiber optic Gyroscope coils typically have tens of layers of fiber which can build up an overall coil thickness of several tenths of an inch. For instance, a 40 layer coil using 250 micron diameter fiber will have a coil thickness (measured radially from the inner diameter to the outer diameter) of about .35" outside the jog zone

and .40" inside the jog zone of the coil. That means that the flange depth must be at least .40" deep to provide support for the entire coil, and correspondingly the guide wheel must have a reach of .40" to be able to guide fiber starting from the base layer.

This combination of long reach and thin walls is where the difficulty with guide wheels lies. With such a long thin structure the guide wheel is very susceptible to warpage as a result of machining stresses when being manufactured. As mentioned before, the idea for the use of a guide wheel originated from a subcontractor to the Customer who had been using the idea for their own semi-manual winding machine. This subcontractor had worked out a manufacturing process for producing guide wheels with axial runouts of no better than .001". However, this was a long (and thus costly) process involving several steps from wire EDM to surface grinding and heat treatments which took up to a day for a single guide wheel. This process was proprietary to the subcontractor, and so it was the MIT/MI's goal to design a guide wheel and work with a machine shop to develop a process by which to manufacture guide wheels with comparable or better quality. There was also a drive to reduce the cost of the guide wheels because it was anticipated that several would be needed throughout the winding experimentation process.

#### **4.2.2. Guide Wheel Development**

##### *4.2.2.1. Single-Piece Guide Wheel*

The first attempt at a guide wheel redesign centered on minimizing the number of sources of possible runout. The typical design involved a very thin disc, i.e. the guide wheel itself, and a hub and retainer structure (as seen in figure 2.9) to support the thin guide wheel. This assembly would then be fitted with high grade ball bearings for rotation about a shaft. The redesign sought to reduce the part count in the assembly from three pieces to only one piece under the assumption that the greater the number of pieces the greater the probability that one of the

pieces would have a relatively large amount of runout which would contribute to the guide wheel's overall runout.

A local machine shop collaborated on the design of the new guide wheel and went on to produce a few for testing. Figure 4.3 shows the new single-piece asymmetric design. The design incorporated the support structure, which formerly consisted of a separate hub and retainer, into the guide wheel itself. Large radii between the support and the thin section of the guide wheel, which gave it its reach, sought to reduce the local machining stresses.

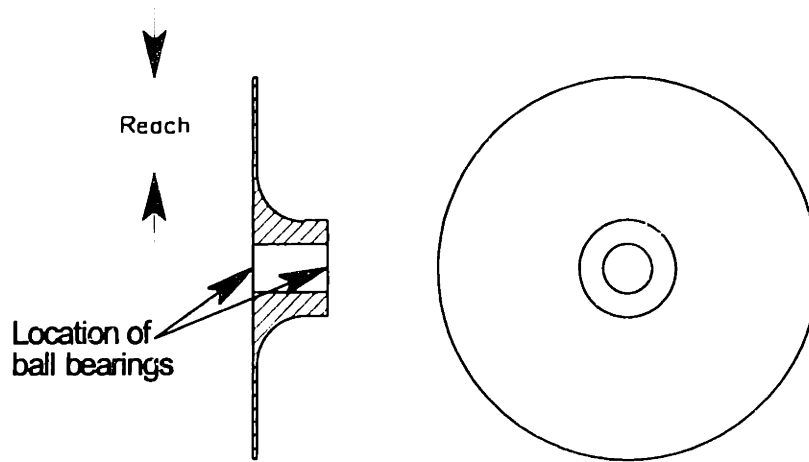


**Figure 4.3: Asymmetric guide wheel incorporates support structure into the guide wheel itself.**

The first guide wheels were made from stress relieved steel using basic lathe work to produce the part. The manufacturing time on the part was a few hours. The runout on these guide wheels, as measured visually under a high magnification vision system, ranged from about .0015" to .0025". These guide wheels were successfully used in several winding experiments on the test-bed winding machine. However, a small lag angle generally had to be employed to prevent the fiber from causing a gap error (see chapter 2) as a result of the runout.

An attempt to reduce the runout on this guide wheel design centered on changing the material from stress-relieved steel to a machinable ceramic which would not suffer from the same stress problems. However, this attempt failed as

the guide wheel groove wall thickness of only .005" was too thin for the relatively brittle material.

#### *4.2.2.2. Optimized Hub and Retainer Guide Wheels*

The single-piece guide wheel attempt was abandoned because it was not able to produce guide wheels of comparable runout to the original design. The next iteration in the design process focused on improving the original hub and retainer design. The original hub and retainer design sought to serve a general purpose guide wheel by having a reach of 0.5", thus being able to be used for even the largest of coils. In addition, the overall diameter of the guide wheel was approximately 2.0" leaving the inner 1.0" of the diameter for the support structure. The redesign of the original idea sought to reduce the overall outer diameter of the guide wheel with the belief that the smaller the guide wheel the less susceptible the guide wheel would be to warpage from machining stresses. Reduction in diameter was achieved on two levels. First, the reach of the guide wheel was reduced to just enough to accommodate the baseline coil desired by the Customer utilizing an MIT/MI flange design. Thus, the reach of the guide wheel was cut in half from 0.5" to only 0.25". Second, the size of the hub and retainer were shrunk down as much as possible being only large enough to house the bearings on which the guide wheel assembly would sit, and large enough to still provide a good amount of support for the guide wheel. In this way the guide wheel's overall diameter was reduced to only 1.15" from almost 2.0". Figure 4.4 shows the details of the new guide wheel assembly including the bearings. A cross-section of the original general purpose guide wheel assembly is shown to illustrate the dramatic reduction in size of the new guide wheels.

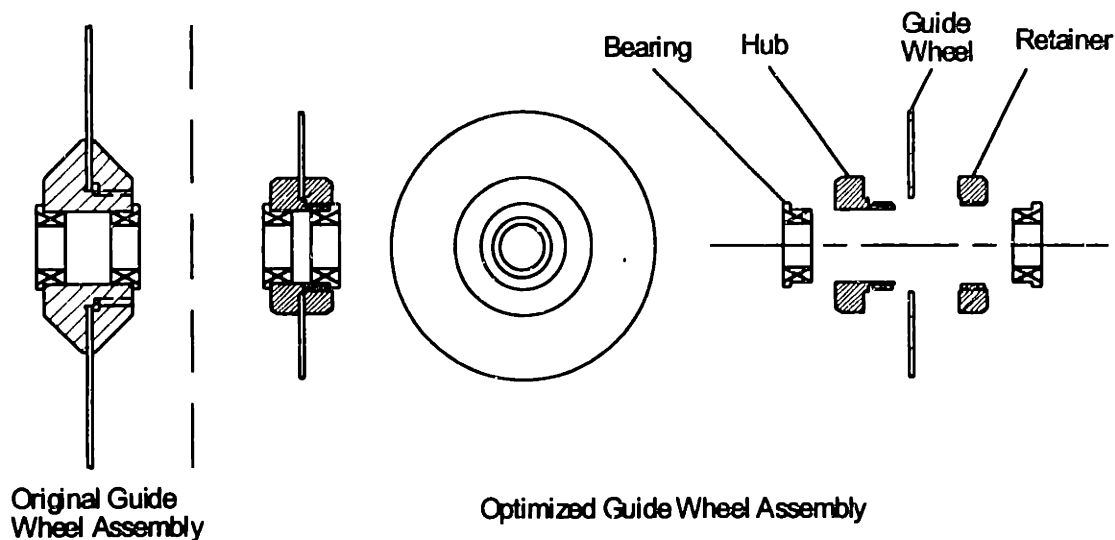


**Figure 4.4: Optimized guide wheel assembly redesign. The redesign of the original guide wheel assembly minimized the overall size of the guide wheel in an attempt to achieve lower runout.**

In addition to the physical changes in the design of the guide wheel assembly the process by which the actual guide wheel itself was changed. Recall that the original design began with a thin slice of stress-relieved steel cut using wire EDM from a larger cylindrical piece. That method require additional machining in the form of surface grinding which is a probably cause of machining stresses causing warpage on the piece. The MIT/MI again worked with the same local machine shop to develop a process for producing a guide wheel. The new design starts with shim stock made of spring steel. The idea was to let the manufacturer of the shim stock worry about keeping a very flat surface and uniform thickness in a stress-relieved material rather than machine the piece to the appropriate thickness. The only machining required would be to shape the outer diameter, place a small groove into it, and machine a center hole for mounting onto the hub. Later, a last step of lapping the thin part was added to increase the flatness of the piece. The orbital motions of the lapping process was preferred over the uniform motions of a surface grinder to randomize the direction of the induced surface stresses. This new technique required only about two hours to manufacture costing only \$120 each.

Runout on the first few guide wheels of this new design ranged from .001" to .0015". Based on the shape of the runout profile taken it was hypothesized that a large contribution of the runout came not from warpage of the guide wheel itself, but from runout of the surface on the hub which the guide wheel was pressed up against. (See the following sub-section for the interpretation of this runout profile).

Measurement of the runout on the hub revealed about .0004" of runout at the edge of the hub which was only 0.3" radially away from the center of rotation. Extrapolating this to the outer edge of the guide wheel, which was at 0.525" from the center, revealed that about one-half of the runout of the guide wheel assembly was coming from the hub alone. Additional hubs were sent out to a high precision shop, and when used in a guide wheel assembly the runout for guide wheels dropped to around and occasionally below .001" based on the quality of each individual guide wheel.

Thus, even though the overall quality of the redesigned guide wheels assemblies was approximately the same as the original one, the manufacturing costs of this very important part were significantly reduced.

### **4.2.3. Interpretation of Guide Wheel Runout Profile**

#### *4.2.3.1. Measurement Technique*

The runout of interest for the guide wheels was the axial runout. That is, the difference in position along the axis about which the guide wheel rotates as measured at the outer circumference of the guide wheel. In order to get an idea of what this runout looked like several measurements (every 45 degrees) along the circumference were taken and compared relative to each other and plotted to produce a runout profile. Measurements at each of the points were taken using the guide wheel registration technique outlined later in this chapter. A quick picture of a guide wheel's runout profile could also be taken using a dial

indicator. However, this technique involves pressing the dial indicator's spring loaded arm up against the surface of the guide wheel which was thought to influence the measurement, and in addition, dial indicators are known to have an inherent amount of backlash which would also affect the perceived amount of runout.

The subcontractor to the Customer indicated that the runout profile of their original guide wheels took on a 'potato chip' shape. That is, the profile had two peaks and two valleys as shown in figure 4.5. Such warpage was believed to be the result of the surface grinding process through which their guide wheels were subjected.

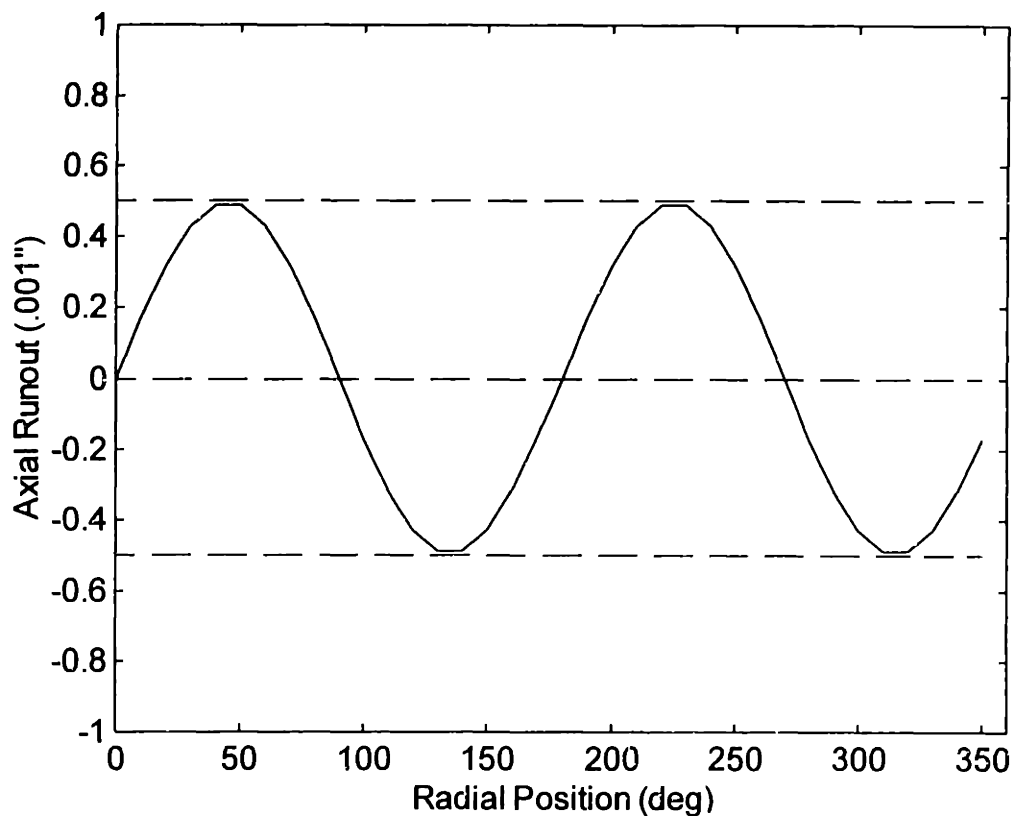


**Figure 4.5: Runout profile of original guide wheel assembly. The 'potato chip' profile is distinguished by its two peaks and two valleys.**



In contrast, the redesigned guide wheel assemblies exhibited a different runout profile as shown in figure 4.6. This profile has only one peak and one valley. The profile suggests that although the guide wheel may be warped, it is also likely that the guide wheel is simply rotating off its ideal axis. To clarify, even if the guide wheel were perfectly flat, if it were rotating about an axis that was not perfectly perpendicular to the plane of the guide wheel then runout resembling that of figure 4.6 would result.

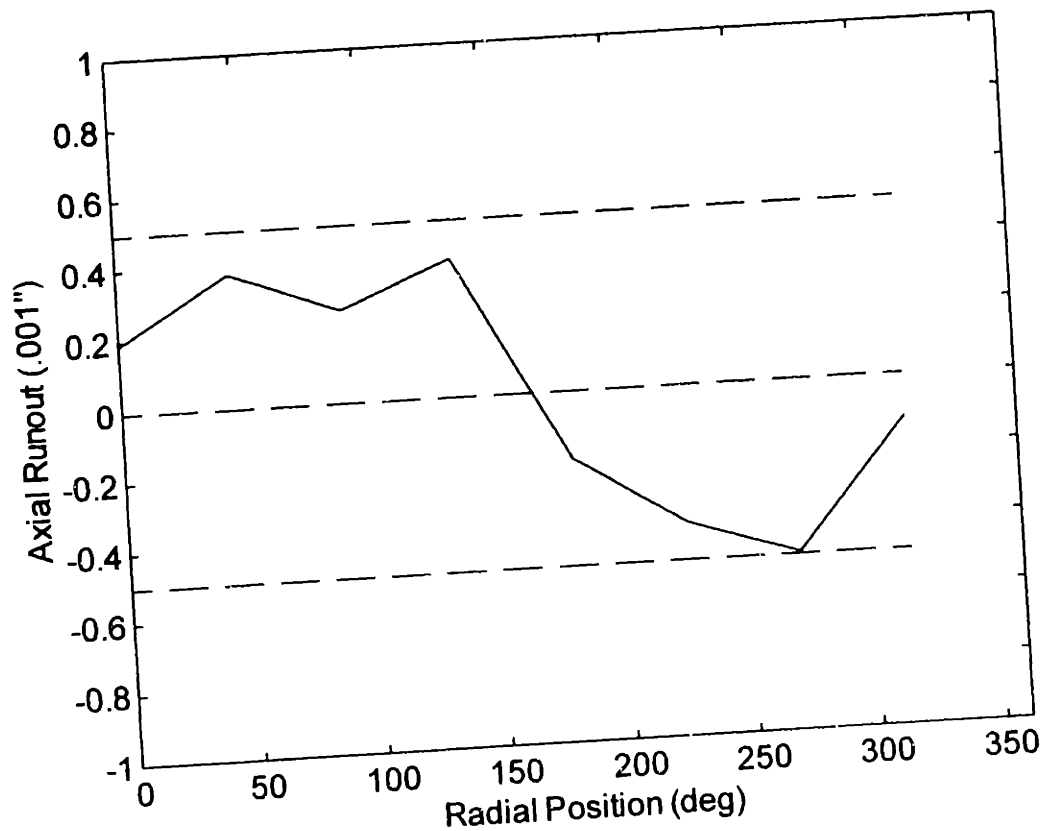


Figure 4.6: Runout profile of an actual redesigned guide wheel assembly. This profile reveals only one peak and valley.

To determine how much of the runout was based on the way in which the guide wheel assembly was seated on top of the two ball bearings a remounting repeatability test was run. In this test the runout profile was taken four times with the guide wheel assembly removed from and remounted on top of its bearing in a different orientation from trial to trial. Figure 4.7 shows the runout profile for each of the trials. Each of the four trials yielded results that were within .0002" of

the other trials at each of the locations where measurements were taken. Thus, it would seem that the interface between the bearings and the guide wheel assembly contributed little to the overall runout of the guide wheel.

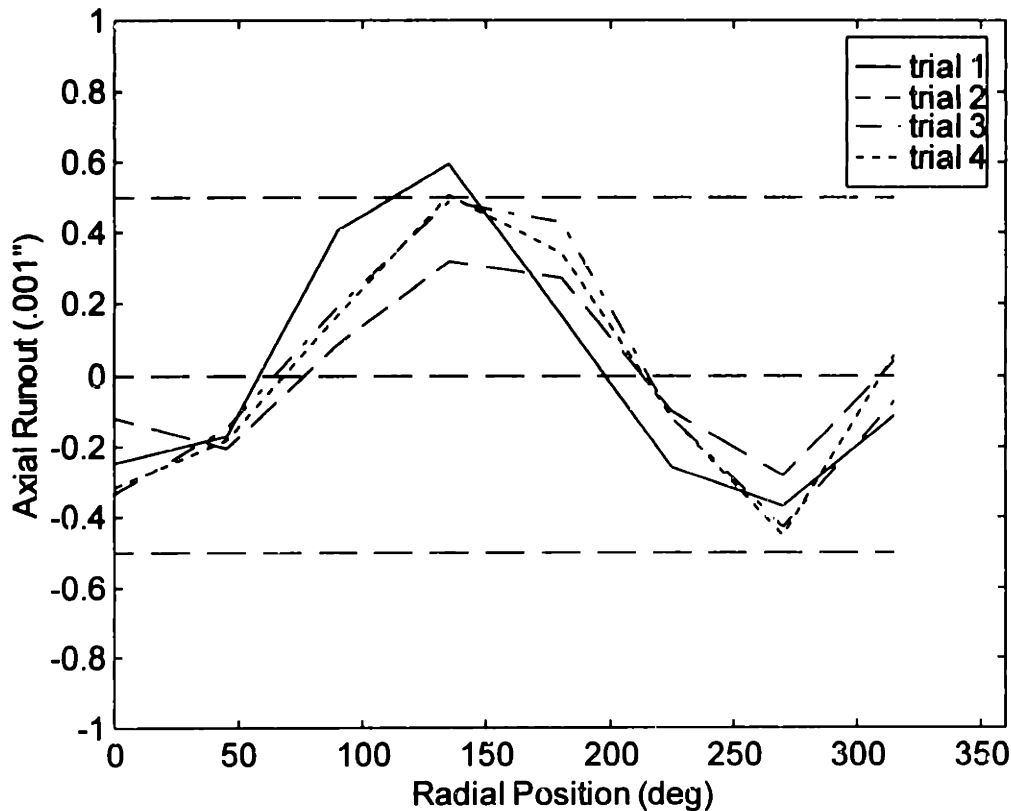


Figure 4.7: Runout profile remounting repeatability test.

#### 4.2.4. Further Improving Runout

The results of profiling the runout of the redesign guide wheel assemblies suggested that the guide wheel itself and the hub on which it is mounted each contributed about half to the total runout of the system. The runout of .001" represents as much as 20% of the smaller fibers used to wind fiber optic coils. While it has been shown to be sufficient for winding coils through numerous winding experiments, improved runout from about .002" to .001" has also been shown to improved the quality of the wind.

Further improvements could possibly be made by obtaining more accurate parts, i.e., adjusting the process to obtain flatter guide wheels and hubs with less runout. Another idea was conceived, but not implemented, to actively try to compensate for the runout of the guide wheel. This method involved knowing what the runout profile of the guide wheel was and also knowing at which orientation it was at any given moment during the winding of a coil. Given this knowledge, the positioning system on top of which the supply unit sits could be rapidly adjusted to shift the entire supply unit and thus the guide wheel to make it seem to the fiber as if the guide wheel had zero runout. A feasibility study was performed which showed that the positioning system could rapidly make small adjustments based on a given profile. The real challenge in implementing a full scale system lies in being able to determine the orientation of the guide wheel at any given time in the wind. The idea was abandoned given the added complexity to the system and the lack of knowledge over the marginal improvement to the winding quality that would have been obtained through a full implementation.

### ***4.3. Guide Wheel Fine Alignment***

#### **4.3.1. Introduction**

Given a perfect guide wheel, as described in the section on guide wheel runout, there would still be problems with guiding fiber with the guide wheel right up against a flange if the guide wheel was not aligned properly. Figure 4.8 shows how misalignment of the guide wheel can affect the guide wheel's ability to guide fiber into a region close to the flange. The figure illustrates a rotation about the Y axis. A similar sort of flange interference would happen if there was misalignment about the Z axis.

Fine alignment of the guide wheel was not designed into the test-bed winding machine and the affects of this could be seen as the first and last couple

of turns on any given layer were the most difficult to guide into the proper position for exactly the reason noted. The winding experiments on the test-bed emphasized the need to provide for such fine alignments. Such alignment mechanisms were also not seen on any of the machines surveyed early on in the project which utilized the guide wheel concept.

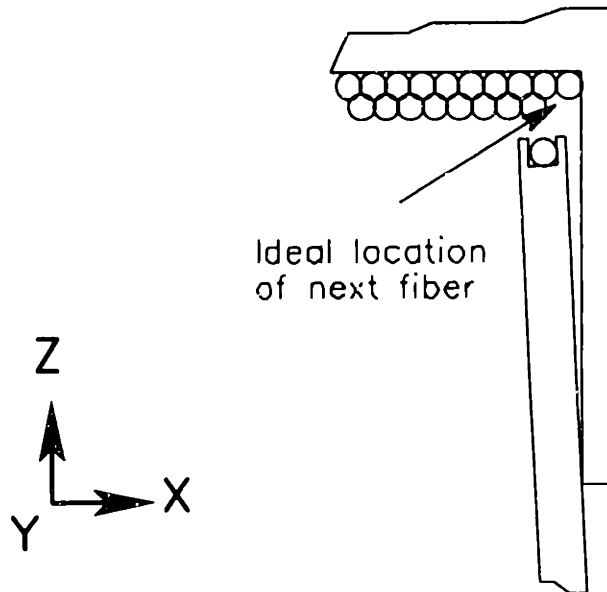


**Figure 4.8: Guide wheel misalignment. Improper alignment of the guide wheel with respect to the flange interferes with its ability to wind against the flange.**

#### **4.3.2. The Fine Alignment Mechanisms**

Given the importance of good alignment of the guide wheel to the flanges of a product spool it is unclear why fine alignment systems were not in place on other winding machine. Fortunately, it was not difficult to incorporate such systems into the supply units. Figure 4.9 shows the fine alignment system for the rotation of the guide wheel about the Y axis. Two opposing set screws are used to adjust and lock down the angle of the guide wheel about its pivot. A dial indicator is placed on the surface of the guide wheel while the supply unit is mounted in place in its payout position. The dial indicator is moved across the surface to measure the angle of tilt and the set screws are adjusted accordingly

to reduce the angle to zero. The particular implementation has one drawback which is that not only do the set screws adjust the angle of the guide wheel, but they also affect its lateral position along the X axis. This unfortunate side effect is a result of the location of the pivot. Ideally, the pivot would be located as close to the top of the guide wheel. However, there was no convenient location for the pivot and opposing set screws near this location which would not interfere with the operation of the guide wheel or interfere with the readings of the load cell. Fortunately, the offset of the guide wheel is easily corrected for in software once the guide wheel is registered to a known location. See the section on guide wheel registration later in this chapter for more information on guide wheel registration.

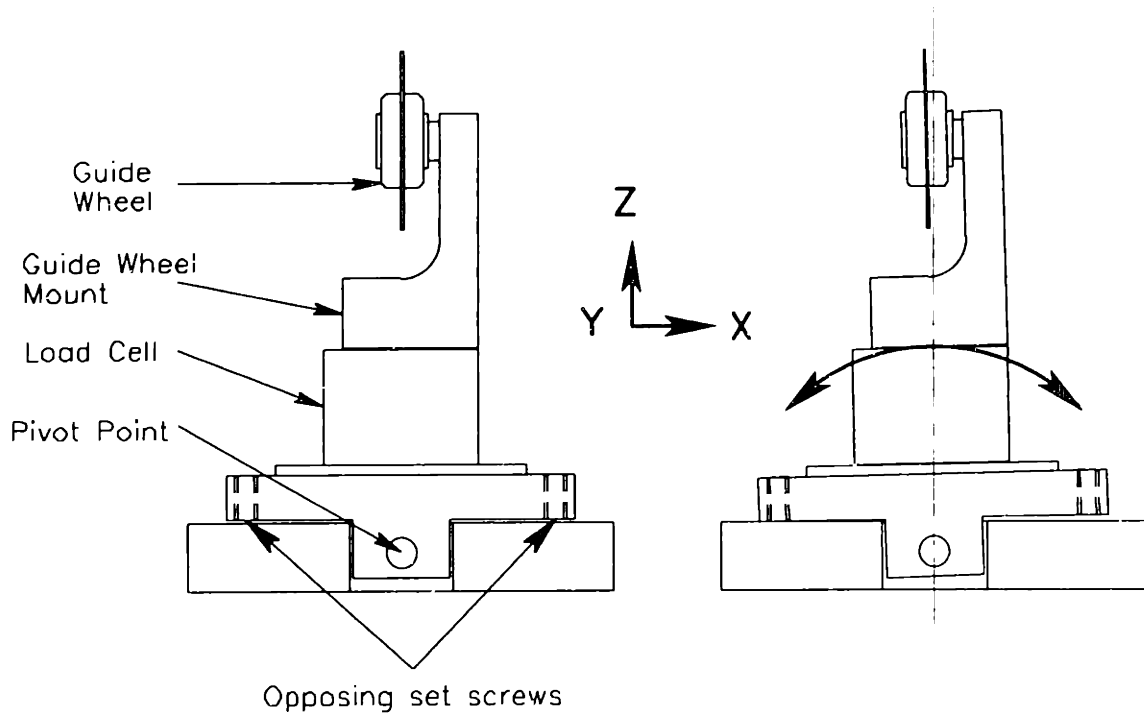


**Figure 4.9: Fine alignment of the guide wheel about the Y axis. Opposing set screws adjust and lock down the angle of the guide wheel about the pivot.**

Figure 4.10 shows the fine alignment system for rotation of the guide wheel about the Z axis. Again, two opposing set screws are used to adjust and

lock down the angle of the guide wheel! This time also the pivot point is not located in its ideal location which is down the center of the guide wheel.

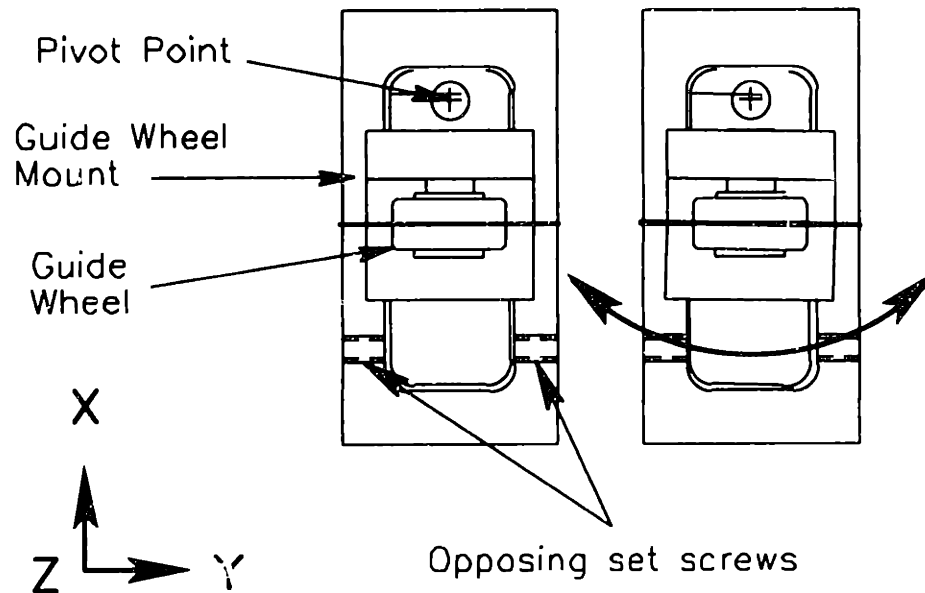


**Figure 4.10: Fine alignment of the guide wheel about the Z axis. Opposing set screws adjust and lock the angle of the guide wheel about the pivot.**

### 4.3.3. Testing and Results

The automated coil winding machine was used in several small (less than ten layers) winding experiments as well as a few large (greater than twenty layers) winding experiments. During these tests the guide wheel was successfully used time and time again to guide fiber onto the coil as close as  $\frac{1}{2}$  of a fiber away from the flange as is illustrated in figure 4.2. This was not the case when using the test-bed winding machine. Thus, the importance and success of the fine alignment system was proved out.

During the winding process the supply unit, and thus guide wheel support structure, is subjected to constant machine vibrations. In addition, the guide wheel itself if physically touched by the flange every time it is registered against a flange which can happen as often as once per layer, and occasionally when it

is winding a fiber near the flange because the alignment to the flange will never be 100% perfect.

To determine the affect that these constant forces on the guide wheel would have on the fine alignment system a repeat alignment was performed after several winding experiments were completed. The realignment test showed that the alignment about the Y axis was off by 0.0015" over a 0.200" distance for one supply unit and less than 0.0003" over a 0.200" distance for the other. About the Z axis, the alignment was off by .0012" and 0.0004" over 0.200" for the supply units, respectively. Both supply units continued to have success guide fiber onto the product spool after a period of time. However, the repeat alignment test showed that at least one guide wheel's fine alignment system needed to be re-adjusted. Such re-adjustment could potentially be avoided by applying thread locking compound to the opposing set screws which control the guide wheels' alignment. Not enough experiments were performed to determine a long term alignment maintenance schedule.

## ***4.4. Guide Wheel Registration***

### **4.4.1. Introduction**

In the last section, the importance of fine alignment of the guide wheel with respect to the flanges was stressed. In this section, the importance of repeatable relative positioning of the guide wheel with respect to the flange will be discussed.

As mentioned before, the supply units must alternatingly wind fiber onto the coil in order to wind a complete fiber optic coil. Each alternation by supply units involves swapping one supply unit out of its ride position back into its payout position while swapping the other supply unit out of its payout position and into its ride position. Ideally, the payout clamp which couples the supply unit

to the main positioning system has 100% repeatability, and the rotational axis on top of which the payout clamp sits also has 100% repeatability. However, as discussed in Chapter 3 the payout clamp does not have perfect repeatability. In addition, the rotational axes have been measured to have as much as 0.3 degrees of backlash. This amount of backlash translates into several thousandth of an inch in lateral offset of the guide wheel with respect to the flange.

If winding were to proceed under the assumption that the guide wheel was in exactly the same position after having swapped a supply unit into payout position as it was the last time the same supply unit was swapped in, then some layers would be wound with the fiber going nicely into place, while other layers would potentially be a horrible mess with winding errors happening frequently. Mis-positioning of the guide wheel by as little as 0.001" has been shown to have a significant effect on the quality of the wind for any given layer. Although, some winding patterns are less affected by guide wheel positioning errors, the automated winding machine developed was responsible for the most sensitive of winding patterns. Thus, there was a need for some form of guide wheel registration to let the machine know where the guide wheel was with respect to some known coordinate. The flanges of the product spool were chosen as the registration surfaces, because once these coordinates were known the location of all the grooves formed by the underlying layer of fiber would also be known.

#### **4.4.2. Registration Concept Selection**

Several concepts were under consideration for the registration of the guide wheel against the flange. They were the use of a high precision sensor external to the guide wheel structure, sensing electrical contact of the guide wheel to the flange, and sensing physical contact of the guide wheel to the flange.



#### 4.4.2.1. High Precision External Sensor

One of the first concepts involved the use of a high precision sensor capable of micron and sub-micron level accuracies. Inductive sensors with such capabilities were identified. Figure 4.11 shows the use of such a device to determine the location of the flange. The sensor would also be mounted to the same supply unit as the guide wheel. Thus, if the relative position of the sensor to the guide wheel is known, then the relative position of the guide wheel to the flange would be known after the sensor was used to register the location of the flange.

However, there are many difficulties involved in using this technique. In order for the sensor to get a measurement of the distance to the flange the sensor must lie somewhere in-between the two flanges of the product spool. This would be difficult because the Customer could potentially wind coils so thin that there would be no room for the sensor in-between the flanges. The sensor would also have to be capable of performing measurements to either flange meaning its orientation would have to be flipped regularly. Finally, the relative position of the guide wheel to the sensor would somehow have to be determined, and this measurement would have to be re-taken each time the guide wheel's fine alignment system was adjusted.

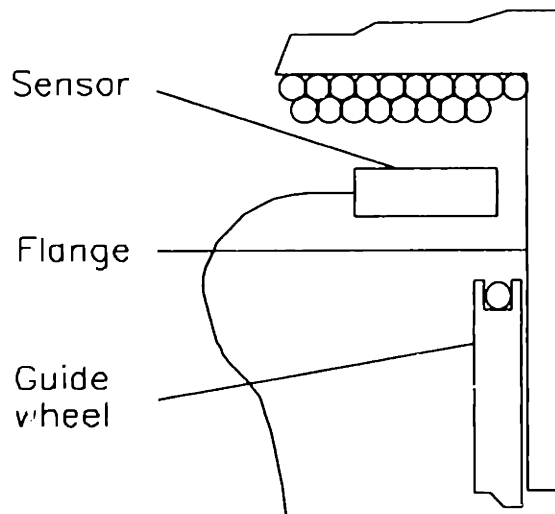


Figure 4.11: Guide wheel registration using a high precision external sensor.

#### *4.4.2.2. Electrical Contact of the Guide Wheel to the Flange*

The need for the sensing device to be able to fit in-between the two flanges of the product spool suggested that the device be very thin. The idea to use the guide wheel itself as a sensing surface grew out of this need. The idea involved using the contact between the guide wheel and the flange to complete an electrical circuit. The guide wheel would be slowly incremented towards the flange, and when the circuit was completed the guide wheel would be registered. Limited tests were performed on the test-bed winding machine to determine the feasibility of this concept.

The tests showed that the method was feasible and repeatable to at least 0.001" if not better. However, complications on the method's implementation on the automated winding machine were noted. The bearing on top of which the guide wheel proved a poor electrical conductor. This necessitated some form of electrical brush from the guide wheel mount to the guide wheel surface itself. Such a brush would have to be cleaned and replaced at some regular interval. More importantly, such a brush would potentially affect the actual tension of the fiber being wound onto the coil as the friction caused by the brushing on the guide wheel would be undefined. Electrical conduction on the flange end of the circuit also suffered from conduction problems through the main shaft's bearings.

#### *4.4.2.3. Physical Contact of the Guide Wheel to the Flange*

The final concept for guide wheel registration involved sensing the physical contact of the guide wheel to the flange. The guide wheel structure is mounted on top of a load cell sensor used to measure the tension on the fiber (see section on active tension control later in this chapter). The idea was to use the load cell to sense a change in force when the guide wheel contacted the flange.

There were a couple of concerns regarding this method. The forces involved in the contact between the guide wheel and flange would apply a

moment on the load cell rather than a downward force. The load cell is designed to resist such moments and a static loading experiment to simulate the sideways loading at the guide wheel tip showed that, in fact, the load cell's output was changed by less than one millivolt (equivalent to about .0125 grams) for a 20 gram load. The constant torquing on the load cell was also a cause for potential concern that the load cell might suffer some permanent damage.

Tests were run to determine the feasibility of the method. Although, the load cell was resistant to static sideways loads it would register a temporary change in load as soon as the load cell contacted the flange. Multiple test trials of registration using this method also showed that the load cell was not permanently affected by the repeated moment loading.

This method of using the load cell to sense the physical contact of the guide wheel to the flange surface was chosen as the method of registration. The method proved at least as accurate in test trials as the electrical contact method described, and was by far the simplest to implement since it involved no additions to the supply unit system. The same method of registration was chosen to locate the guide wheel in the vertical direction by registering the guide wheel vertically against a registration surface of known diameter.

#### **4.4.3. Testing and Results**

A repeatability test was run on the registration method chosen. The test involved registering the guide wheel against the flange several times with the guide wheel being back away from the flange each time it was registered. The position of the X axis which incremented the guide wheel closer and closer to the flange until contact was made was noted. Figure 4.12 shows the results for this test over ten trials. The test shows that the registration repeatability is approximately +/- 0.00025". This data was used to determine that, during winding, a minimum of three registrations of the guide wheel to the flange would be averaged to

determine where the actual location of the flange was, thus increasing the accuracy of the registered location.

This method of registration was successfully used to wind tens of layers of fiber. The implications of such successful winding over a large number of layers suggests that winding a coil follows a very theoretical pattern. That is, the fiber in the coil does not shift around much even after several layers, and the guide wheel can be placed according to a pre-defined pattern and be expected to guide the fiber into the proper spot. The significance of this discovery suggests that to a certain extent fiber optic coils can be wound with open-loop placement of the guide wheel so long as the placement of the guide wheel is well-known (registered), guide wheel runout is low, and mandrel runout is also low. This was not known to necessarily be true from previous winding efforts including the MIT/MI's own test-bed winding machine because of either the relatively poor quality of the wind produced or the amount of manual intervention required to obtain a good quality wind.

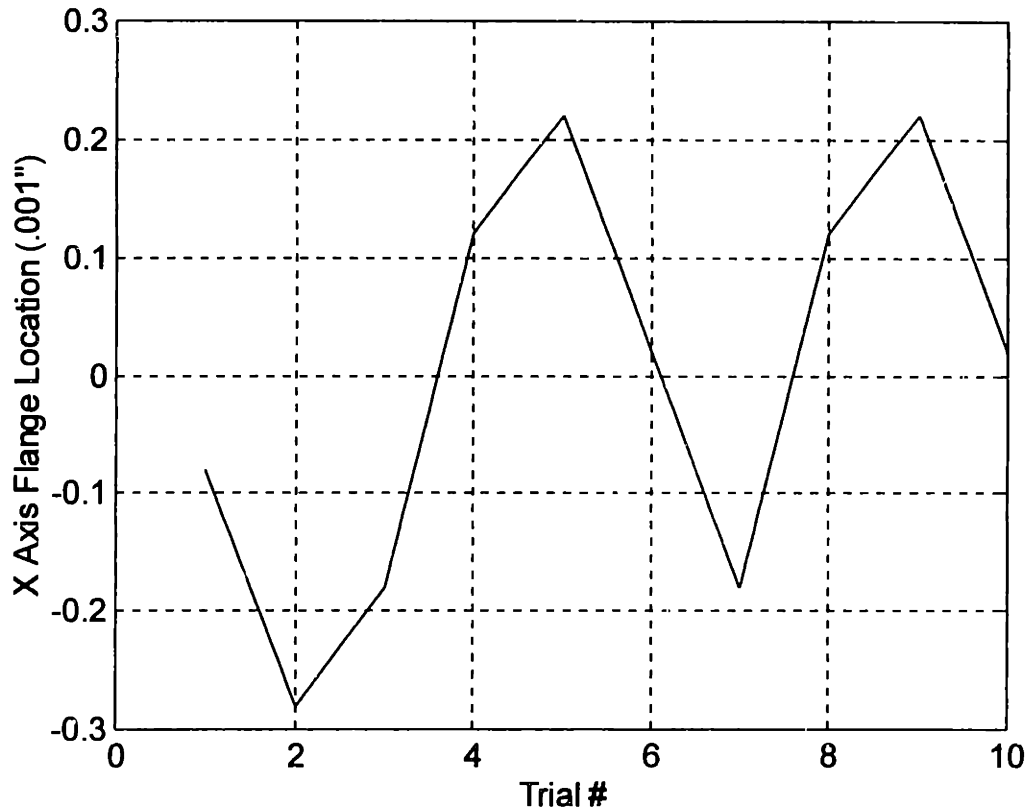


**Figure 4.12: Guide wheel registration repeatability test.**

By noting the registration location of the guide wheel each time a supply unit is swapped back into payout position the importance of registration can be highlighted. Figure 4.13 shows exactly this data for both supply units A and B during an actual winding experiment with the registration location being noted for each layer of the wind. The data collected shows that if it were not for the guide wheel registration performed after each swap in of a supply unit the guide wheel could potentially be off by as much as 0.006" from where it should ideally be. Such distance represents over 100% of the smallest fiber diameter required by the Customer. This data together with the payout clamp repeatability test (see section 3.4) suggests that most of the repositioning error that occurs during a swap in of a supply unit is a result of the backlash of the rotary tables on top of which the payout clamp sits.

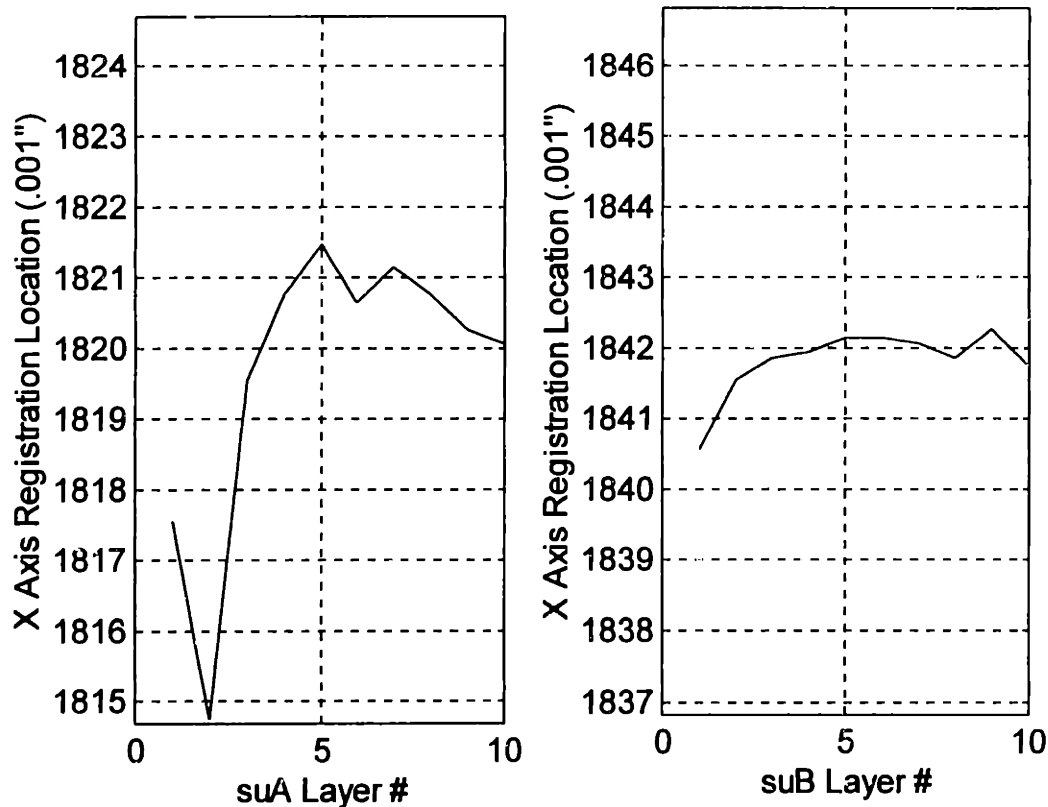


Figure 4.13: Flange registration location data over several layers of winding for supply units A and B.

## 4.5. Inactive Fiber Immobilization

### 4.5.1. Introduction

At any given time during a wind there is one supply unit in payout position paying out fiber onto the product spool while the other supply unit is in ride position rotating with the main shaft. The fiber which goes from the riding supply unit to the product spool is termed the "inactive" fiber while the fiber being paid out is termed the "active" fiber. When a supply unit is being swapped out into its ride position its fiber becomes inactive. If slack is allowed into the inactive fiber line it would threaten to uncoil already wound fiber. In traditional manual winding machines this problem is solved by taping the inactive fiber down to the product

spool's flange, thus immobilizing it. Devising a method for taping down the fiber in this manner is not suitable to automation. Other semi-automated winding machines surveyed continued to apply tension to the inactive fiber to immobilize it. This approach was taken for the automated winding machine.

#### **4.5.2. Concept Generation and Selection**

##### *4.5.2.1. Applying Tension With A Motor Bias*

One idea for immobilizing the inactive fiber involved applying a bias current to the supply spool motor to maintain tension on the line. The difficulty in this method lies in the fact that the supply unit requiring the bias current is rotating in its ride position with the main shaft. Two methods were available to supply the bias current. The first involves using an electrical slip ring to provide a rotating electrical contact. The second involves using a battery to provide the necessary current.

The difficulties with using an electrical slip ring surround the fact that the supply unit must lock into ride position at different locations throughout a wind and also depending on the size of the coil to be wound, so that a single point contact is not sufficient for supply power. The issues surrounding the use of a battery for power involve the lifetime of the battery.

The test-bed winder's supply units were designed with the battery alternative in mind. Figure 4.14 depicts the use of a battery to apply a bias current to the supply spool motor. Several winding experiments were successfully completed using this concept for immobilization. However, use in the test-bed also highlighted the concept's limitation which centered on battery life and thus battery replacement. The pair of standard AA batteries contained enough stored energy to supply current to the supply spool motors for a moderate size wind, but would not last through the full wind of larger coils required by the Customer. The idea of switching to rechargeable batteries was explored. Although, rechargeable batteries offer lower energy densities than

standard alkaline batteries, it was thought that the ability to recharge the batteries during a wind would allow for similar sized or smaller batteries to be used. The main issue concerning rechargeable batteries involved the complexities of actual recharging of the batteries which would occur whenever a supply unit was locked into payout position and fiber immobilization was not needed.

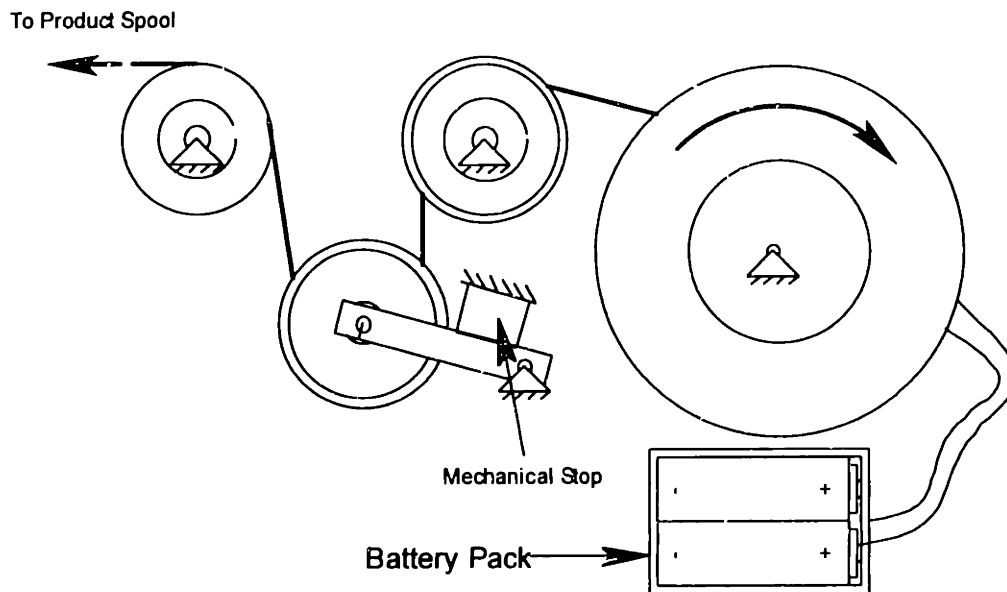


**Figure 4.14: Inactive fiber immobilization using battery power to apply a bias current to the supply spool motor.**

#### **4.5.2.2. Applying Tension Using a Spring**

Another concept for fiber immobilization involved using a tension spring and a brake. In this idea, the fiber is required to be routed through a dancer pulley attached to the end of a dancer arm. Figure 4.15 illustrates this concept. Just before a supply unit is released from its payout clamp into its ride position the fiber is pulled with enough tension such that the dancer arm rises up and presses against a tension spring. At this time, the supply unit's brake engages the supply spool and prevents it from rotating, thus, the tension spring pushing on the dancer arm continues to provide tension to the fiber line.



The disadvantages of this method include the addition of the brake mechanism and the actuator to operate it. Also, the method relies on the existence of a dancer pulley which assumes a certain form of active tension control (see section on active tension control later in this chapter), whereas the motor bias method works just as well with or without a dancer pulley.

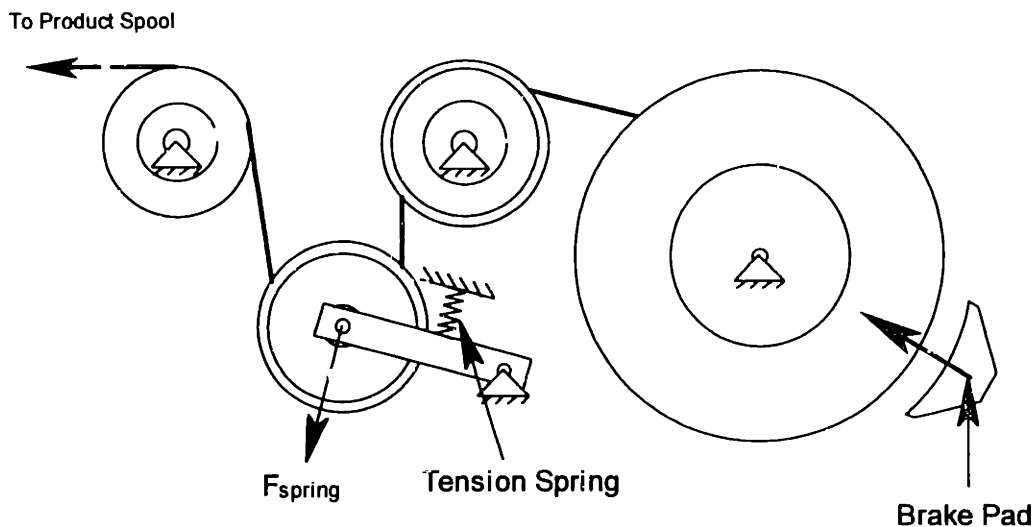


**Figure 4.15: Inactive fiber immobilization using a tension spring to apply a tension to the fiber through a dancer arm and pulley. The brake pad engages the supply spool to prevent it from rotating and releasing tension from the line.**

In the end, the tension spring method was chosen over the motor bias method for several reasons which had little to do with the limitations or complexities of any of the motor bias methods. The added complexity of a brake had additional uses other than for fiber immobilization. A brake could be used during the loading of both supply units on to the machine, the only time when fiber can freely move from one supply unit to the other. Here, a brake could prevent the fiber from doing just that. Without a brake, there would be no way to prevent unwanted movement of the fiber. In addition, the actuator for the brake mechanism was able to be off-loaded from the supply unit to the payout clamp, thus saving space on the supply unit itself and eliminating the need to any additional electrical connections to the detachable supply unit.

## **4.6. Active Tension Control**

### **4.6.1. Introduction**

The Customer considered active tension control over the fiber as it is being wound onto the product spool to be one of the more important issues regarding the automated winding machine. Poor control over winding tension has been shown to degrade the performance of a coil. The Customer placed tight specifications on the average winding tension when considering the winding speeds needed to achieve the desired throughput. The desired winding tension levels ranged from close to zero grams to tens of grams of tension. It was believed early on from talking with fiber optic coil winding experts, that the ability to spike the tension while winding would prove useful in winding error prevention and correction. In addition, a model was in development during the project which suggested that applying a special profile to the winding tension throughout the course of winding a full coil would produce a more uniform final tension in the final coil, and thus lead to better gyroscopic performance.

There are some factors which complicate the control of tension on the fiber during winding. The fiber is not guaranteed to be wound very neatly onto the supply spools from which they are payed out. Thus, the variations in the way the fiber comes off of the supply spool must be accommodated by the tension control system. In addition, because the tension control system was to be housed in the supply unit, it was desired to minimize the overall size and weight that the control system added to the supply unit which would be spun around the main axis for 50% of the time of a total wind.

This section will present the various tension control schemes which were considered. Theoretical models for two of the control schemes were developed and will also be presented. Experimental data taken on the test-bed winding

machine and the final automated machine will be compared and contrasted to the theoretical models. And, finally, the benefits of the final tension control scheme implemented will be discussed in the context of actual winding experiments conducted.

#### **4.6.2. Tension Control Methods**

##### *4.6.2.1. Constant Tension Control Methods*

Among the possible tension control methods available the easiest and perhaps the most common are the constant tension control methods. These methods either employ a spring loaded pulley or pulley pair, or a dancer pulley (gravitational spring), with positional feedback to maintain a constant level of tension on the fiber throughout the entire wind. These methods were ruled out early in the design stage because they did not satisfy the desire to be able to profile and spike the tension on the fiber during the winding process.

##### *4.6.2.2. Inertia De-coupled Tension Control Using A Magnetic Brake*

A method seen by the MIT/MI implemented at a sub-contractor to the Customer's site sought to achieve good tension control over the fiber by de-coupling the tension control mechanism from the inertia of the fiber payout system. Figure 4.16 shows the components and layout for this method. The payout system utilizes a servo driven motor attached directly to the supply spool. A high precision rotary position sensor feeds back the position of the dancer pulley to the supply spool motor. The payout rate of the fiber is kept at the required rate by maintaining the position of the dancer pulley. After the fiber routes around the dancer pulley, it then goes around another pulley before going to the guide wheel. The fiber is pinched between this pulley and another wheel connected to a variable resistance magnetic brake. The tension on the fiber when the brake is not engaged (i.e. the wheel is free-spinning) essentially is determined by the

weight of the dancer pulley. A load cell on top of which the guide wheel is mounted is used to monitor the out-going tension of the fiber. The braking resistance of the brake is determined by a second feedback loop from the load cell to the brake.

In this way, the tension on the fiber can be maintained at a constant rate or continuously adjusted through the load cell to brake feedback loop. The reason behind de-coupling the inertia of the fiber payout system from the tension control system is to achieve a higher bandwidth tension control system. Depending on how the supply spool is designed, it can represent a significant inertia. In addition, in the case of the sub-contractor's actual system, the supply spool drive motor represented a large inertia when compared to that of the supply spool and other pulleys in the system.

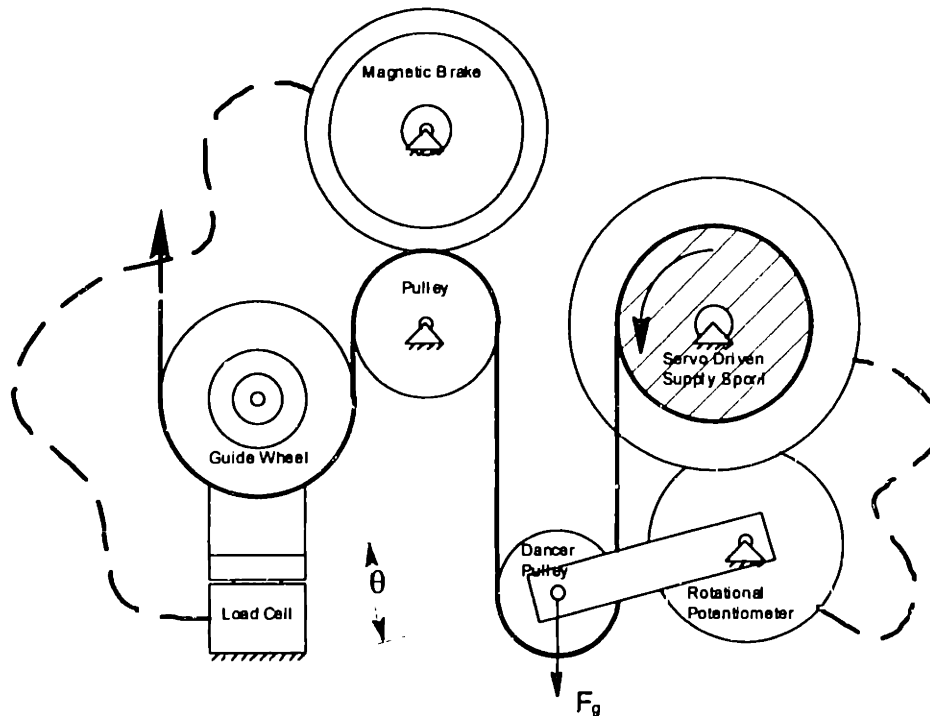


**Figure 4.16: Inertia de-coupled tension control method using a magnetic brake. Feedback loops are indicated by the dashed lines.**

This tension control method has the potential for very good control over the tension on the fiber while also allowing full tension profiling during winding. The disadvantages of this approach include the method's complexity and size. The particular components used by the sub-contractor occupied quite a bit of space. The system could be optimized by more carefully selecting components more suited to the task at hand. For instance, the supply spool motor could easily support a fiber payout rate many times the actual rate required. However, the Customer also voiced concerns over the possible damage to the fiber caused by the pinching of the fiber between the pulley and the wheel connected to the magnetic brake. For these reasons this method was not really pursued beyond conceptual consideration.

#### *4.6.2.3.Dancerless Tension Control*

In an effort to minimize the complexity of the tension control system a system was proposed which involved nothing more than a tension sensor, a servo driven supply spool, and a stationary pulley whose only purpose was to feed the fiber from the relatively wide supply spool to the narrow guide wheel. Figure 4.17 shows the layout for this approach. In this approach, the only form of closed loop control that exists is from the load cell measuring tension to the supply spool's drive motor. This feedback allows for tension profiling as discussed previously.

The method relies on designing a very low inertia supply spool and driving it with an even lower inertia and low friction motor. The idea seeks to use the small supply spool motor as a torque source to provide variable resistance to the fiber which is pulled off of the supply spool as the motor is back-driven. The supply spool motor size would be optimized to be able to provide no more continuous torque than required amounting to only one or two ounce-inches of torque.

The benefits of such a simple system are clear. The concerns over this approach was whether the system's inertia and friction could be kept low enough to allow a high enough bandwidth system to achieve good tension control. Also, it was also not clear how robust the system would be to variations in fiber payout from the supply spool due to a poor pre-wind onto the supply spool.

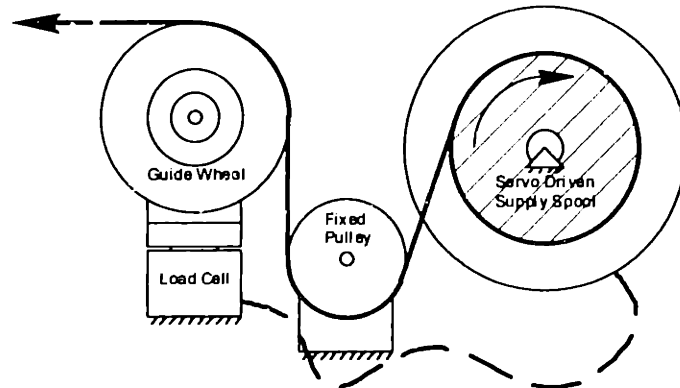


**Figure 4.17: Dancerless tension control system. The dashed line indicated a feedback loop from the load cell to the supply spool motor.**

#### *4.6.2.4.Active Dancer Tension Control*

The final method for tension control that was under consideration involved the use of what is termed an “active dancer” and sought to represent a compromise between the two previous methods. Figure 4.18 shows the layout for this tension control scheme. The magnetic brake and associated pinching of the fiber have been eliminated from this approach and instead replaced with a low-inertia and low-friction servo motor (with encoder) acting as the pivot point to the dancer pulley. The encoder attached to the dancer motor is used as positional feedback not for the dancer motor, but for the supply spool motor. The tension level feedback from the load cell is used by the dancer motor to maintain a desired tension level.

Once again, the dancer pulley seeks to de-couple the tension control from the inertia of the supply spool. It does not succeed to the extent that the magnetic brake with a dancer pulley does. However, whereas the dancerless tension control scheme is directly affected by the inertia of the supply spool, in the active dancer method the supply spool motor's inertia has an indirect affect on tension by limiting the system's ability to compensate for positional changes of the dancer pulley.

The base tension applied to the fiber is a function of the dancer pulley's weight. With feedback from the load cell to the dancer turned off, this system reduces to the simple case of constant tension level control mentioned earlier. However, with load cell feedback of the actual tension to the dancer motor, full tension profiling capabilities are possible.

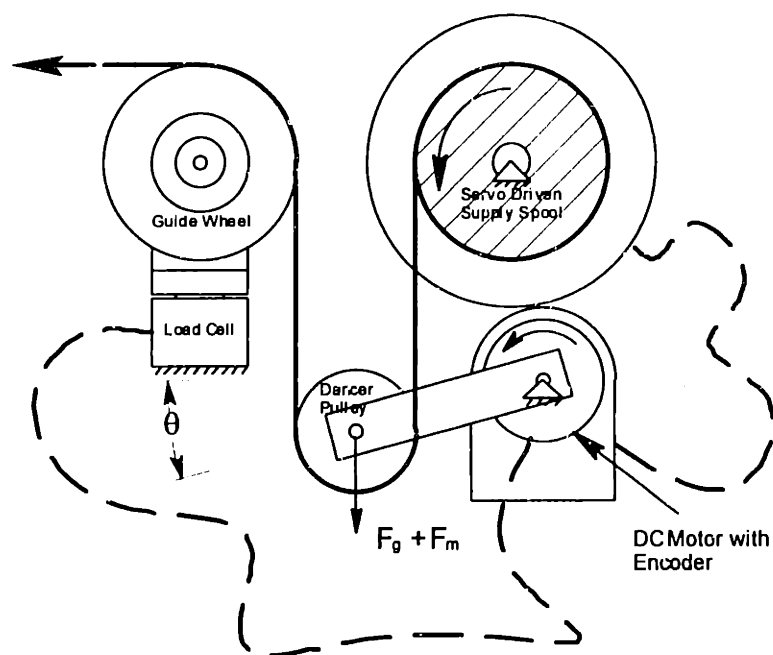


Figure 4.18: Active dancer tension control method.

### 4.6.3. Tension Control Models

#### 4.6.3.1. Introduction

Models of the dancerless and active dancer tension control methods were produced to examine the two methods' ability to maintain good control over tension on the fiber while winding a coil. The development of these models will be presented as well as the results gathered from winding simulations performed using the Mathworks' Matlab™ Simulink™ simulation software.

#### 4.6.3.2. Dancerless Tension Control Model

The dancerless tension control model is based on the concept drawing depicted in figure 4.17. Figure 4.19 shows the idealized mechanical model of the dancerless tension control system. The model is based on the following assumptions:

- The inertia of the supply spool motor is negligible when compared to the inertia of the supply spool itself which is mounted directly onto the motor.
- The inertia of the guide wheel is negligible.
- Friction is negligible for all pivot points.
- There is no slippage of the fiber with any of the wheels around which it is routed.
- Fiber in tension is extremely stiff. The spring and dampers modeled are not a result of fiber in tension, but rather a result of the fact that fiber does not naturally route around the small radii of the supply spool, intermediate pulley, and guide wheel.

The variables  $R_g$ ,  $R_d$ , and  $R_s$  are the radii of the guide wheel, intermediate pulley, and supply spool, respectively.  $J_\theta$ ,  $P_\theta$ , and  $J_s$ ,  $P_s$  are the rotational inertia and angular momentum of the intermediate pulley and supply spool, respectively.  $K_1$ ,  $K_2$ , and  $B_1, B_2$  represent the spring stiffnesses and damping constants for the



portions of fiber indicated.  $V_c$  is the fiber velocity source which determines at what rate the fiber is being drawn from the supply spool onto the coil. And,  $X_1$ ,  $X_2$ , and  $X_d$  are the linear displacements as shown with  $X_{k1}$  and  $X_{k2}$  (see figure 4.20) as the spring extensions.

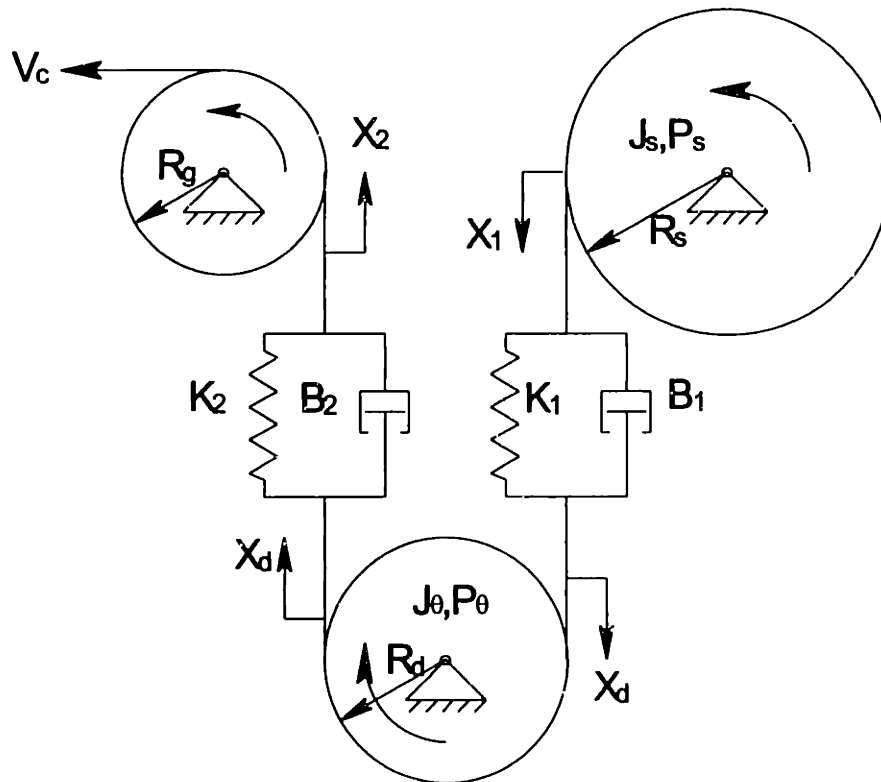


**Figure 4.19: Idealized mechanical system for the dancerless tension control method.**

A bond graph representation of the model was made of the idealized mechanical system<sup>19</sup>. The bond graph is shown in figure 4.20.

<sup>19</sup> The bond graph developed is based upon the methods detailed in Introduction To Physical System Dynamics by Rosenberg and Karnopp.

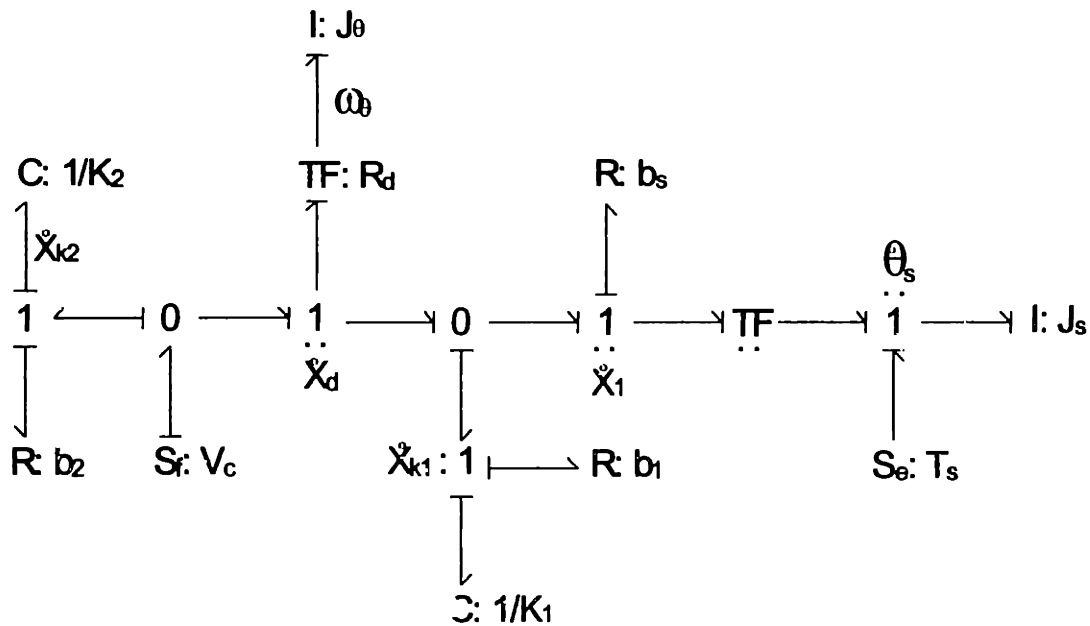


Figure 4.20: Bond graph representation of the dancerless tension control system.

From the bond graph, a state-space representation of the dancerless tension control was derived. The state-space equations are shown below in matrix form. The state variables were chosen to be the extensions  $X_{k1}$  and  $X_{k2}$  of the two springs, and the momenta  $P_s$  of the supply spool, and  $P_\theta$  of the intermediate pulley. The tension  $T_f$  on the fiber is the only output from the system.

**State-Space:**

$$\dot{X} = AX + BU$$

$$Y = CX + DU$$

where,

$$X = [X_{k1} \quad X_{k2} \quad P_s \quad P_\theta]^T$$

are the state variables,

$$U = [V_c \quad T_s]^T$$

are the input velocity  $V_c$  of the fiber and torque  $T_s$  on the supply spool motor.

$$Y = [T_f]$$

is the tension  $T_f$  on the fiber.

And,

$$\mathbf{A} = \begin{bmatrix} 0 & 0 & -R_s/J_s & R_d/J_d \\ 0 & 0 & 0 & -R_d/J_d \\ R_s K_1 & 0 & -R_s^2(B_1+B_s)/J_s R_s R_d B_1/J_d \\ -R_d K_1 & R_d K_2 & B_1 R_s R_d/J_s & -R_d^2(B_1+B_2)/J_d \end{bmatrix}$$

$$\mathbf{B} = \begin{bmatrix} 0 & 0 \\ 1 & 0 \\ 0 & 1 \\ R_d B_2 & 0 \end{bmatrix}$$

$$\mathbf{C} = [0 \quad K_2 \quad 0 \quad -R_d B_2/J_d]$$

$$\mathbf{D} = [B_2 \quad 0]$$

are the remaining matrices in the state-space representation.

#### 4.6.3.3. Active Dancer Tension Control Model

A similar model of the active dancer tension control system was developed based on the concept drawing depicted in figure 4.19. Figure 4.21 shows the idealized mechanical model of the active dancer tension control system. The model is based on the same assumptions made for the dancerless tension control model. In addition, the following assumption is made:

- The inertia of the dancer arm which connects the dancer pulley to the dancer motor is negligible when compared to the inertia of the dancer pulley itself.

The variables in this model are as follows.  $R_d$  and  $R_s$  are the radii of the dancer pulley and supply spool, respectively.  $J_d$ ,  $P_d$ , and  $J_s, P_s$  are the angular inertias

and momenta of the dancer pulley and supply spool, respectively.  $M_d$  and  $P_d$  are the mass and linear momentum of the dancer pulley, respectively.  $K_1, K_2$  and  $B_1, B_2$  are once again the stiffnesses and damping constants of the sections of fiber indicated. And, the inputs  $V_c$ ,  $T_s$ , and  $T_d$  are the fiber velocity, the torque on the supply spool, and the torque on the dancer arm, respectively. Gravity  $g$  acts on the system.

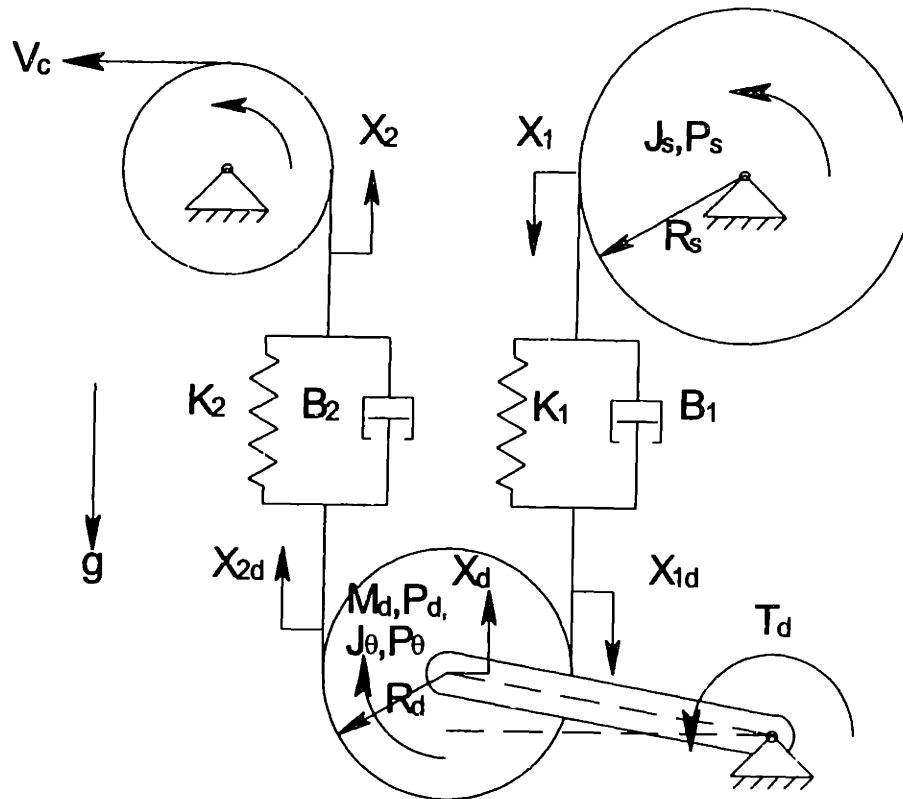


**Figure 4.21: Idealized mechanical system for the active dancer tension control method.**

As before, a bond graph representation of the active dancer tension control system was developed<sup>20</sup>. This bond graph is shown in figure 4.22. The state-space equations were derived from the bond graph model and placed in matrix form as shown below. The state variables were chosen to be the extensions  $X_{k1}$  and  $X_{k2}$  of the two springs in the system, and the rotational momenta  $P_s$  of the supply spool and  $P_\theta$  of the dancer pulley, and the linear momentum  $P_d$  of the

<sup>20</sup> The bond graph developed is based upon the methods detailed in Introduction To Physical System Dynamics by Rosenberg and Kamopp.

dancer pulley. The output variables are the tension  $T_f$  on the fiber and the vertical position  $X_d$  of the dancer pulley.

**State-Space Equations:**

$$\mathbf{X}' = \mathbf{A}\mathbf{X} + \mathbf{B}\mathbf{U}$$

$$\mathbf{Y} = \mathbf{C}\mathbf{X} + \mathbf{D}\mathbf{U}$$

where,

$$\mathbf{X} = [X_{k1} \quad X_{k2} \quad P_s \quad P_d \quad P_\theta]^T$$

are the state variables,

$$\mathbf{U} = [V_c \quad T_s \quad M_d g + T_d/L]^T$$

are the inputs,

$$\mathbf{Y} = [T_f \quad X_d]^T$$

are the outputs, and

$$\mathbf{A} = \begin{bmatrix} 0 & 0 & -R_s/J_s & -1/M_d & R_d/J_d \\ 0 & 0 & 0 & -1/M_d & -R_d/J_d \\ R_s K_1 & 0 & -R_s^2(B_1+B_s)/J_s & -B_1 R_s/M_d & R_s R_d B_1/J_d \\ K_1 & K_2 & -B_1 R_s/J_s & -(B_1+B_2)/M_d & R_d(B_1-B_2)/J_d \\ -R_d K_1 & R_d K_2 & B_1 R_s R_d/J_s & R_d(B_1-B_2)/M_d & -R_d^2(B_1+B_2)/J_d \end{bmatrix}$$

$$\mathbf{B} = \begin{bmatrix} 0 & 0 & 0 \\ 1 & 0 & 0 \\ 0 & 1 & 0 \\ B_2 & 0 & -1 \\ R_d B_2 & 0 & 0 \end{bmatrix}$$

$$\mathbf{C} = \begin{bmatrix} 0 & 0 & 0 & 1/M_d & 0 \\ 0 & K_2 & 0 & -B_2/M_d & -R_d B_2/J_d \end{bmatrix}$$

$$\mathbf{D} = \begin{bmatrix} 0 & 0 & 0 \end{bmatrix}$$

$B_2$                      $0$                      $0]$

are the remaining matrices in the state-space representation.

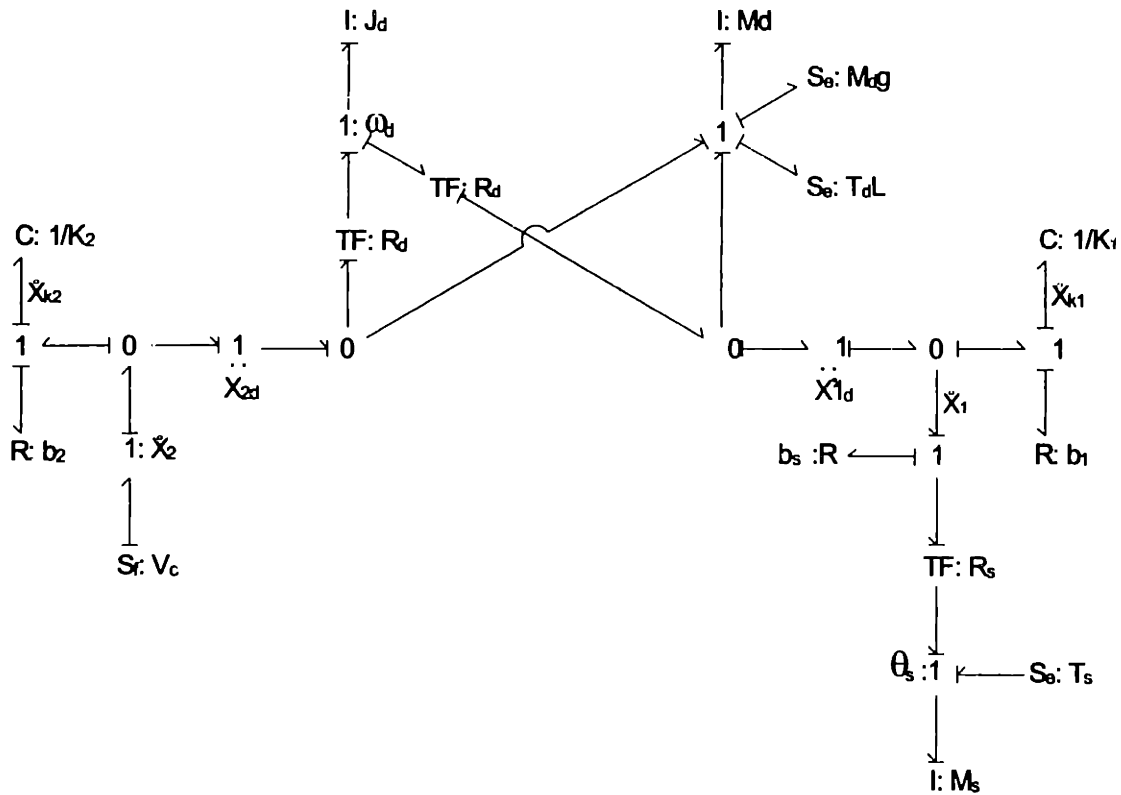


Figure 4.22: Bond graph representation of the active dancer tension control system.

#### 4.6.3.4. Simulated Tension Control Results

The ability of each tension control method's ability to maintain good control over tension while winding were simulated using the Mathworks' Matlab™ Simulink™ simulation software and the state-space representations of the two systems. Values for all the constants in the system were estimated to grossly approximate what the values in the real physical system might be. These values for both models are:

$$J_s = 5e^{-5} \text{ kgm}^2$$

$$J_d = 1.6e^{-6} \text{ kgm}^2$$

$$M_d = 0.020 \text{ kg}$$

$$R_d = 0.0127 \text{ m}$$

$$R_s = 0.0206 \text{ m}$$

$$B_1 = .08 \text{ N/(m/s)} \quad B_2 = .08 \text{ N/(m/s)}$$

$$B_s = .05 \text{ N/(m/s)}$$

$$K_1 = 1.1 \text{ N/m} \quad K_2 = 1.1 \text{ N/m}$$

The Simulink™ block diagram representation of the dancerless tension control system is shown in figure 4.23.

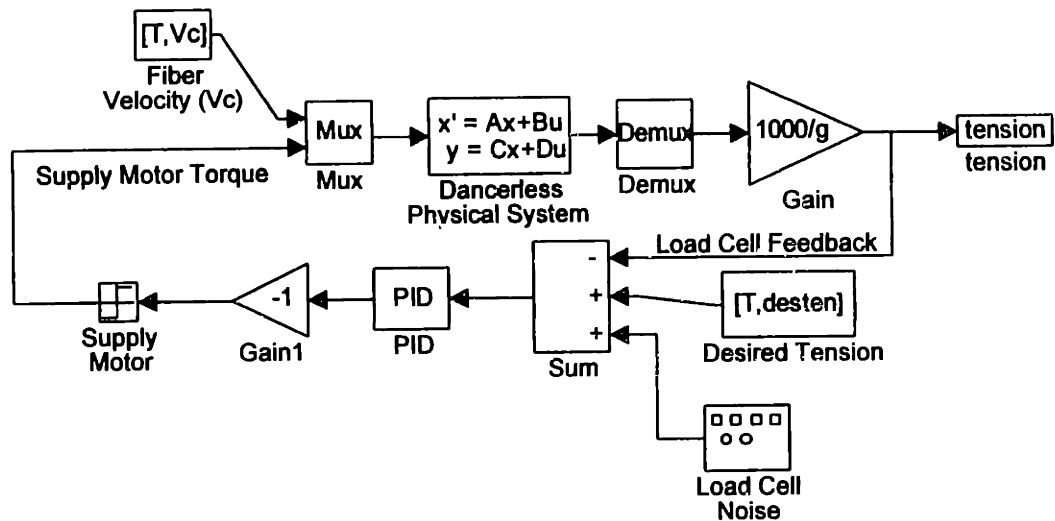


**Figure 4.23: Simulink™ block diagram model of the dancerless tension control system.**

In order to make the dancerless system model more realistic, the output from the motors were limited to a maximum torque of .015Nm which is just enough to allow the motor to handle the maximum tension control requirements, thus, keeping in line with the design goal of minimizing the inertias of the motors to increase the bandwidth of the systems. In addition, a small amount of static friction amounting to about 0.1 grams as seen at the fiber was modeled in the motor to represent the friction of the motor's brushes. These affects are governed by the block entitled "Supply Motor". A noisy feedback signal from the load cell was also worked into the model using the block entitled "Load Cell Noise" to add a broad-band low amplitude (50 milligrams) noise signal to the system to determine how the system might react to environmental noise.

The dancerless tension control system model was first subjected to a normal winding situation where the fiber velocity starts at 0.0m/s and accelerates at  $0.60\text{m/s}^2$  to a typical feed rate of 0.15m/s, winds at constant speed for a while, and then decelerates back down to 0.0m/s. Then, in addition to the acceleration and deceleration, the desired tension on the fiber was suddenly changed from 10.0 grams of tension to 15 grams of tension for a short period of time, thus obtaining the system's step response and revealing the system's ability to profile tension while winding as discussed before. The gains of the PID control loop were selected to achieve good tension control performance. Figure 4.24 shows the results of these simulated tests.

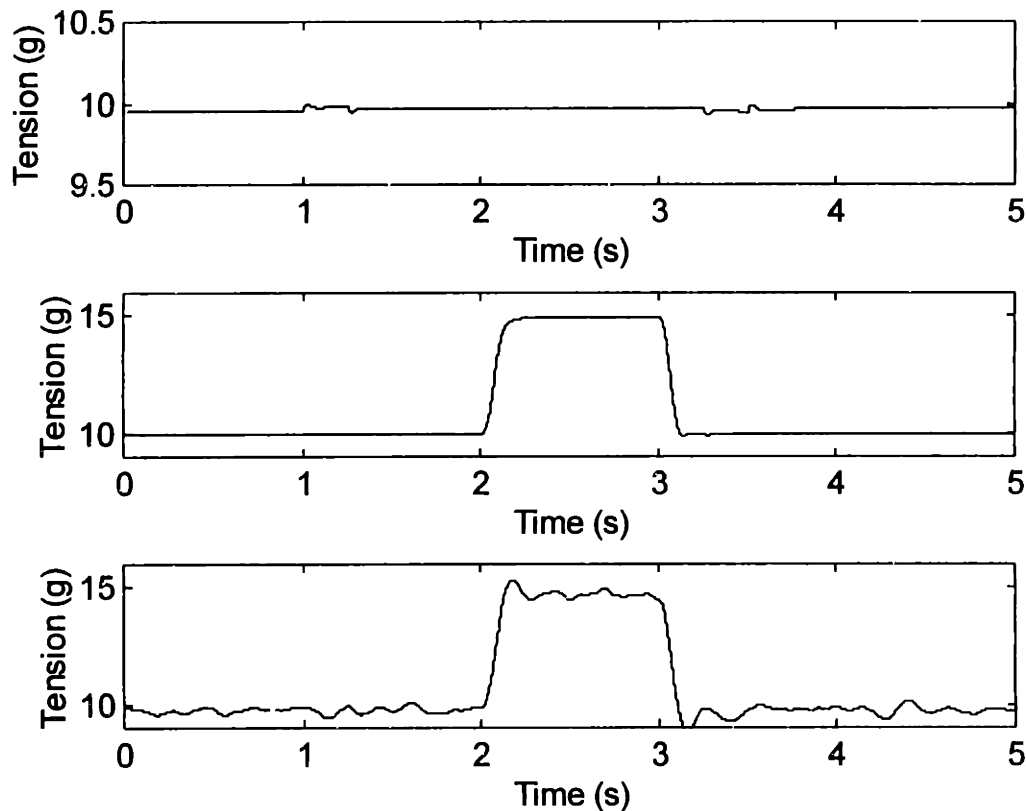


**Figure 4.24: Results from simulated winding tests on the dancerless tension control model. Top: Normal winding. Fiber accelerates to constant speed and then decelerates back to zero. Mid: Desired tension is stepped in the middle of winding. Bot: A low amplitude broad band noise signal is inserted in to the feedback line.**



The top plot shows the results of the normal winding test. The plot shows that the dancerless tension control method is very much capable of maintaining tight control over the tension on the fiber under normal circumstances. Only small changes in tension can be seen in two places in the top plot each corresponding directly to the acceleration and deceleration of the fiber velocity. The middle plot shows the system's reaction to a step in the desired tension level. Again, the system seems quite capable of handling such tension profile requests. The somewhat slow rise time of the step is a result of the limitations placed on the maximum motor output as discussed. Faster rise times were obtained when the motor output was not so limited. The bottom plot again shows the step response while winding, but this time the low amplitude broad band noise signal has been inserted into the load cell feedback signal. This plot shows the importance of having as clean a feedback signal as possible. Although, the noise signal level was only 50 milligrams in amplitude, the response of the system shows that it has a much greater affect on the output tension.

The Simulink™ block diagram representation of the active dancer tension control system is shown in figure 4.25.

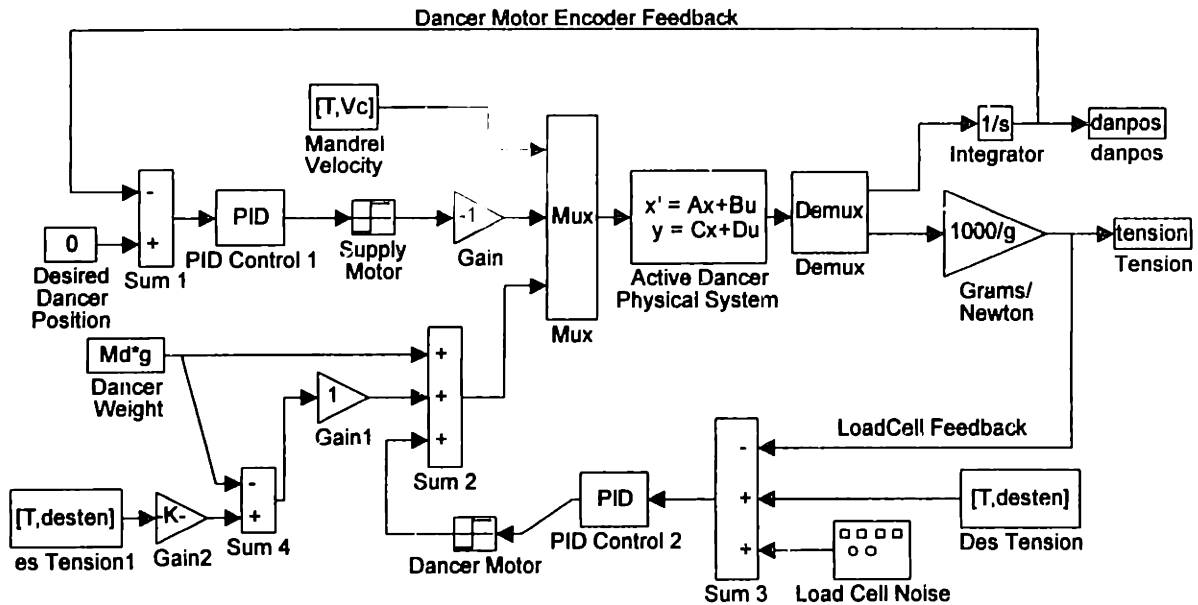


**Figure 4.25: Simulink™ block diagram model of the active dancer tension control system.**

Similar to the dancerless tension control system modeled in Simulink™ this control system has been modeled with limitations placed on both the supply spool motor and the dancer motor, and the model has the ability to insert noise into the load cell feedback signal to determine its affect on the system. A feature of the model not mentioned before is the open-loop torque applied to the dancer arm to achieve the desired tension level as represented by the "sum 4" block which compares the desired tension to the weight of the dancer and estimates the additional motor torque output to achieve the desired tension level. This open-loop signal is intended to allow the system to more rapidly achieve the desired tension for large changes in the desired tension.

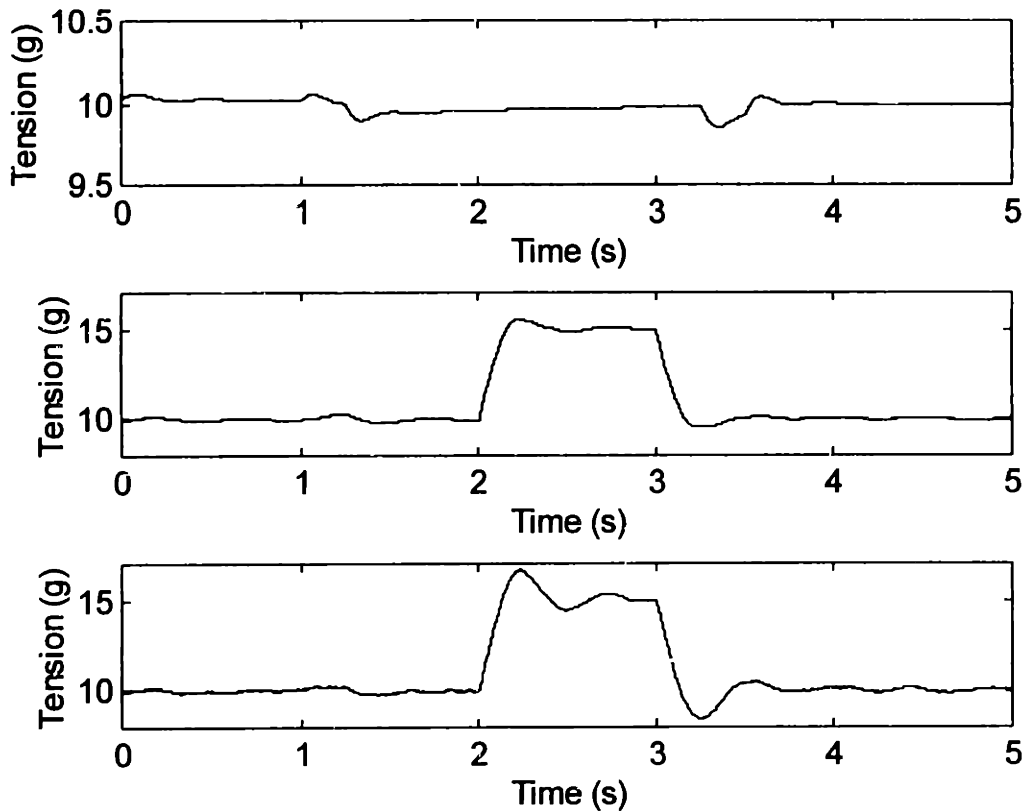


**Figure 4.26: Results from simulated winding tests on the active dancer tension control model. Top: Normal winding. Fiber accelerates to constant speed and then decelerates back to zero. Mid: Desired tension is stepped in the middle of winding. Bot: A low amplitude broad band noise signal is inserted in to the feedback line.**

The same tests which were run on the dancerless system were run again on the active dancer system. Figure 4.26 shows the results of these tests. The top plot shows the results of the normal winding test. As with the dancerless method, the active dancer method appears quite adequate to the task of maintaining tension during normal winding allowing only small changes in the tension during the acceleration and deceleration phase of winding. The middle plot shows the system's step response. The system does not seem to have a problem handling the requested change in desired tension level. Again, the somewhat slow rise time is a result of the limitations placed on the maximum output of the motor. The bottom plot shows the same step response with the low amplitude (50 milligrams) broad-band noise inserted in to the load cell feedback signal. As the

plot shows, the system is adversely affected by the noise, although not to the same extent as the dancerless system.

#### **4.6.4. Choosing A Tension Control Method: Experimental Results**

##### *4.6.4.1. Introduction*

Theoretical models are useful for getting an idea of how a system will behave, but when possible, actual experimental results provide the best information for decision making. In this case, obtaining experimental results for both the dancerless and active dancer tension control methods was possible. The test-bed winding machine was designed with a modular supply unit base to allow accommodation of both control methods. Experiments were performed using both types of tension control to determine each method's ability to maintain a tight control over the average winding tension, and to determine each method's ability to profile the tension while winding.

##### *4.6.4.2. Load Cell Noise*

A load cell was used to measure the tension levels on the fiber while winding. In an ideal system this feedback would represent the exact tension on the fiber and be free of system noise. However, this is generally not the case in a real physical system. The noise levels of the load cell's signal were measured experimentally to use as a basis for interpreting the results from the tension control experiments. The setup involved routing the fiber from the supply spool to the product spool as if winding would be taking place. Tension was applied to the fiber, but no actual winding took place. The raw tension data was rather noisy, so a low-pass filter was constructed with a cutoff frequency of 300 Hz for the tension signal. The results of all the experiments presented in this section were filtered this way.

Figure 4.27 shows the results from the tension noise level measurement including both the tension data and the results of a Fourier transform on the data. The dashed lines on the data indicate the  $\pm 0.5$  and  $\pm 1.0$  gram levels. As the results show, there was less than  $\pm 0.5$  grams worth of noise in the tension signal. The major frequency components of this signal, as indicated, were at about 16 Hz and 70 Hz. The 16 Hz component, while never isolated, was suspected to have come from the vibrations from the support structure of the main positioning system on top of which sat the supply unit and load cell. The 70 Hz component was identified as the natural frequency of the main shaft to which the product spool was attached. The vibrations traveled from the shaft through the fiber to the load cell.

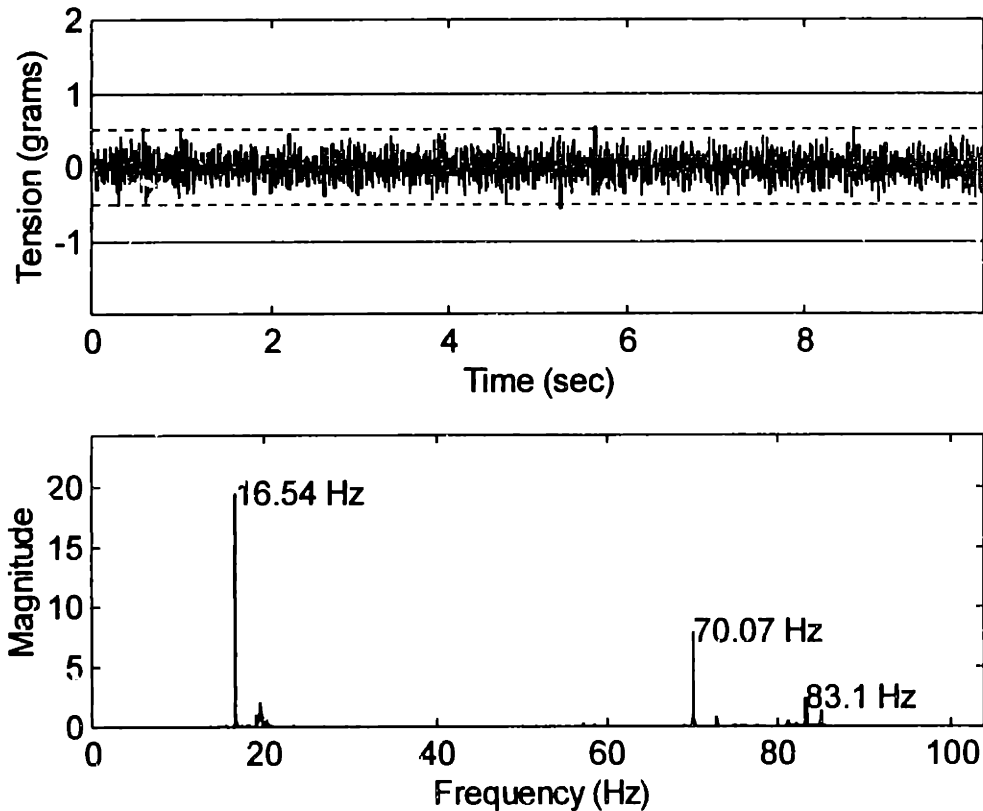


**Figure 4.27: Load cell noise. Fiber is routed from supply spool to the product spool, but tension control is not active, and no winding is taking place.**

#### 4.6.4.3. Tension Control While Winding

The first criteria for the tension control system was to be able maintain tight control over the average winding tension. At the time that the original tension control experiments were performed certain aspects of fiber optic coil winding were true. Winding at a rate of about half a turn per second was considered a fast rate, constant speed winding was the norm, and 10 grams of tension was considered a typical winding tension level. The experiments first conducted were run under these circumstances.

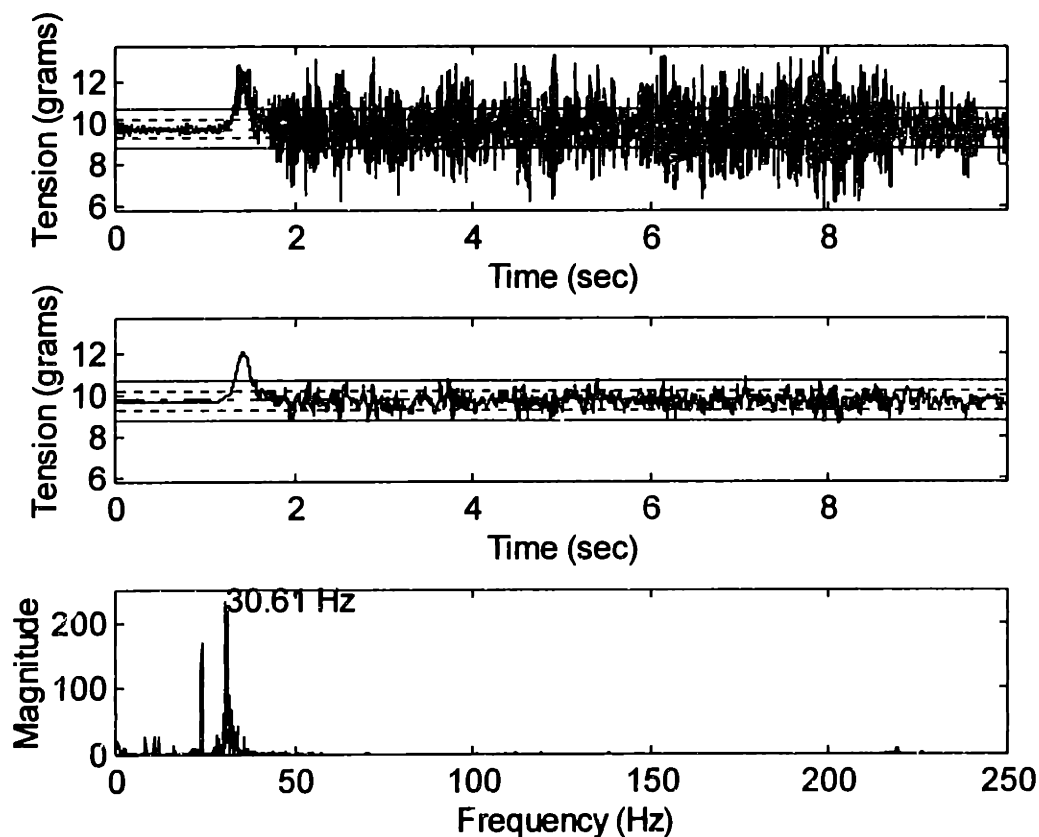


**Figure 4.28: Dancerless tension control. Winding at approximately 0.5 rps while sampling tension at 500 Hz. Top: Raw tension data. Mid: tension averaged over 50 milliseconds. Bottom: Tension frequency spectrum.**

Winding with dancerless tension control was tried first. Figure 4.28 shows the results from a typical winding experiment. The top plot shows the tension data which was sampled at a rate of 500 Hz. The +/- 0.5 and 1.0 gram lines are drawn on the plot. Thus, the instantaneous tension on the fiber while winding

exceeded +/- 2.0 grams of tension. The middle plot shows the same data only averaged over 25 samples, or every 50 milliseconds. This amount of averaging was considered very reasonable given the 0.5 rotations per second (rps) winding speed at which the experiment was conducted. Except for the initial surge in tension associated with the acceleration of the main shaft up to its constant winding speed, the average tension during the several seconds of winding remained, for the most part, well within the +/- 1.0 gram lines and generally within the +/- 0.5 gram lines.

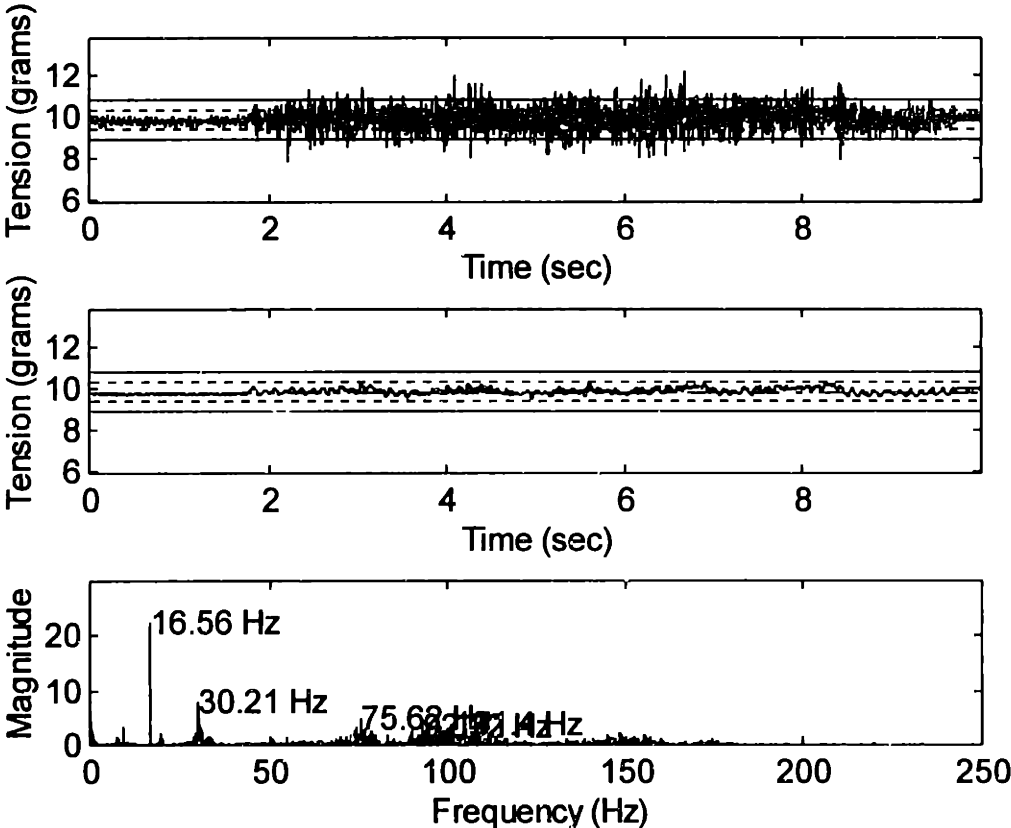


**Figure 4.29: Active dancer tension control. Winding at approximately 360 dps while sampling tension every 2 milliseconds. Top: Raw tension data. Mid: Tension averaged over 50 milliseconds. Bottom: Tension frequency spectrum.**

Similar tension control experiments were performed using the active dancer tension control method. The results from a typical experimental run are shown in figure 4.29. Again, the top plot shows the sampled tension data. Here, the instantaneous tension data almost stays within +/- 1.0 grams from the target.

The middle plot shows the 50 millisecond averaged tension. This time it stays well within  $\pm 0.5$  grams of the target tension.

#### 4.6.4.4. Tension Profiling While Winding

The second criteria for the tension control system was the ability to profile tension while winding, both in the form of control over the target tension level throughout the wind, and in the form of quick tension spikes. A second series of experiments were run to determine each method's ability to profile tension. The experiments were similar to the first set of typical winding experiments, only this time the target tension level was stepped up several grams for a brief period of time during the wind.

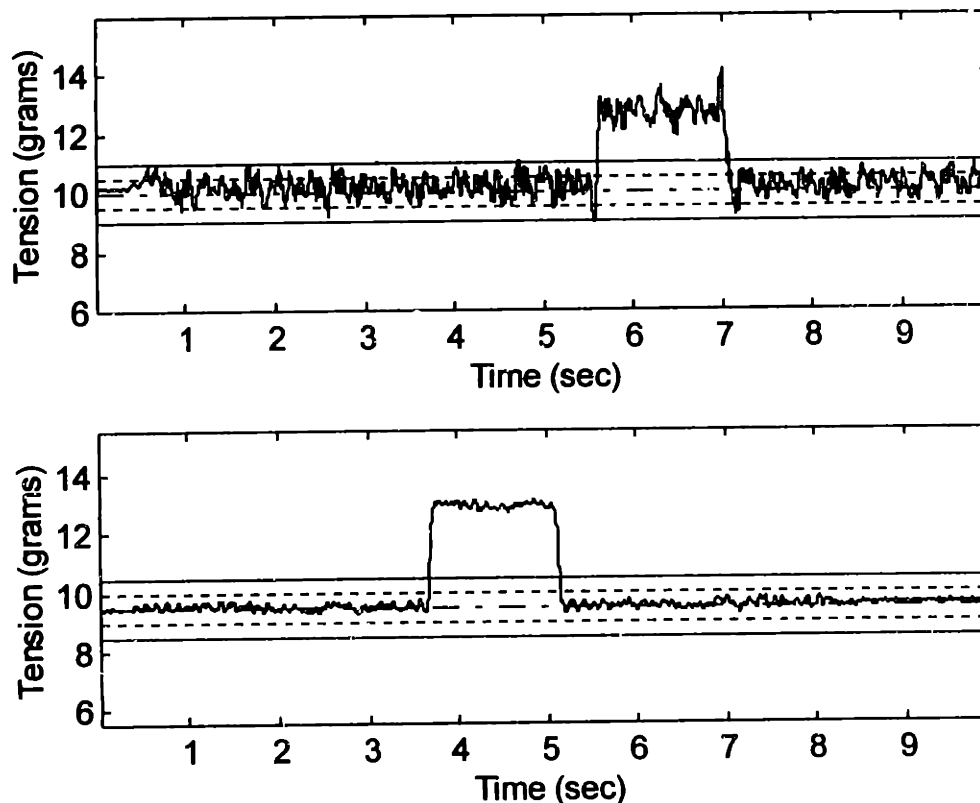


**Figure 4.30: Tension profiling tests conducted by inducing a tension step while winding. Top: Results using dancerless tension control. Bottom: Results using active dancer tension control.**



The results of this experiment using both the dancerless and active dancer tension control methods are shown in figure 4.30. The top plot shows the (50 millisecond) averaged data while winding using the dancerless tension control method. The bottom plot shows the same results using the active dancer tension control method. The results reveal that both methods are equally capable of tension profiling. As soon as the target tension level is stepped up the actual tension level follows and both the tension control methods are able to immediately compensate for the increased tension levels, thus maintaining tight control over the tension. This is also true when the target tension is dropped back down to the original level. As before, it is clear from the results that the tension on the fiber using the active dancer tension control method is much cleaner than the results using the dancerless tension control method.

#### *4.6.4.5.Making The Choice*

The results of the tension control experiments conducted showed that either the dancerless or the active dancer tension control methods were capable of meeting the basic needs of the automated winding machine. It was clear that the active dancer method was able to maintain tighter control over the instantaneous and average tension on the fiber. It is possible that the dancerless method suffered from a much greater reliance on the noisy load cell signal which was the only form of control feedback in that system. However, it was not clear whether the improvement in tension control was worth the added complexity to the system.

The decision was made to go with the more complicated active dancer control method for several reasons. The multiple winding experiments performed revealed that the dancerless system was dependent on a good clean pre-wind of the fiber onto the supply spool. Snags of the fiber around itself while paying out from the supply spool as a result of poor pre-winding would occasionally lead to sudden spikes and subsequent sudden losses in tension.

While pre-winding of the fiber was slated to be performed automatically using another machine which would presumably do a nice job, the MIT/MI did not wish to depend on such unwritten guarantees. The active dancer method suffered much less from such fiber snags as the dancer pulley acted as a buffer to such sudden changes in fiber payout rate.

In addition, the fiber immobilization method discussed previously was easier to implement using a method which involved a dancer pulley. And, of course, the results of the tension control experiments worked in favor of selecting the active dancer. If going with the active dancer would have meant a large amount of added complexity to the supply unit, then perhaps another decision would have been made. However, as it was, the active dancer system was able to fit into approximately the same space as the dancerless system, and required only an additional small servo motor and servo control axis per supply unit

#### **4.6.5. The Automated Coil Winder: Tension Control Experiments**

##### *4.6.5.1. Introduction*

The active dancer tension control method which was chosen for most of the experiments run on the test-bed winding machine was again chosen for the final automated coil winding machine. A few changes to the original design were made. An additional pulley was placed in-between the supply spool and the dancer pulley as shown in figure 4.15. This intermediate pulley served to make the funneling of the fiber from the relatively wide supply spool to the narrow guide wheel more gradual by taking two steps rather than one. At the request of the Customer, the supply spool drive motor and the dancer motor were both re-selected to achieve a higher level of potential target tension levels. There was some concern over the effect that the larger motors, having greater breakaway friction, would have on the tension control, but the decision to go ahead with the larger motors was made. The length of the dancer arm was nearly doubled to avoid geometric interference in the new supply unit. The resolution of the

encoders used on the dancer motors were doubled to compensate for the potential loss in the ratio of encoder counts to degrees of motion of the dancer arm which would affect the resolution of the dancer arm's feedback loop.

In addition to these changes to the mechanics of the tension control system, there were changes to the machine itself and the fiber wound. The baseline fiber used during all winding experiments on the automated winding machine was nearly half the diameter of that used on the test-bed winder. Greater attention was made to stiffen up the machine structure and dampen out possible environmental vibrations. The automated nature of the machine and the many possible positions of the main positioning system precluded placing the amplifier for the load cell signal as close to the load cell as it was on the test-bed winder. This provided a possible source of increased noise in the tension control system.

This section will present and discuss the results of several winding experiments conducted using the active dancer control method implemented on the automated coil winding machine.

#### *4.6.5.2. Load Cell Noise*

As with the original tension control experiments one of the first experiments conducted was to measure the level of noise coming from the load cell output. In this experiment, the supply unit is seated in payout position, but no fiber connects it to the product spool on the main shaft. However, the main is rotated at 360 dps to see how the vibrations from the main motor and main shaft affect the load cell output. The top plot of figure 4.31 shows the results from this experiment. In the bottom plot the same situation exists, but in addition to the main shaft turning, the supply unit is jogged laterally once per revolution of the main shaft as if real winding were occurring.

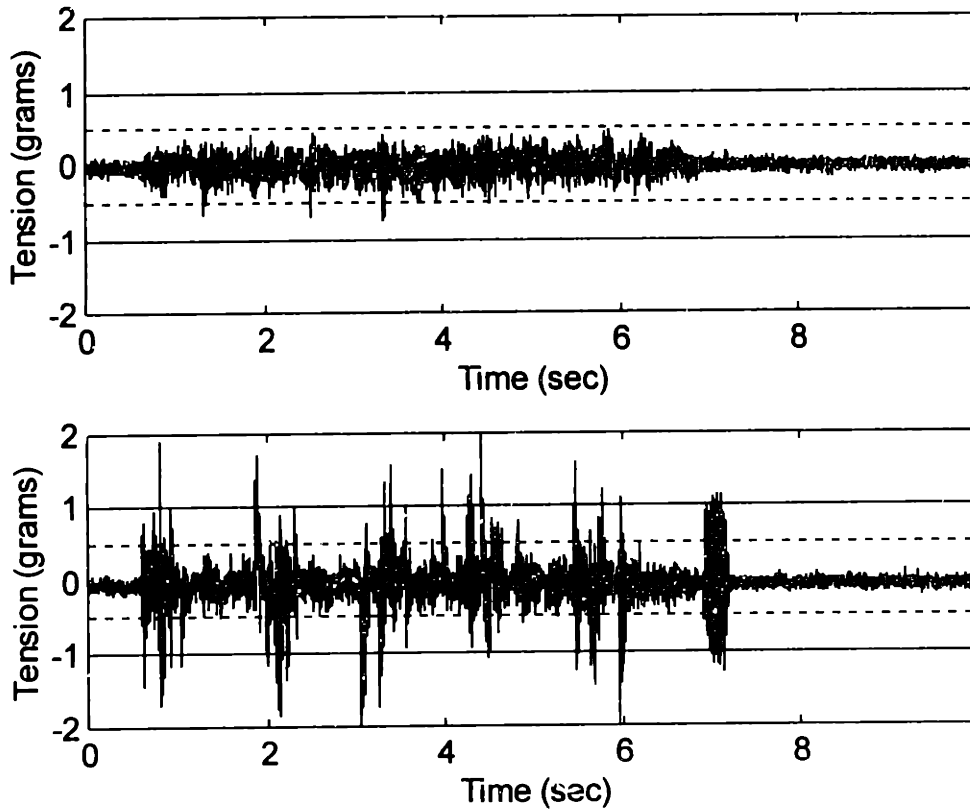


**Figure 4.31: Tension noise levels on the automated coil winder. Top: Main shaft is turning, but no fiber connects the supply spool to the product spool. Bottom: same situation but the supply unit is jogged as if winding were occurring.**

As the plots reveal, the amplitude of the relatively low noise load cell signal more than doubles when the main shaft is turning and has periodic spikes averaging more than 1.5 grams when the supply unit is jogged.

#### *4.6.5.3. Tension Control While Winding At Constant Speed*

Figure 4.32 shows the results from typical constant speed winding experiment. As before, the tension data was sampled at 500 Hz and then averaged over 50 milliseconds. The winding speed for the data shown was 240 dps, and the target tension level was 9 grams. As the top plot shows, the instantaneous tension level exceeds the  $\pm 1.0$  gram lines. Even the 50 millisecond averaged tension occasionally breaks 1.0 gram line although for the most part it remains at around  $\pm 0.5$  grams.

To a certain extent, these results were disappointing considering the results obtained on the test-bed winder using the same tension control method. Much of the loss in control over the tension level is attributed to the greater levels of friction present in the motors selected for the automated machine as mentioned before.

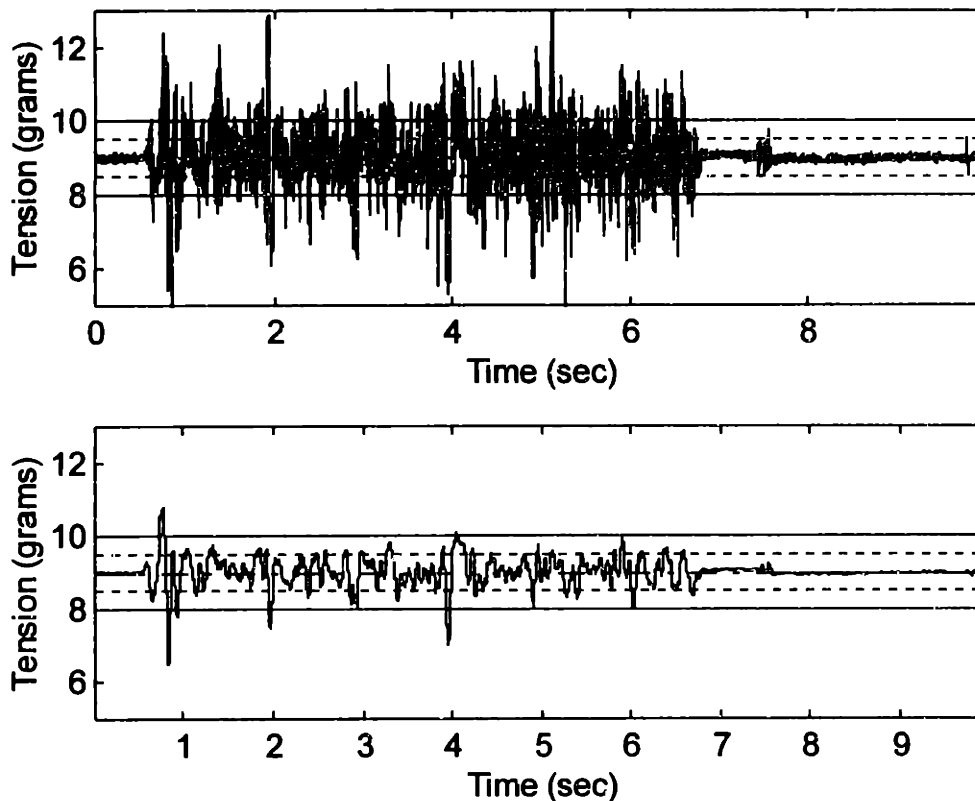


**Figure 4.32: Active dancer tension control while winding at a constant speed of 240 dps on the automated winder. Tension is being maintained at 9 grams. Top: Raw tension data. Bottom: Averaged tension data.**

#### *4.6.5.4. Tension Control While Winding With A Slow Down Zone*

It was discovered that it was helpful to wind more slowly through the jog zone of a coil during certain layers of some winding patterns. This allowed the guide wheel to more accurately place the fiber onto the product spool, and also gave more time for tension profiling techniques (see next sub-section) to take effect. At times, the speed at which winding occurred in the jog zone became as low as

60 dps. However, it was unacceptable to slow down the speed of winding an entire layer to this speed as it would at a minimum quadruple the winding time for that layer. Thus, the winding velocity was decelerated down to 60 dps to wind through the jog zone and then immediately accelerated back up to full speed on every turn for a given layer. This form of winding was termed winding with a "slow down zone".

An experiment was conducted to determine how this periodic acceleration and deceleration of the winding velocity would affect the control over the target tension level. Figure 4.33 shows the results from this experiment plotting both the instantaneous tension data and the averaged tension data. The periodic acceleration and deceleration is clearly having a detrimental affect on the tension control system's ability to maintain an average target tension as the averaged data regularly breaks out of the +/- 1.0 gram line however brief it may be.

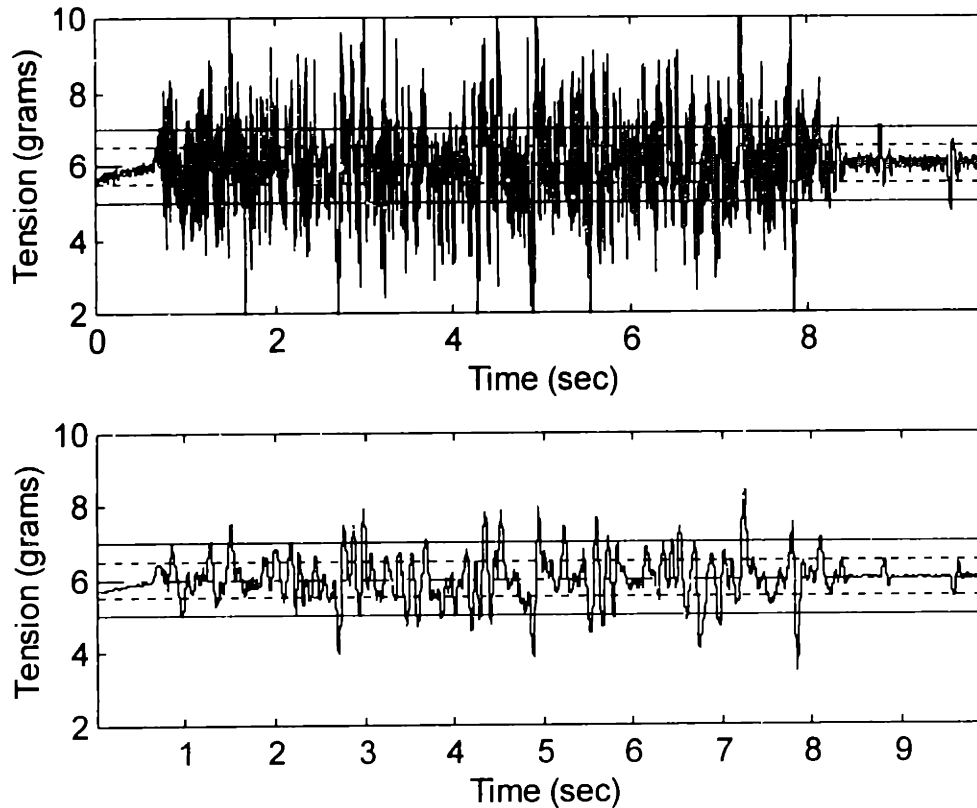


**Figure 4.33: Tension control while winding with a slow down zone. Full winding speed at 360 dps with a slow speed of 60 dps through the jog zone. Tension is being maintained at 6 grams.**

#### 4.6.5.5. Tension Profiling While Winding With A Slow Down Zone

It was discovered that certain forms of tension profiling while winding through the jog zone would help seat the fiber into it's proper place for some pattern types. These types of profiling include tension spiking and tension dithering. To give time for these profiling methods to take effect the slow down zone was also used in conjunction with the tension profiling.

Figure 4.34 shows the averaged tension results from both tension spiking and tension dithering while winding inside the jog zone. In the first plot, tension is being spiked from its normal target tension of 9 grams to a temporary target of 15 grams. As the figure shows, the tension control scheme has no problem dealing with this periodic tension spiking.

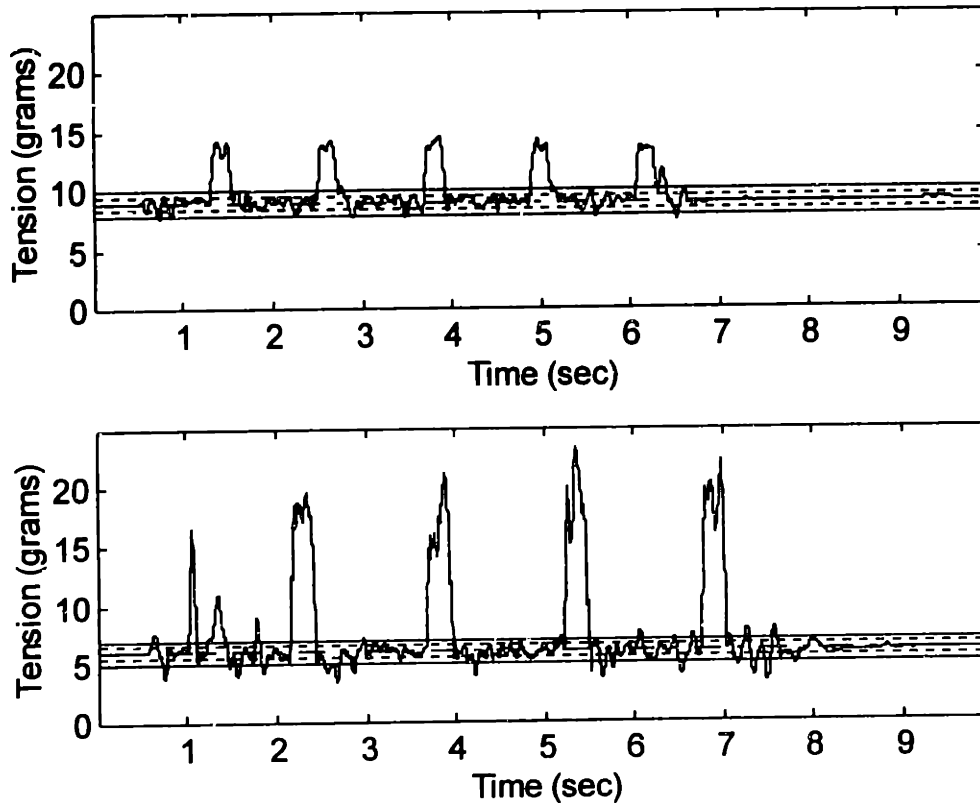


**Figure 4.34: Top: Average tension while winding with tension spiking inside the jog zone. Bottom: Average tension while winding with tension dithering inside the jog zone.**

The bottom plot shows the averaged results while dithering the tension in the jog zone. The tension level was being maintained at 6 grams. When winding inside the jog zone a sinusoidal dithering tension profile of 20 grams at 100 Hz was superimposed onto the constant 6 gram tension profile. The averaging performed on the tension data shown averages out the 100 Hz component, but the temporary elevated tension level is clear.

The averaged tension data appears similar for both tension spiking and tension dithering. However, the ability of tension dithering has been shown to be more effective in “vibrating” the fiber into its proper position in certain situations.



#### **4.6.6. Auto Load Cell Calibration**

The load cell used to measure the tension level on the fiber was shown to drift slightly over time, as much as 0.5 grams over an hour. It would take several hours to wind one of the longer coils desired by the Customer, so this potential drift in load cell readings cannot go unchecked. The solution to this issue was to implement an automatic way of calibrating the load cell.

The auto load cell calibration procedure involves maintaining the dancer arm in its normal tension control position, i.e., parallel to the base of the supply unit. The supply unit brake is then engaged and the tension control system shutdown. At this point, the tension registered on the load cell is strictly a result of the weight of the dancer pulley on the fiber routed around it. This value will not change over time and thus can be repeatedly used to calibrate against. Fortunately, although the load cell's zero position has been known to drift over time, the load cell's scaling factor has been shown to be very steady.

## **5. Automated Control of the Coil Winding Process**

### ***5.1. Introduction***

Without an intelligent automation scheme the winding machine developed would be little better than a traditional manual winding machine. There were several complicating factors in automating the process of winding a fiber optic gyroscope coil on the machine developed. The simplest of these factors to solve was the flexibility requirements imposed by the Customer. The Customer required that the machine be capable of winding three patterns using a wide range of fiber diameters. Solutions to this issue were plentiful. The more difficult issues centered around developing an automation scheme that was also flexible enough to allow modification of the winding process by the Customer without the need for re-programming of the winder software, that allowed for easy and rapid development of the required and future winding processes, and that allowed for error handling and recovery.

The winding process development for a fiber optic gyroscope coil is a particularly difficult one. The difficulty lies in the long serial nature of the process combined with the need for each step of the process to be tweaked out. Performed individually, tweaking out the various steps of a process seems not to present much of a problem. First, take one process step, get it to work as desired, then take the next and so on until the whole process is working right. This is not so easily done with fiber optic coil winding. The entire act of winding a complete fiber optic coil is one long process from start to finish. There is no tweaking of step five without having gotten steps one through four to work properly. One cannot tweak the process for winding the first couple of turns of the third layer of the coil without first having figured out exactly how to start the

wind, wind the first couple of turns near the flange, continue with the orthocyclic winding across the base layer, performing a layer transition, etc...

The severe hardship imposed by this long serial process on the process development is as follows. If one attempt to get a process step to work fails, what is required before another, slightly different attempt, is made? In order to guarantee that the new changes are in fact an improvement to the process, the same conditions must be reproduced. Normally, this means winding a new coil up to the point where the new changes will be inserted. This would quite painful since there are no shortcuts in getting back to that point in the process.

This issue of what happens when something is not quite right with the process while winding a coil further complicates the automation scheme when error handling and recovery is considered. In order to correct an error, whether automatically or manually, the process must first be stopped, the process undone to a point before the error occurred, and then the process resumed with corrective actions taken.

The core of the solution to all the issues discussed for the automation scheme lies in a scripting language developed for the control of the machine. First, the scripting language itself will be covered. Then, the solution to the automation issues through the use of the scripting language will be covered.

## ***5.2. The Scripting Language***

One of the fundamental choices made in the software automation scheme was the choice to develop a scripting language to control the machine functions during a winding process rather than hard-coding the entire process plan for a coil. The possibility of hard-coding automation instructions directly into the software was abandoned early on in the software development. Such an approach would not have satisfied the more difficult issues regarding easy and

rapid process development and error handling and recovery. This section will only cover the scripting language developed and the functionality supported.

### **5.2.1. Basic Operation - Cmd File Execution**

The basic unit of instruction in the script files is the "cmd" (pronounced "command"), and thus the script files themselves are referred to as cmd files. The series of cmds which comprise a cmd file is called a cmd list. The operation of the winding machine as run from a cmd file is as follows. The cmd file is presented to the machine's cmd list manager. The cmd list manager starts at the beginning of the list and works its way through each cmd until the end of the list is reached. Each cmd in the list is successively passed to the machine's cmd interpreter which parses the cmd and executes the proper machine instructions.

### **5.2.2. Basic Unit Of Instruction - The Cmd**

The cmds which comprise a cmd file are the basic unit of instruction in the scripting language. The following shows the format for a generic cmd:

```
<Cmd ID> <parameter 1> <parameter 2> <parameter 3> ...
```

The cmd is broken up into two parts, the cmd ID, and a parameter list. The cmd ID, as the name suggests, is used by the machine's interpreter to identify which function call should be made. The parameter list, which can be comprised of zero or more parameters, can be used to specify how a function behaves. Support for various types of cmds was extended to all the basic functionality of the machine including simple motor and stage movements and piston actuation, as well as to the higher machine functions such as guide wheel registration and coordinated motions for supply unit swapping.

### 5.2.3. Flow Control

The flow control supported by the cmd language is limited. As mentioned, a cmd file is executed from start to finish. The only deviation from this course allowed is the ability for the execution of one cmd in a cmd file to result in the execution of the cmds in another cmd file. This sort of flow control is similar to calling a function in a programming language and is illustrated in figure 5.1.

```
START script_one
instruction_1.1 <parameter 1>
instruction_1.2 <parameter 1> <parameter 2>
RUN script_two
instruction_1.3 <parameter 1>
instruction_1.4
RUN script_two
instruction_1.5 <parameter 1> <parameter 2>
END script_one

START script_two

instruction_2.1 <parameter 1>
instruction_2.2 <parameter 1>
END script_two
```

**Figure 5.1: Making multiple calls to a cmd file from another cmd file.**

In the example, two “run” calls to script\_two are made from script\_one. Each one of these run calls will result in the cmd manager temporarily stopping execution of script\_one while it moves over to script\_two. Control is returned to script\_one when script\_two has been fully executed. This sort of cmd list calling was useful for implementing series of process steps that repeated periodically through the wind of an entire coil.

#### **5.2.4. Interactive Control And Cmd Development**

The cmd list manager developed to control the execution of a cmd list not only is able to move through the cmd list executing each cmd in order, but also gives the machine operator interactive control over the cmd list. The cmd list manager allows the operator to selectively step through the cmd list executing cmds one by one or in groups. Executed cmds are marked to indicate their executed state. In addition, during the execution of a series of cmds the manager allows the operator to intercede and stop the execution.

An operator is also able to use the cmd list manager to interactively modify the cmd list and its cmds. At any given point in the cmd list the operator can choose to insert a new cmd, modify, or delete an existing cmd.

### ***5.3. Undo Support***

The scriptable control over the winding machine was a fundamental concept to the automation scheme. An equally important concept was that of undoing cmds which had already been executed. The ability to undo cmds suddenly gives the operator the freedom to try out a certain combination of cmds with little concern over what would happen should the cmds not work out quite as expected because the cmds could simply then be undone.

It was believed that this freedom would greatly facilitate the rapid development of the winding process. For this reason the decision to support undo capability in one form or another for all cmds available to the operator was made early on in the machine's software development.

Support for undo was implemented at the cmd level. For each cmd supported, such as movement cmds, it was determined what information would be necessary to return the state of the machine to what it was prior to the execution of the cmd. This undo-information was then stored into the actual cmd itself ready to be used when such time as the operator or the machine decided to

undo the cmd. A simple example is the case of an absolute movement cmd to a particular axis, such as:

```
move_abs z to 1500
```

which commands the machine to move the Z axis to the absolute position of 1500 milli-inches from its home position in the positive direction. After the cmd is executed undo-information is stored in the cmd and the cmd then reads:

```
move_abs z to 1500 FROM 1200
```

which indicates that the Z axis was previously located at 1200 milli-inches away from its home position in the positive direction. Undoing the cmd would cause the axis to return to this position.

#### ***5.4. Rapid Process Development***

It may not be clear exactly how a scriptable machine control language which supports undo capabilities facilitates rapid process development for coil winding. To illustrate the point figure 5.2 shows one cmd file developed for maneuvering the main positioning system of the machine in order to get the second fiber turn on a layer into place. Recall, from the section on fiber guiding, that the guide wheel is not able to lie between the flanges if the first fiber turn lies up against the flange wall.

The cmds shown assume that the first turn of the layer has already been wound and that the guide wheel is not in-between the flanges. Automatic jogging is turned off since that depends on the guide wheel guiding the fiber very close to the coil. Fiber is wound up until the point where it is suppose to begin jogging. The guide wheel is shifted over part way in the direction of the jog where it can now be inserted between the flanges. A small series of movements,

```

START manu.cmd #SIDE
// Manuevers 2 fibers over and
// winds 1 turn
set_jog dir off
set_wind speed 90
wind_to jog_start
xshift 0.5 fiber #SIDE
insert_gw
wind_to zero
tension_spike 15 500
tension_spike
xshift 1.5 fiber #SIDE
wind_to camera
set_jog dir on
set_wind speed nom
END intbmanu.cmd

```

**Figure 5.2: Cmd list for maneuvering the main positioning system to properly wind the second fiber turn of a layer where the first turn lies up against the flange.**

alternately turning the main axis and moving the jogging axis, is performed in conjunction with a tension spike to get the fiber to lay down correctly into place.

This seemingly simple series of cmds involves quite a bit of tweaking to determine the right combination and magnitude of movements necessary to place the fiber just right to allow winding to continue.

#### **5.4.1. Development And Tweaking On The Fly**

The example shown in figure 5.2 is just one of many cases where process steps need to be tweaked out. One of the advantages of having a scriptable language which can be interactively controlled and modified is the ability for the process developer to begin developing the majority of the process based solely upon the theoretical requirements. That is, based solely on the pattern to be wound, the process developer can determine which axes need to be at what locations to



achieve a perfect wind. So, without ever having placed any fiber on the machine, the process developer can quickly sketch out everything the machine will have to do to wind the coil desired. Of course, the script he writes will produce junk if it is run blindly believing that it will correctly wind the coil on the first try. However, if the script is run interactively, as soon as problems with the wind are detected the developer can go right into the script and make changes on the fly. It is this ability to make changes to the script at will *while the machine is still running* that allows rapid development of the winding process. The machine should never have to be stopped except in the case of fiber breakage.

#### **5.4.2. Automatic Process Steps History Generation**

When the winding automation project was started in the Fall of 1995 and the MIT/MI went out to research the state of the art in coil winding knowledge, most winding “experts” produced slightly different versions of winding details such as when and where a jog zone should stop and start, where the fiber should be just before swapping it out, and how to get the fiber to wind during certain situations. In many cases, it was not possible to extract expertise from the experts into hard process steps. Why the variation between expert opinions on a process which seems quite definable? And, why the difficulty in turning those opinions into process steps? The answer lies in the fact that the experts were expert at manually winding a fiber optic coil. Manual winding almost always takes the form of an operator hovering over the coil as it is wound using a tool to keep the fiber in place. The operator’s skilled hands make so many small movements sometimes it is hard for the operator’s themselves to know exactly what they are doing to make the fiber go into place correctly. In addition, they are making no special effort to document what they are doing and their machine is in no way helping them.

Even the test-bed manual winding machine developed by the MIT/MI, which did not use any form of special tool for enforcing the fiber location,

suffered from this problem of no process documentation. Too often, in the experiments run on the test-bed, several adjustments to the positioning of the guide wheel had to be made before the fiber would wind correctly. With many adjustments being made at a rapid pace in a process that takes hours to complete there is little desire to document the adjustments and so the collective outcome of those adjustments are lost.

Herein lies yet another benefit of developing a scripting language for the winding machine. The script itself is the document of the history of process steps which are required to correctly place the fiber into any given situation. When the process developer interactively runs a script for the first time the script requires some major modifications and some tweaking. All of these changes are made to the script itself and it there for review by the process developer when it is finally gotten to the point where the set of process steps are as good as they will get and work can begin on the next set of steps. Thus, the scripting language inherently enforces the documentation of the process as it is being developed with no extra effort on the process developer's part.

## ***5.5. Error Handling And Recovery***

Despite having defined and tweaked out a full process plan for winding an entire fiber optic coil the process is not immune to potential errors. Errors can come in the form of winding errors where the placement of the fiber is not correct, or from machine errors where the machine takes in some bad data (e.g. guide wheel registration) or fails to correctly execute an instruction. Whatever form an error presents itself in, the automation scheme must be prepared to handle the error and recover from it.

The scripting language developed and the undo functionality supported represent the solution for allowing graceful error handling and recovery. When a winding error is sensed by the vision system on the machine, the cmd list

manager first halts execution of the cmd list and passes control of the cmd list to an error handling routine. In the case of most winding errors the error handling routine proceeds to undo backwards through the cmd list just past the point where the error occurred. Corrective actions such as readjustment of the position of the guide wheel are taken, and then control of the cmd list returns to the cmd list manager. In other cases, such as the fiber falling out of the groove in the guide wheel, cmd list execution is halted and the operator called in since the machine cannot correct such problems itself. The operator can choose to resume execution of the cmd list when the machine is once again ready.

## **5.6. Results And Conclusions**

The rapid process plan development strategy of working out a theoretical process plan first, and then interactively tweaking out the details of the plan was successfully used to develop a full process plan for winding what is considered to be one of the most difficult winding patterns by the Customer in under two man-weeks. In addition, in the process of delivering the machine to the Customer, one of the Customer's engineers was successfully trained on the process development technique and was able to come up with the theoretical process steps for winding a quadrupole patterned coil. This training took less than two days demonstrating the great flexibility of control over the machine given to the Customer. Note that the new process developed involved zero modifications to the machine's software.

It should be noted that scriptable control over the machine is probably not the only possible way that the machine could have been automated. However, this author cannot imagine how to otherwise support automatic process step history generation and undo capability which allows for rapid process plan development and error handling and recovery.

The greatest disadvantage to scriptable control over the machine as it was implemented is possibly that it gives the operator and process developer too much flexibility and control over the machine. A process developer might write a cmd script which makes no sense at all. The operator is exposed to the script while the machine is running, and should the need for operator intervention arise, the operator may need to modify the script on the fly. This necessitates that the operator be skilled in the use of the scripting language just as a CNC machine tool operator might be skilled in the use of G-codes. However, given the advantages of choosing this particular automation scheme these concerns seem small by comparison.

## 6. Conclusions

Figure 6.1 shows the very first full length fiber optic gyroscope coil wound using the automated winding machine. The coil stands as the fastest wound coil of its pattern type and length, and also with the least amount of operator involvement. This despite some necessary tweaking of the cmd script written to wind the coil while the coil was being wound, and some minor software bugs which have since been corrected. The coil was inspected by a manual coil winding expert and validated as having as few visible defects as the expert had ever seen.



**Figure 6.1: First full length fiber optic gyroscope coil wound on the automated fiber optic gyroscope coil winding machine.**

Many factors contributed to the success of the automated coil winding machine without which automated winding would not be possible. First, there was the commitment to use special flange designs to allow the fiber to be routed out of the main winding area as soon as possible when swapping to the alternate supply spool. This eliminated the problem which plagues most other winding machines, which is the need to use a special tool guided with human dexterity to maneuver the fiber from the alternate supply spool around the fiber which is routed out around the outside edge of the flange. (See section ??? for more details). The use of a guide wheel aligned to the flanges using a fine alignment

system allowed guiding of the fiber directly onto the product spool in all cases except for fibers which lie directly against the flange. The relative runout of the guide wheel and the product spool caused problems early on. However, the runout of the guide wheel was brought down to acceptable levels through redesign. Also, the runout of the main shaft, and thus the product spool attached to it, was also brought down to acceptable levels. (This topic is addressed in a document by Brian Sonnichsen entitled "Design Of A Fiber Optic Gyroscope Coil Winder."

The supply unit concept allowed the machine to wind any of the patterns requested by the Customer. However, this necessitated the clamping and de-clamping of the supply unit from its payout position. Registration of the guide wheel to the flange surface before the start of every layer helped to ensure that the guide wheel was always in a known position so that fibers were laid down properly. Despite this, fibers still managed to get slightly out of place especially in the jog zone, not enough to cause an error, but enough to cause potential problems on subsequent layers. Tension spiking and dithering were used as necessary to reduce these variations. The roller was designed to correct any remaining problems with the wind after the completion of each layer.

All of the above provided the machine with the physical capabilities of winding a fully automated coil. However, the difficult task of developing a complete winding process with all its little adjustments and maneuvers at particular times in the wind remained. This is where development of scriptable control, which supported full undo capability, over the machine's basic and more advanced capabilities provided an enabling tool for making automation of the machine possible. Interactive development of the winding process for a particular winding pattern was developed in about one week using scriptable control.

Thus, it was the combined results of several design choices which contributed to the success of the automated fiber optic gyroscope coil winding machine.

## **7. Bibliography**

Baron, Heidelberg et al. "RPM Measuring Device Utilizing An Optical Fiber Coil and Winding Method For Making The Coil" United States Patent, Patent No. 4,781,461

Belsley, Kendall and Smith, Ron. "Exploratory Studies Of Optical Fiber Gyro Coil Winding Automation." Optelecom, Inc.

Crandall, Kamopp, Kurtz, Pridmore-Brown. Dynamics of Mechanical and Electromechanical Systems, Robert E. Krieger Publishing Company Inc., FL 1982.

Davis, James Lawrence. "Inertial Rotation Sensing Using a Fiber Sagnac Interferometer," Thesis (Ph.D.), MIT, Department of Electrical Engineering, 1981.

DeFazio, Thomas L. "Development Issues For Quadrupole-Pattern Optical-Fiber Coil-Winding Machinery For Interferometric Fiber-Optic Gyro Manufacture and Automation" Draper Laboratories, 1992

Herdman, Craig T. "Fiber Optic Gyroscopes." Honeywell Technology Center.

Lefevre, Herve C. "Fundamentals of the Interferometric Fiber-Optic Gyroscope." Photonetics.

Lenders, W. L. L. "The Orthocyclic Method of Coil Winding," Phillips Technical Review, Volume 23, October, 1962, No. 12. p. 365-404.

Litton Systems Canada Ltd. "Fiber Optic Sensing Coil," United States Patent, Patent No. 4,793,708, Dec. 27, 1988.

Nauck, LCDR M. H. "Fiber-Optic Gyroscopes. History, Theory, And Application To Naval Systems." Multi-Redcom Technical Training Session, 1997

Rosenberg, Ronald C. and Karnopp, Dean C. Introduction To Physical System Dynamics. McGraw-Hill, Inc, New York, 1983

Slocum, Alexander H. Precision Machine Design. Prentice Hall, New Jersey, 1992

V.Vali and R.W. Shorthill. "Fiber Ring Interferometer," Applied Optics, 1976. p. 15, 1099.